



# QEX

March/April 2007

\$5

## A Forum for Communications Experimenters

Issue No. 241



**K8ZOA** offers the "Z90 Digital Panadapter" to display the received-signal spectrum of your receiver. The DDS-based PIC microcontroller circuit will work with receiver IFs between 50 kHz and 60 MHz.

**ARRL** *The national association for*  
**AMATEUR RADIO**

225 Main Street  
Newington, CT USA 06111-1494



# HL-1.5K<sub>FX</sub>

## HF/50MHz Linear Power Amplifier



Available Now with  
12m and 10m Built-in!

**NEW!**



Auto Band Set

This compact and lightweight 1kW desktop HF/50MHz linear power amplifier has a maximum input power of 1.75kW. Our solid-state broadband power amp technology makes it the **smallest and lightest self-contained amplifier in the industry.**

Typical output power is 1kW PEP/SSB on HF and 650W on 6m band with the drive power of 85-90W. Bands set automatically with the **built-in band decoder.** You can forget about the band setting when the amplifier is connected to your modern radio through **supplied band data cables for ICOM CI-V, DC voltage (ICOM, Yaesu), and RS-232C (Kenwood).** Manual band setting selectable as well.

All these data cables are included with the amplifier.

### Features

- Lightest and most compact 1kW HF amplifier in the industry.
- The amplifier's decoder changes bands automatically with most ICOM, Kenwood, Yaesu.
- The amp utilizes an advanced 16 bit MPU (microprocessor) to run the various high speed protection circuits such as overdrive, high antenna SWR, DC overvoltage, band miss-set etc.
- Built in power supply.
- AC 230V (200/220/240V) default and AC 115V, (100/110/120V) (selectable).
- Equipped with a control cable connection socket, for the HC-1.5KAT, auto antenna tuner by Tokyo Hy-Power Labs.
- Two antenna ports selectable from front panel.
- Great for desktop or DXpedition!

Watch for our  
**NEW PRODUCTS**  
to be  
announced soon!

### Specifications

- Frequency:**  
1.8 ~ 28MHz all amateur bands including WARC bands and 50MHz
- Mode:**  
SSB, CW, RTTY
- RF Drive:**  
85W typ. (100W max.)
- Output Power:**  
HF 1kW PEP max.  
50MHz 650W PEP max.
- Matching Transceivers for Auto Band Decoder:**  
Most modern ICOM, Yaesu, Kenwood
- Drain Voltage:**  
53V (when no RF drive)
- Drain Current:**  
40A max.
- Input Impedance:**  
50 OHM (unbalanced)
- Output Impedance:**  
50 OHM (unbalanced)
- Final Transistor:**  
SD2933 x 4 (MOS FET by ST micro)
- Circuit:**  
Class AB parallel push-pull
- Cooling Method:**  
Forced Air Cooling
- MPU:**  
PIC 18F452 x 2
- Multi-Meter:**  
Output Power – Pf 1Kw  
Drain Voltage – Vd 60V  
Drain Current – Id 50A
- Input/Output Connectors:**  
UHF SO-239
- AC Power:**  
AC 230V (200/220/240V) – 10A max. (default)  
AC 115V (100/110/124V) – 20A max.
- AC Consumption:**  
1.9kVA max. when TX
- Dimension:**  
10.7 x 5.6 x 14.3 inches (WxHxD)/272 x 142 x 363 mm
- Weight:**  
Approx. 20kgs. or 45.5lbs.
- Accessories Included:**  
AC Power Cord  
Band Decoder Cables included for Kenwood, ICOM and Yaesu  
Spare Fuses and Plugs  
User Manual
- Optional Items:**  
Auto Antenna Tuner (HC-1.5KAT)  
External Cooling Fan (HXT-1.5KF for high duty cycle RTTY)



TOKYO HY-POWER LABS., INC. – USA  
487 East Main Street, Suite 163  
Mount Kisco, NY 10549  
Phone: 914-602-1400  
e-mail: thpusa@optonline.net

TOKYO HY-POWER LABS., INC. – JAPAN  
1-1 Hatanaka 3chome, Niiza Saitama 352-0012  
Phone: +81 (48) 481-1211 FAX: +81 (48) 479-6949  
e-mail: info@thp.co.jp  
Web: http://www.thp.co.jp



Exclusively from Ham Radio Outlet!

[www.hamradio.com](http://www.hamradio.com)

- |                                     |  |
|-------------------------------------|--|
| Western US/Canada<br>1-800-854-6046 | Mid-Atlantic<br>1-800-444-4799               |
| Mountain/Central<br>1-800-444-9476  | Northeast<br>1-800-644-4476                  |
| Southeast<br>1-800-444-7927         | New England/Eastern Canada<br>1-800-444-0047 |



# QEX

QEX (ISSN: 0886-8093) is published bimonthly in January, March, May, July, September, and November by the American Radio Relay League, 225 Main Street, Newington, CT 06111-1494. Periodicals postage paid at Hartford, CT and at additional mailing offices.

POSTMASTER: Send address changes to: QEX, 225 Main St, Newington, CT 06111-1494 Issue No 241

Harold Kramer, WJ1B  
Publisher

Doug Smith, KF6DX  
Editor

Larry Wolfgang, WR1B  
Managing Editor

Lori Weinberg, KB1EIB  
Assistant Editor

L. B. Cebik, W4RNL  
Zack Lau, W1VT  
Ray Mack, W5IFS  
Contributing Editors

**Production Department**  
Steve Ford, WB8IMY  
Publications Manager

Michelle Bloom, WB1ENT  
Production Supervisor

Sue Fagan  
Graphic Design Supervisor

Devon Neal, KB1NSR  
Technical Illustrator

Joe Shea  
Production Assistant

**Advertising Information Contact:**

Janet L. Rocco, W1JLR  
Business Services  
860-594-0203 direct  
800-243-7768 ARRL  
860-594-4285 fax

**Circulation Department**

Cathy Stepina, QEX Circulation

**Offices**

225 Main St, Newington, CT 06111-1494 USA  
Telephone: 860-594-0200  
Fax: 860-594-0259 (24 hour direct line)  
e-mail: [qex@arrl.org](mailto:qex@arrl.org)

Subscription rate for 6 issues:

In the US: ARRL Member \$24,  
nonmember \$36;

US by First Class Mail:  
ARRL member \$37, nonmember \$49;

Elsewhere by Surface Mail (4-8 week delivery):  
ARRL member \$31, nonmember \$43;

Canada by Airmail: ARRL member \$40,  
nonmember \$52;

Elsewhere by Airmail: ARRL member \$59,  
nonmember \$71.

Members are asked to include their membership control number or a label from their QST when applying.

In order to ensure prompt delivery, we ask that you periodically check the address information on your mailing label. If you find any inaccuracies, please contact the Circulation Department immediately. Thank you for your assistance.

Copyright ©2007 by the American Radio Relay League Inc. For permission to quote or reprint material from QEX or any ARRL publication, send a written request including the issue date (or book title), article, page numbers and a description of where you intend to use the reprinted material. Send the request to the office of the Publications Manager ([permission@arrl.org](mailto:permission@arrl.org)).



## About the Cover

Jack Smith, K8ZOA, describes his Z90 and Z91 panadapters. Using a DDS-based PIC microcontroller, the panadapters operate with receiver IFs between 50 kHz and 60 MHz. Build one with an LCD for stand-alone operation or without and use Windows control and display software. Michael Warden, W2PY photo.



## Features

### 3 The Z90 and Z91 Digital Panadapters

By Jack Smith, K8ZOA

### 19 IsoCat: USB Transceiver Control and Sound Card Interface

By William Buoy, N5BIA

### 28 In Search of New Receiver-Performance Paradigms, Part 3

By Doug Smith, KF6DX

### 35 On the Crossed-Field Antenna Performance, Part 2

By Valentino Trainotti and Luis A. Dorado

### 46 A Low Budget Vector Network Analyzer for AF to UHF

By Professor Dr Thomas C. Baier, DG8SAQ

### 55 Ceramic Resonator Ladder Filters

By Dave Gordon-Smith, G3UUR

## Columns

### 59 Upcoming Conferences

### 60 Out of the Box

By Raymond Mack, W5IFS

### 60 New Books

By Doug Smith, KF6DX

### 61 Letters

### 62 Next Issue in QEX

## Mar/Apr 2007 QEX Advertising Index

American Radio Relay League: 18, 34, 58,  
62, 63  
ARA West: 64  
Array Solutions: Cov III  
Atomic Time: 54  
Communications Specialists: 59  
Down East Microwave, Inc: 64

Elkins Marine Training International: 64  
Kenwood Communications: Cov IV  
National RF: 64  
Nemal Electronics International, Inc: 34  
Teri Software: 34  
Tokyo Hi-Power Labs, Inc: Cov II  
Tucson Amateur Packet Radio Corp: 27



The American Radio Relay League, Inc, is a noncommercial association of radio amateurs, organized for the promotion of interest in Amateur Radio communication and experimentation, for the establishment of networks to provide communications in the event of disasters or other emergencies, for the advancement of the radio art and of the public welfare, for the representation of the radio amateur in legislative matters, and for the maintenance of fraternalism and a high standard of conduct.

ARRL is an incorporated association without capital stock chartered under the laws of the state of Connecticut, and is an exempt organization under Section 501(c)(3) of the Internal Revenue Code of 1986. Its affairs are governed by a Board of Directors, whose voting members are elected every three years by the general membership. The officers are elected or appointed by the Directors. The League is noncommercial, and no one who could gain financially from the shaping of its affairs is eligible for membership on its Board.

"Of, by, and for the radio amateur," ARRL numbers within its ranks the vast majority of active amateurs in the nation and has a proud history of achievement as the standard-bearer in amateur affairs.

A *bona fide* interest in Amateur Radio is the only essential qualification of membership; an Amateur Radio license is not a prerequisite, although full voting membership is granted only to licensed amateurs in the US.

Membership inquiries and general correspondence should be addressed to the administrative headquarters:

ARRL, 225 Main Street, Newington, CT 06111 USA.

Telephone: 860-594-0200

FAX: 860-594-0259 (24-hour direct line)

## Officers

**President:** JOEL HARRISON, W5ZN

528 Miller Rd, Judsonia, AR 72081

**Chief Executive Officer:** DAVID SUMNER, K1ZZ

The purpose of *QEX* is to:

- 1) provide a medium for the exchange of ideas and information among Amateur Radio experimenters,
- 2) document advanced technical work in the Amateur Radio field, and
- 3) support efforts to advance the state of the Amateur Radio art.

All correspondence concerning *QEX* should be addressed to the American Radio Relay League, 225 Main Street, Newington, CT 06111 USA. Envelopes containing manuscripts and letters for publication in *QEX* should be marked Editor, *QEX*.

Both theoretical and practical technical articles are welcomed. Manuscripts should be submitted in word-processor format, if possible. We can redraw any figures as long as their content is clear. Photos should be glossy, color or black-and-white prints of at least the size they are to appear in *QEX* or high-resolution digital images (300 dots per inch or higher at the printed size). Further information for authors can be found on the Web at [www.arrl.org/qex/](http://www.arrl.org/qex/) or by e-mail to [qex@arrl.org](mailto:qex@arrl.org).

Any opinions expressed in *QEX* are those of the authors, not necessarily those of the Editor or the League. While we strive to ensure all material is technically correct, authors are expected to defend their own assertions. Products mentioned are included for your information only; no endorsement is implied. Readers are cautioned to verify the availability of products before sending money to vendors.

## Research and Development

Also known as R&D, research and development is a term that was unknown before the industrial revolution. Since then, it has become an important byword of technically advanced cultures. Even more recently, the intimate connection between basic research and technological development was accentuated by certain discoveries that have rocked the world.

Innovative design is difficult in our fast-paced commercial world; but the foundation of every innovation is either invention or discovery. And every invention or discovery comes from careful, studied and sustained inquiry. Sometimes, trial and error is the best approach. So do not be surprised if errors sometimes appear on these pages; but it is our policy to correct all proven errors and we have a few to correct this time around. See the Letters Column.

Ultimately, the goal of research is to solve some problem or fill some need. In actual fact, that process is what drives our economy and makes life better. The first serious attempts to harness scientific knowledge to achieve those goals were done in the 18<sup>th</sup> and 19<sup>th</sup> Centuries by a few talented individuals, such as those who developed the telegraph, radio, airplane, computers and so on.

Research must be conducted in controlled laboratories. The same goes for test facilities that must adhere to the same rules as the researchers do. All theories have to be tested in some way. We each build on the work of others and the citation of such edification is quite important in what we publish. I'm probably as guilty as the next guy for not citing all my sources, but it's really important because we could be at risk of reinventing the wheel.

Much basic research is done at universities; however, it makes sense eventually to have the applied engineering done as closely as possible to the place where a product will be manufactured. Therefore, a symbiotic relationship exists between academia and industry. Government also has an important role. The two World Wars brought that out stunningly. Even today,

governments are the leading sponsors of industrial research. Advanced communication systems, for example, have largely been sponsored with governmental support because of military and security reasons.

A steady flow of R&D is necessary to keep any manufacturing operation cranking. Once you stop designing, things go downhill rapidly. Still, only about 25% of proposed product ideas actually succeed. Some concepts are ideas whose time has come — and gone. Take bubble memory for example. Massive amounts of research dollars went into developing that technology and it went nowhere.

The movement of products from conception into production is a critical act in engineering. The modern way is to involve all personnel along the chain from the earliest stages. Numerous technical, financial and managerial issues must be coordinated with various teams. Each company must weigh their R&D investments against the consequences of withdrawing to alternatives for their funds.

The tendency in Japan has been to look to the long term while too many companies here in the US are focused only on their monthly bottom lines. Now, however, the burgeoning economic power seems to be China; but outstanding basic research does not seem to be coming from there, other than in military matters. They are evidently centered on manufacturing.

Human factors have sometimes been largely ignored in engineering. That's true whether we're talking about theoretical studies or product design. The so-called ergonomics of technology is often elusive, but is critical to its success. The science of human-factors engineering gets little press, perhaps because it's so difficult to define for most designers. But we must define human factors in two steps: 1) integrating the human being into the machine interface by logical rigor, and 2) experimentation, often by trial and error.

My messages are: 1) keep those projects going, 2) do, and document, your research to give credit where due, and 3) don't be afraid to try something different and new, even if the results aren't what you wanted. **QEX**



# The Z90 and Z91 Digital Panadapters

*This article describes a frequency-agile, DDS-based PIC Microcontroller-equipped panadapter, with a choice of LCD or computer display.*

**Jack Smith, K8ZOA**

Since readers may not all be familiar with the term “panadapter,” a brief explanation is in order. A panadapter is a special-purpose spectrum analyzer that connects to a receiver’s mixer or IF amplifier chain. The panadapter then provides a visual display of signals near the frequency to which the receiver is tuned, with frequency on the horizontal axis and signal amplitude on the vertical axis. The panadapter was invented in the 1930s by Marcel Wallace, who founded the Panoramic Radio Corporation to manufacture his invention.<sup>1</sup> (Units manufactured by the

Panoramic Radio Corporation are identified as “panadaptors” but modern usage prefers the panadapter spelling.) To provide a useful sweep width, of course, the IF must be sampled ahead of the receiver’s selective filters.

I recently decided to build a second panadapter to use with a new receiver. The first one I built was all analog, with a surplus 1 × 4 inch rectangular electrostatic cathode ray tube display, and it functioned only with a 455 kHz IF receiver. The small electrostatic deflection CRT has largely vanished from the surplus market, so I decided to use a graphic liquid crystal display (GLCD) for my new design. As the GLCD is a digital device, a microcontroller or microprocessor is required to interface between the panadapter’s analog and digital elements. Having gone that far, replacing the analog sweep oscillator with

direct digital synthesis made sense as well. Since a stable, synthesized signal source might have other uses, I added a buffered DDS output. And, of course, since most of us have a computer in the shack now, why not also write a *Windows* control and display program as well? Six months later, the result is two variants of the same basic design:

- Z90 — A panadapter with a 240 × 320 pixel, 5.6 inch (diagonal) GLCD display and RS-232 serial interface for computer control (see Figure 1); and
- Z91 — A Z90, without an LCD display, for use with an RS-232 link for computer control. See Figure 2.

Complementing the Z90 and Z91 is *Z90 Control* software, compatible with *Windows 2000* and *Windows XP*, providing control and

<sup>1</sup>Notes appear on page 17.

7236 Clifton Rd  
Clifton, VA 20124  
[Jack.Smith@cliftonlaboratories.com](mailto:Jack.Smith@cliftonlaboratories.com)



Figure 1 — The Z90 Digital Panadapter has an LCD display.



Figure 2 — The Z91 Digital Panadapter is similar but provides data only output for use with a compatible PC program.

display of both Z90 and Z91 panadapters.

The basic specifications of the Z90 and Z91 panadapters are:

- Flexible receiver intermediate frequency — operates with receiver IFs between 50 kHz and 60 MHz, with no hardware changes.<sup>2</sup> The firmware has many popular IFs built-in, and allows the user to program in three custom IFs.
- Flexible span selection — built-in firmware-defined spans between 5 kHz and 200 kHz, with three user-programmable custom spans.
- Multiple bandwidths — two resolution bandwidths (RBW) are provided, 200 Hz and 1 kHz, under either manual control, or automatic firmware control, with RBW linked to span selection.
- High sensitivity — minimum discernable signal approximately 2  $\mu$ V with 1 kHz RBW and 4  $\mu$ V with 200 Hz RBW.
- Dynamic range — at least 60 dB.
- Vertical accuracy —  $\pm 2$  dB over a 60 dB range.
- Third-order intermodulation — with two equal signals of  $-43$  dBm level, third order products are at least 55 dB below the input signals.
- Scan rates — range from approximately four scans/second to 1.2 seconds/scan, depending upon user settings. But, since the GLCD (and the Z90 Control program) update at the end of a scan, the display

does not fade during a scan.

- Accuracy and stability — all frequencies and span widths are derived from a crystal time base, typically 10 parts per million (ppm) stability over normal indoor temperature ranges.
- Open interface — the RS-232 command structure is fully documented and is open.

### Circuit Overview

Figure 3 is a block diagram of the Z90 panadapter, operating with a 455 kHz IF receiver. The Z91 is identical, but without the GLCD and user interface switches.

The input signal enters a two-section switchable attenuator that allows the user to manually select 0, 10, 20 or 30 dB of attenuation. The input signal is amplified by a broadband monolithic microwave integrated circuit and feeds a double-balanced diode mixer. The mixer's swept local oscillator signal is provided by an AD9851, a direct digital synthesis device. The mixer output is amplified by a 2N5109 stage, with IF selectivity provided by switchable 200 Hz and 1 kHz bandwidth Gaussian crystal filters. The filters have a nominal 8 MHz center frequency. The crystal filter feeds an AD8307 logarithmic detector that converts the signal level to a dc voltage proportional to the signal strength, in decibels.

The controller, a PIC18F4620 device from

Microchip, reads the AD8307 logarithmic output with its internal 10-bit analog-to-digital converter. We'll refer to this as an 18F4620. It also controls the AD9851 by sending frequency-set commands, communicates with the GLCD and reads the status of the six front panel soft key switches (in the Z90).<sup>3</sup> In addition, it communicates with any external computer program over the RS-232 port.

### Detailed Circuit Description

I've divided the Z90 circuitry into seven modules, both for convenience and because it matches how I developed and tested the circuitry.

- Module 100 — DDS Amplifier
- Module 200 — Mixer
- Module 300 — Crystal filter
- Module 400 — Log amplifier
- Module 500 — Microcontroller and power
- Module 600 — Soft key switches
- Module 700 — DDS

### Modules 100 and 700 — DDS and Signal Generator Output Port

The DDS and related amplifier chain are closely related and will be discussed together. The local oscillator signal is generated with an Analog Devices AD9851 direct digital synthesis chip, U701.<sup>4</sup> Analog Devices describes the AD9851 as follows:

The AD9851 is a highly integrated de-

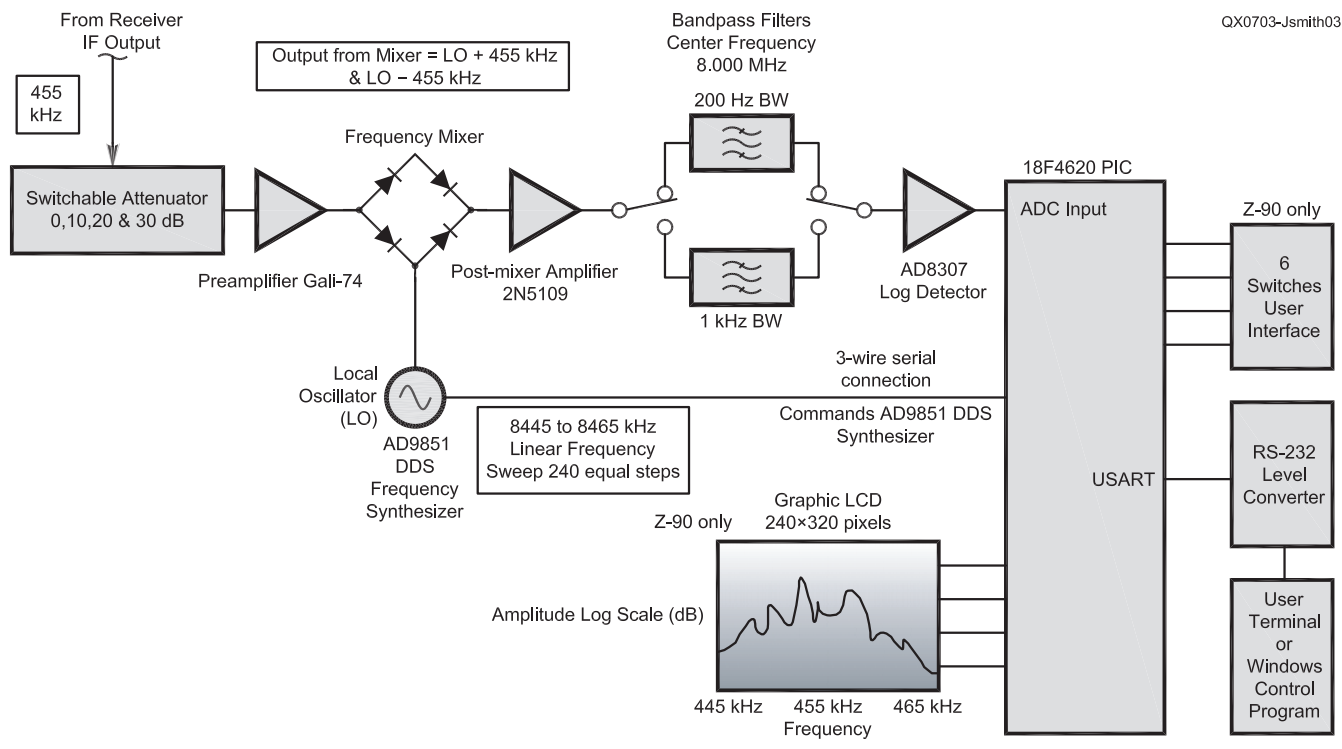


Figure 3 — Z90 Block Diagram.

vice that uses advanced DDS technology, coupled with an internal high speed, high performance D/A converter, and comparator, to form a digitally programmable frequency synthesizer and clock generator function. When referenced to an accurate clock source, the AD9851 generates a stable frequency and phase-programmable digitized analog output sine wave. This sine wave can be used directly as a frequency source, or internally converted to a square wave for agile clock

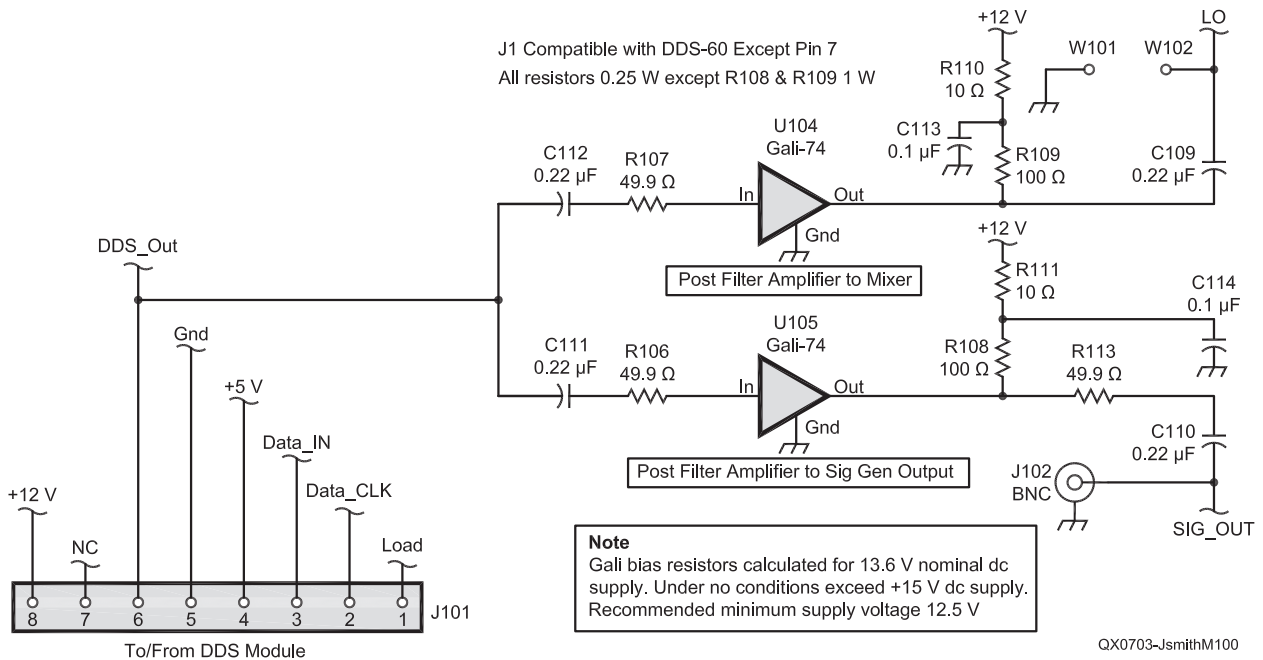
generator applications. The AD9851's innovative high speed DDS core accepts a 32-bit frequency tuning word, which results in an output tuning resolution of approximately 0.04 Hz with a 180 MHz system clock.<sup>5</sup>

My DDS design is based upon pioneering work by Paul Kiciak, N2PK, and the AmQRP Club's DDS-60 plug-in synthesizer board.<sup>6,7</sup>

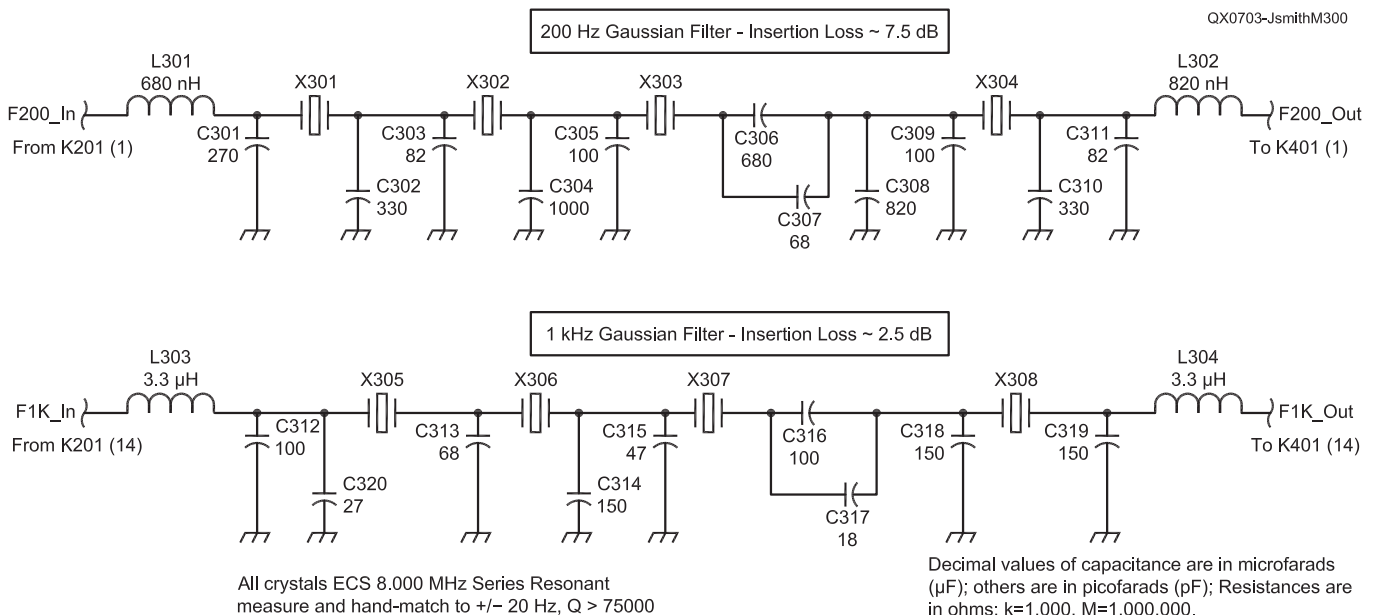
The AD9851's system clock is derived

from U702, a 30 MHz oscillator module, with the AD9851's internal 6 times PLL providing a 180 MHz effective clock frequency. Since our panadapter has a modest dynamic range objective, we accept the PLL's increased phase noise as an acceptable trade for saving the expense of a low-phase-noise 180 MHz oscillator.

The AD9851's digital-to-analog converter is current-driven, with the output current programmed at 10 mA with R704, resulting in

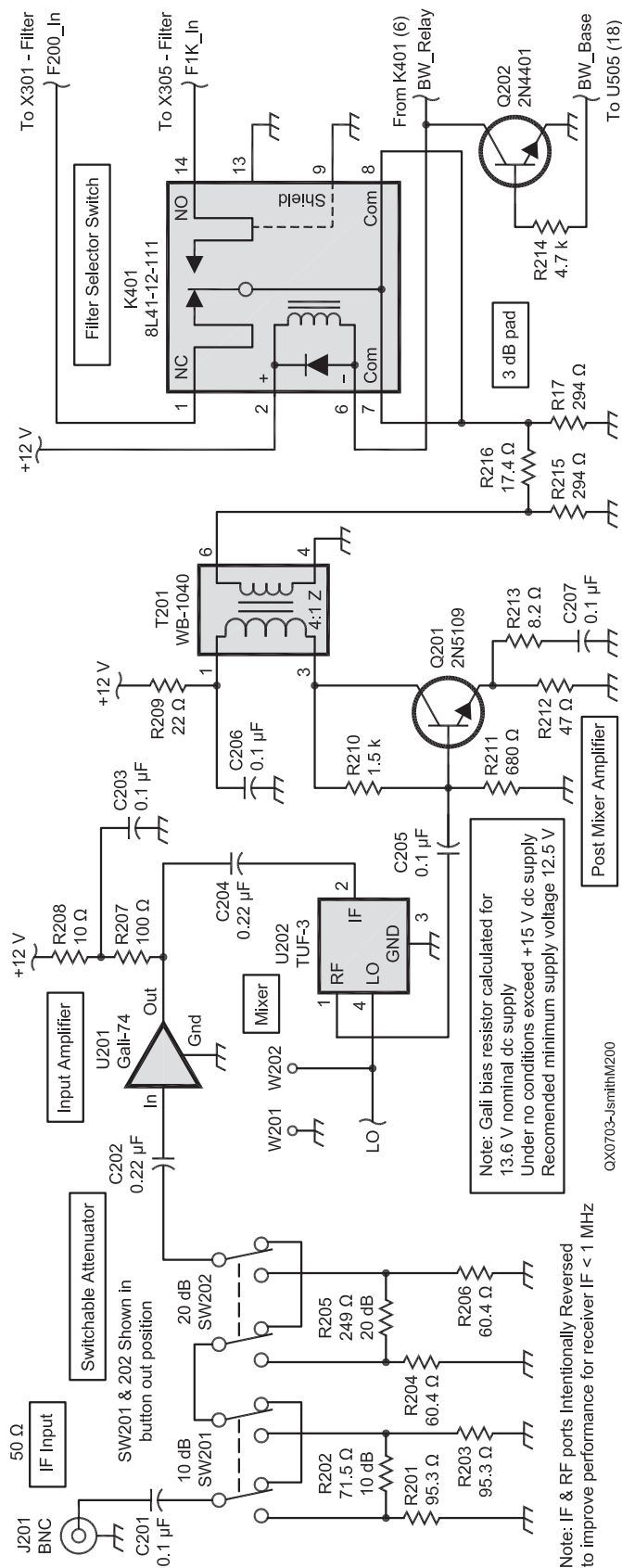


**Module 100** — This section of the panadapter is the amplifier circuit board for the direct digital synthesizer.



**Module 300** — The 200 Hz and 1 kHz Gaussian crystal filters make up this module.





a peak-to-peak signal level of 250 mV when operated into the 25 Ω load presented to it. The output is doubly terminated with R712 at the input to the 60 MHz low-pass filter, FL701, and again at the FL701's output with the input impedances of U104 and U105. Low-pass filter FL701 is a modular seven-section elliptical filter manufactured by Coilcraft Inc, with a 60 MHz cutoff frequency, and which controls spurious emissions from the DDS resulting from the digital-to-analog conversion process. It's important to remember, however, that FL701 will not remove all spurious frequencies, as some fall within the FL701 passband.<sup>8</sup>

FL701's output is coupled to U104 and U105 with a 6-dB-loss resistive splitter. Since the input impedances of both U104 and U105 are 50 Ω, adding a 49.9 Ω series resistor to each yields two amplifier chains, each with 100 Ω input impedance. The parallel combination of the two amplifiers is thus 50 Ω, providing the correct termination impedance for FL701. The resistive coupler is a cost-saving measure. However, it permits signals from the IF input port to appear at the signal generator output port, albeit reduced by the mixer's IF-to-LO isolation and U104's reverse isolation, typically totalling 40 to 50 dB. If greater purity is desired, the IF input should be disconnected when using the signal generator function.

U104 and U105 are Mini-Circuits Gali-74 MMIC broadband gain blocks rated for a maximum power output of +19.2 dBm. In the Z90 they provide gain of approximately 23 dB. The Gali-series amplifiers are simple-to-use RF amplifiers. Their main drawback is a GHz-range bandwidth, far more than necessary in the Z90, which carries with a risk of oscillation in the GHz range without careful attention to PCB layout. This slight drawback is a reasonable exchange for a low-priced, broadband, high-performance and simple-to-use amplifier.

U104's output feeds the mixer, U202, while U105 provides a buffered copy of the DDS signal to rear panel connector J102, where it may be used as a general purpose generator signal, when in signal generator mode. In addition, the signal output at J102 is used during master oscillator calibration.

U105 is protected from short circuits via a series 49.9 Ω resistor, R113, and from dc voltages by C110. The output impedance at J102 is approximately 100 Ω. Using a simple series resistor instead of an attenuator is an intentional design decision. If U105's output were terminated with a 6 dB 50-Ω pad, it would be protected from short circuits and the signal generator output would have a 50 Ω output impedance. However, at frequencies below the point where C110's reactance becomes appreciable, the 6-dB pad would severely reduce the output signal, even into a high impedance load. The current design permits increased signal levels when the AD9851 is commanded

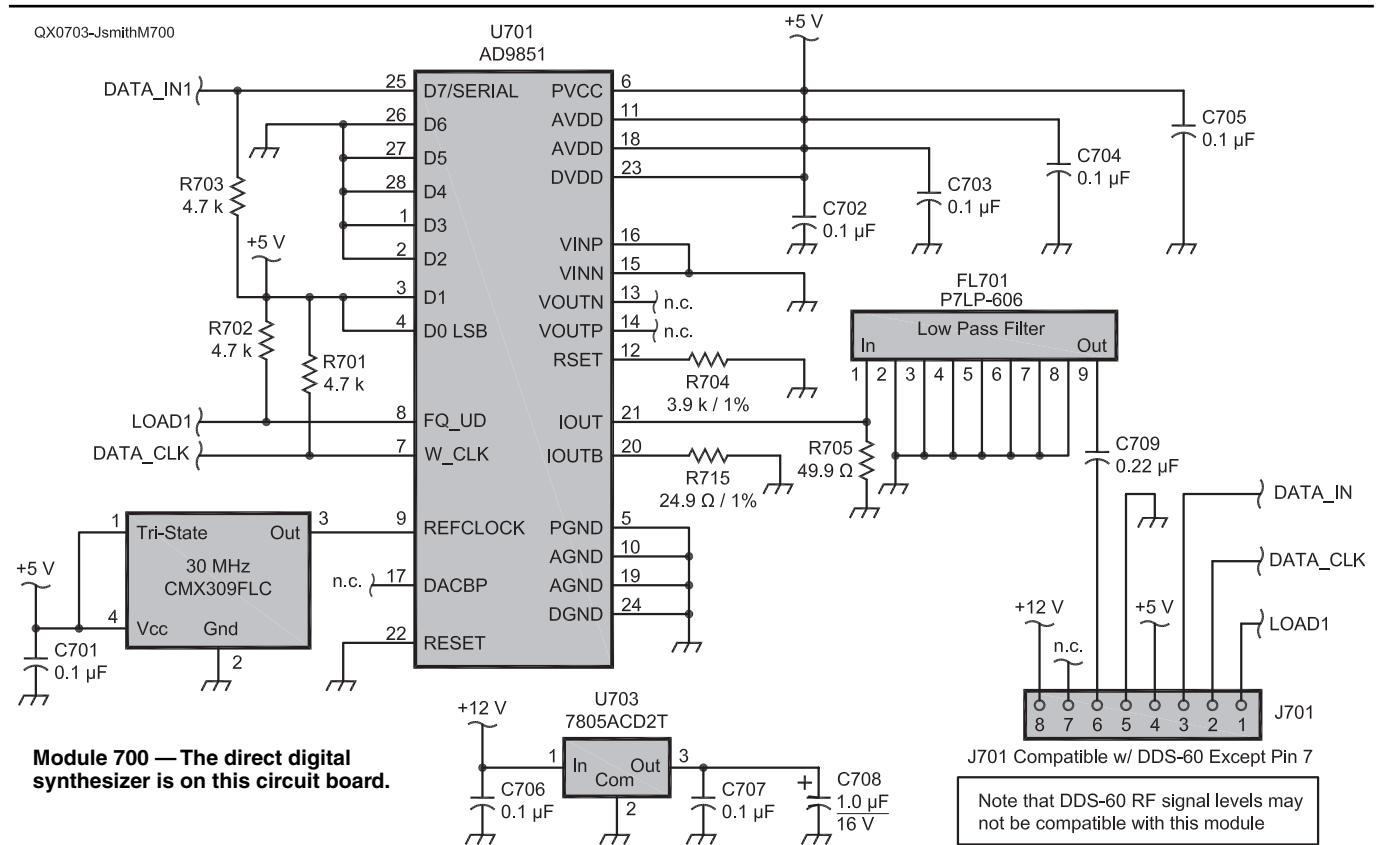
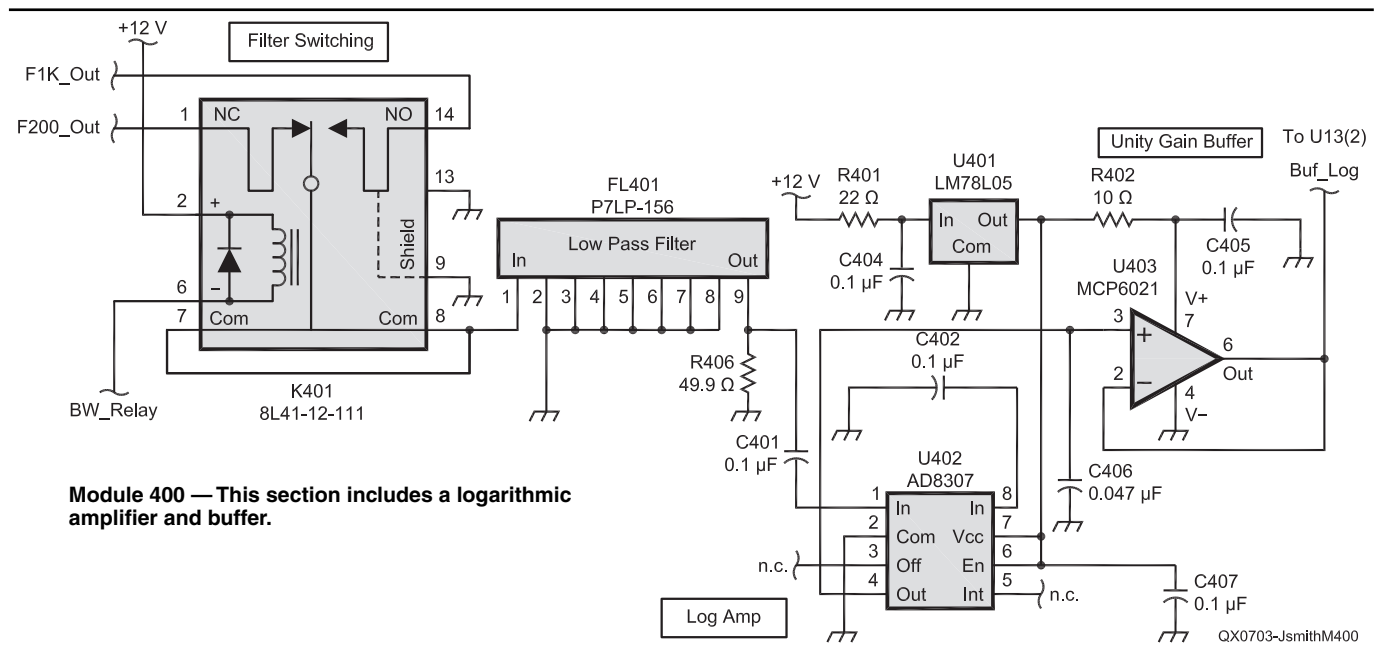
Module 200 — This section is the input and mixer portion of the circuit.

to frequencies below 100 kHz, as long as the auxiliary signal generator output is terminated into a high impedance load. J102 provides approximately +5 dBm into a 50 Ω load over the range 50 kHz to 60 MHz, and reduced voltages outside this range. The AD9851 may be

commanded to operate at frequencies between 1 Hz and 75 MHz for signal generation purposes, either through Z90 Control, or via the Z90's front panel soft keys.

Module 700 is constructed as a separate small plug-in PCB, and is broadly pin-com-

patible (but not output-level or output-level-control compatible) with AmQRP Club's DDS-60 board. Keeping the DDS on a separate PCB is useful for two reasons. First, it reduces the level of radiated RFI into the AD8307 log amplifier input, and second, it



moves the most expensive and difficult-to-install IC to a small daughter board that can be professionally assembled, if necessary, and repaired without damaging the main PCB.

### Module 200 — Input Stage and Mixer

The input connector, J201, is followed by a switchable attenuator, comprising a 10 dB pi attenuator (R201, R202 and R203) and a 20 dB pi attenuator (R204, R205 and R206), providing 0, 10, 20 or 30 dB input attenuation. Input attenuation may be necessary for receivers with a high degree of amplification ahead of the IF output port. For example, the Racal RA6790/GM 455 kHz IF peak output

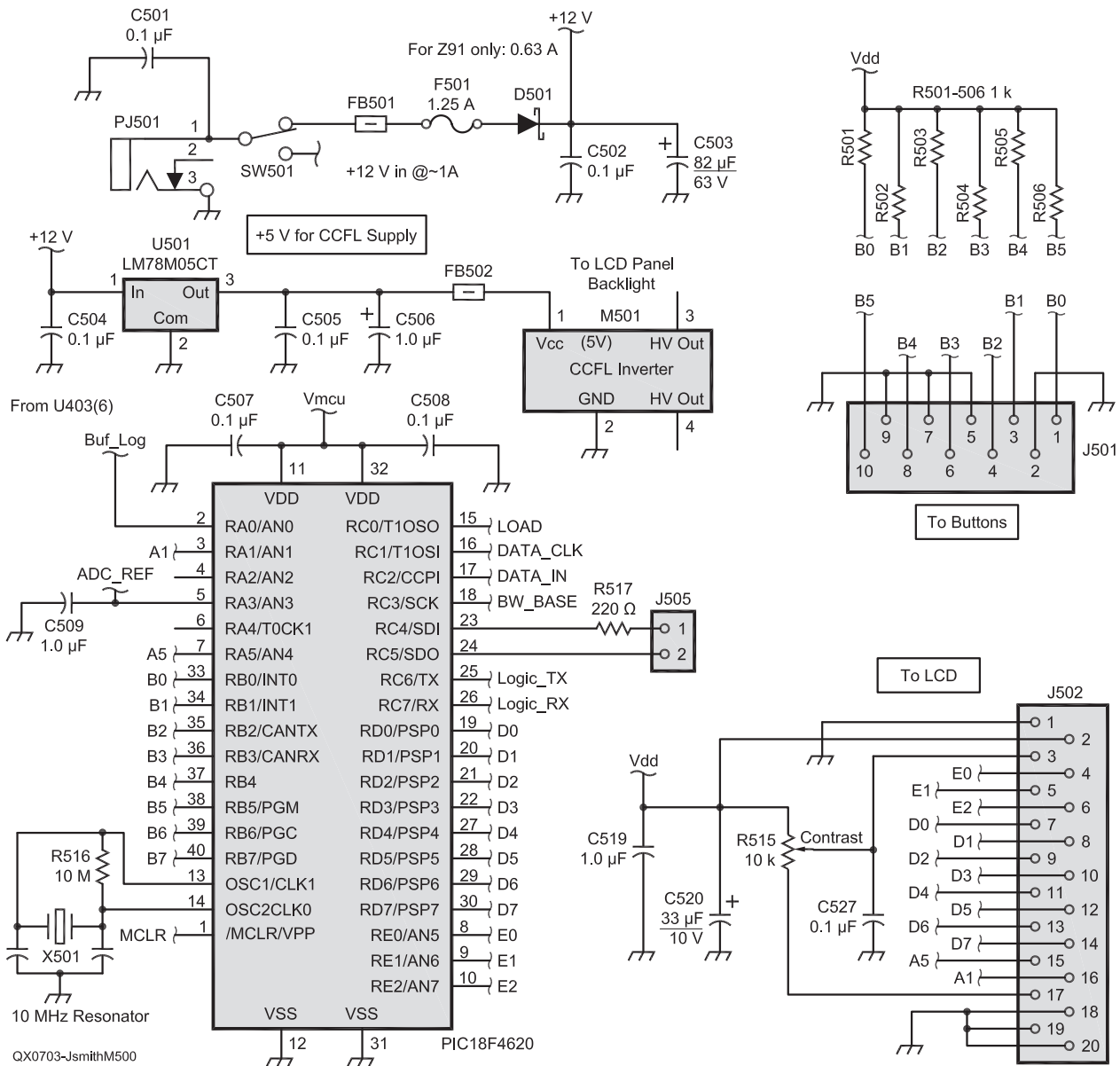
level is approximately  $-20$  dBm, requiring 10 dB attenuation to maintain the Z90's  $-30$  dBm maximum recommended input level.

U201, a Gali-74 MMIC, is a 23 dB broadband gain block identical to those used in Module 100. The Gali-74 and, for that matter, other members of Mini-Circuit's MMIC line, are "current-fed" devices, requiring a series "bias" resistor to limit the current to safe levels, with the resistor value depending upon the supply voltage. Second- and third-order intermodulation performance severely degrades if the Gali-74's bias current drops below 60 mA. To maintain the design target

85 mA bias current requires the Z90's supply voltage to be between 13.5 and 14.5 V. Operation with a supply voltage above 16 V risks damaging the Gali-74. A possible future revision to the Z90 is a 15 V supply voltage clamp.

U201's output feeds a Mini-Circuits TUF-3+ level-7 double-balanced mixer, U202. To better accommodate low IFs, the mixer's IF and RF port connections are reversed, permitting input frequencies down to dc. However, U201's coupling capacitors are designed to roll off gain for input frequencies below approximately 50 kHz.

The mixer output is coupled to a 2N5109



Module 500 — The power supply and microcontroller are on this circuit board.



amplifier based on a design by Wes Hayward, W7ZOI, using negative feedback to provide a 50 Ω input with good strong-signal performance.<sup>9</sup>

Mixer performance is critically dependent upon all ports being terminated in their design impedances: 50 Ω for the TUF-3+. The Gali-74 amplifiers (U201 on the signal input; U104 on the local oscillator input ports) present broadband 50 Ω impedances to the mixer. To better match the IF filter input, and, because the input impedance of the 2N5109 stage is determined to a significant degree by that stage's output load impedance, a 3-dB pi pad (R215, R126 and R217) is interspersed

between the 2N5109 and the crystal filter input. The pad helps assure that the mixer output and filter input both "see" 50 Ω.

The TUF-3+ mixer is intentionally slightly overdriven. Its design drive level is +7 dBm, and U104 provides approximately +10 dBm output, corresponding to about 3 dB of overdrive. This is well within the ratings for the TUF-3+.

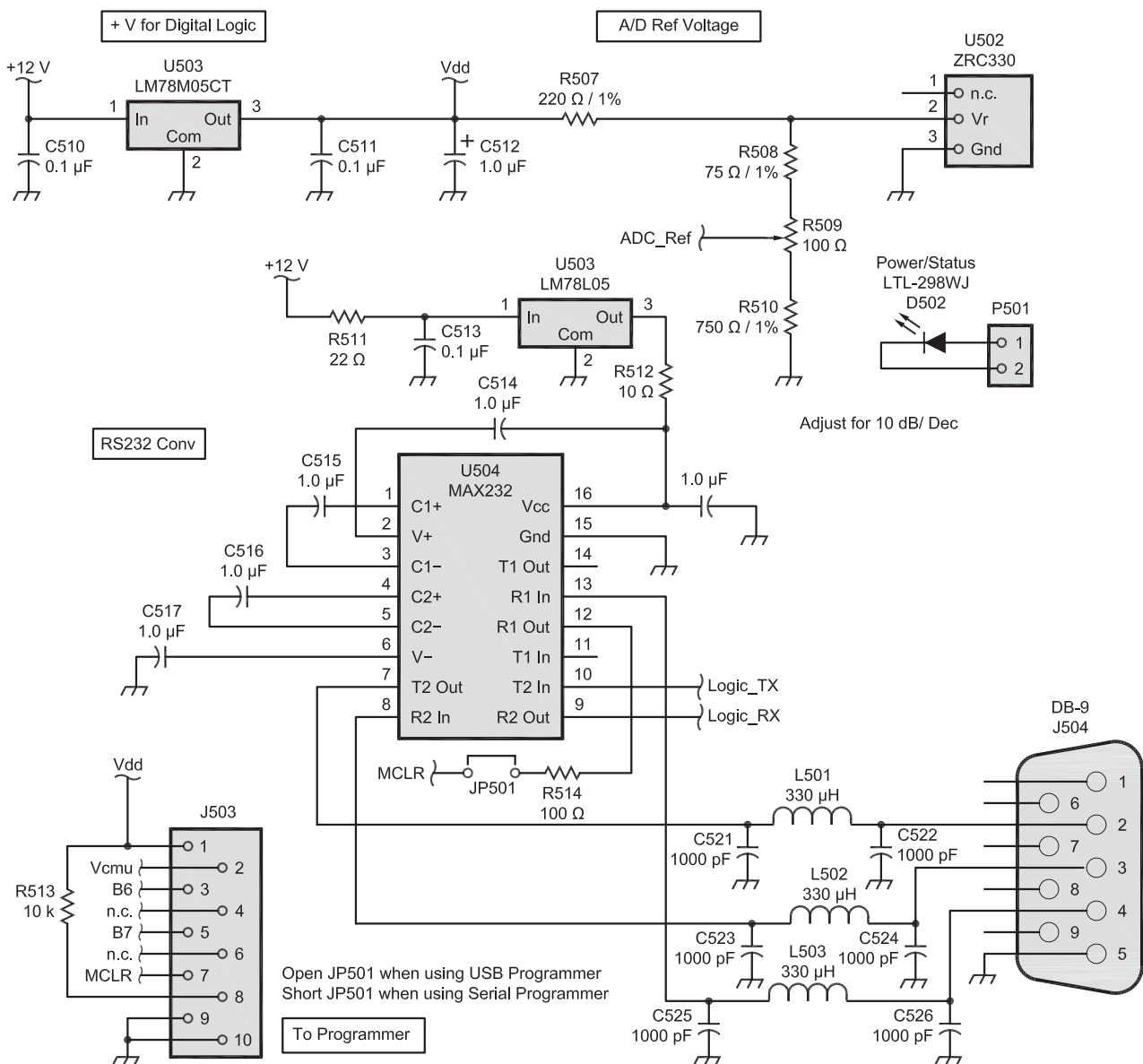
### Module 300 — Crystal Filters

IF selectivity is provided by two Gaussian crystal filters. A Gaussian filter has a rounded "nose" and a relatively gentle flank rejection slope and is used, instead of a flat

topped filter with steep flanks, because it offers a non-amplitude-distorting response to a swept frequency input signal.<sup>10</sup>

The number of crystals — four — used in each filter is based on the desired dynamic range and the necessity to limit the filter complexity for a circuit to be built without adjustment. Filter skirt selectivity is the limiting factor in the Z90's dynamic range.

To aid in development, I designed the filter module with 50 Ω impedance, adding an LC network to each filter's input and output to match the design impedance to 50 Ω. Figure 4 shows a stand-alone crystal-filter test PCB I developed to evaluate



the crystal filter designs.

The filters are of classical ladder design, with a nominal center frequency of 8 MHz. The Z90's firmware finds the exact center frequency of both filters and compensates for any difference between the nominal and true center frequency. Relays K201 and K401 operate under firmware control and select either the 200 Hz or 1000 Hz filter.

Figures 5 and 6 show the amplitude and group delay performance of a prototype 1 kHz Gaussian filter built on the stand-alone test board. It displays the rounded passband and flat group-delay characteristic of a Gaussian filter, with slightly nonsymmetrical flanks, chiefly caused by holder capacitance. It is possible to compensate for holder capacitance, but at the cost of significant additional complexity and a difficult alignment procedure.<sup>11</sup> Hence, the slight asymmetry at levels of -40 dB or more is an acceptable trade-off for a filter intended to be built and used without adjustment. A detailed discussion of the filter's design is presented in a follow-on article, "Designing the Z90's Gaussian Crystal Filter."

#### Module 400 — Log Amplifier and Buffer

The output of the filter selector relay, K401, is connected to a 15 MHz low-pass filter module, FL401, and then to U402, an Analog Devices AD8307 log amplifier. A 50 Ω resistor terminates FL401's output and U402's input. FL401 attenuates any high frequency signals that make it through the crystal filter, necessary because the AD8307's bandwidth exceeds 500 MHz and a crystal filter has little rejection at frequencies significantly above its design center, where the series crystals look more like capacitors than frequency-selective elements.

U402's output (Pin 4) provides a voltage proportional to the logarithm of the input signal, with a slope of 25 mV per dB input, and 0 V corresponding to -80 dBm input:

$$\text{Signal (in dBm)} = -80 + \text{Pin 4 voltage} / 0.025 \quad (\text{Eq 1})$$

The AD8307's internal noise produces approximately 250 mV output at Pin 4 with no signal input, corresponding to an internal noise floor of about -70 dBm. External trim resistors make it possible to adjust the slope and intercept of the AD8307, but I have chosen not to implement that feature.

Noise coupled into the AD8307's input from the Z90's digital circuitry increases Pin 4's output under zero signal input conditions to approximately 350 mV, amounting to a 4 dB increase over the chip's internal noise floor, and corresponds to -66 dBm, *measured at the input to U402*. U402 saturates at approximately +20 dBm input, but the Z90 gain stages will saturate at approximately +3 dBm into U402, thus limiting the dynamic range to approximately 65 dB.

Figure 7 illustrates the typical linearity of the Z90. Over an input signal range of -90 to -30 dBm, the maximum departure from linearity is 0.9 dB. Over the range -100 dBm to -20 dBm, the maximum error is 5.1 dB, mostly occurring at the lower end of the input range, where noise is a significant contributor to total error.

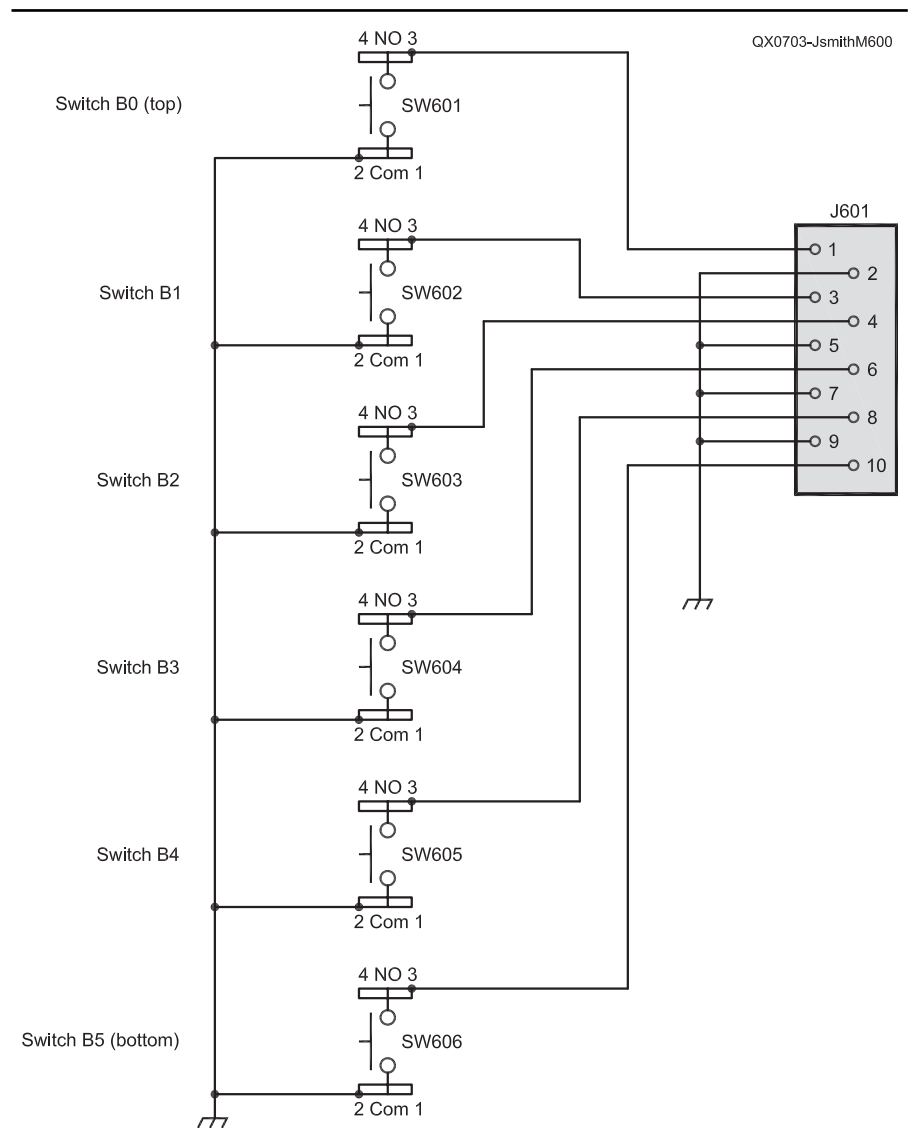
It is important to note that the Z90 does not provide an exact numerical correspondence between input level and displayed dBm value, as this is not a necessary feature of a panadapter. In Figure 7, the offset between input to the Z90 and indicated signal level happens to be almost exactly 30 dB. Achieving an exact offset in dBm was not a design goal but is rather a happenstance of the particular prototype unit being tested. However, linearity is preserved. In other words, a 10 dB change in input level,

within the range of -90 to -30 dBm will be reflected in a 10 dB change in displayed level, within the ±2 dB linearity error budget.

U402's output impedance is approximately 15 kΩ, which, combined with C406, a 0.047 μF capacitor, form an RC low pass filter with a time constant of approximately 700 μs. This provides some video filtering ahead of any averaging performed by the 18F4620 microcontroller. The RC filtered output is buffered by U403, an MCP6021 low offset operational amplifier, thereby presenting a low impedance driving source to the 18F4620's A/D converter.

#### Module 500 — Microcontroller and Power Supply

The heart of the Z90 is a Microchip 18F4620 flash memory microcontroller. This



**Module 600 — The six momentary-contact switches on this board control various Z90 operations, depending on the controller condition at the time they are pressed.**

particular device has 64 K of flash program memory, nearly 4 K of user RAM and 1 K of nonvolatile EEPROM, as well as an internal 10-bit analog-to-digital converter (ADC). At present, approximately 50% of the program memory is used, providing ample expansion room for future software improvements. Because program code is held in flash memory, it can be easily updated to add new features or fix bugs. The program code includes a boot loader, permitting updated code to be uploaded to the 18F4620 over the RS232 interface, without any special programmer hardware. The PCB layout has provisions for a programmer socket compatible with MikroElektronika's PICflash2 USB 2.0 programmer, but for normal use the socket is wired to bypass the programmer.<sup>12</sup>

The 18F4620 reads U403's output voltage level with its internal 10-bit ADC. The ADC's reference voltage is derived from U502, a 3.3 V regulator through a voltage divider chain. U502 is not a precision regulator, but provides adequate accuracy. The ADC reference voltage is nominally 2.94 V, corresponding to 3 ADC units per dB. This value simplifies converting ADC values to pixel positions on the GLCD and avoids floating point arithmetic.

U504, a MAX232 level converter, translates 5 V logic level signals to the  $\pm 15$  V RS232 serial data signal levels. The relatively old MAX232 chip is an intentional choice, as its flying-capacitor voltage multiplier circuit runs at a lower frequency than newer devices, and thus offers less potential radio frequency interference. U503, a 78L05, provides dedicated +5 V power to the MAX232, an additional noise control measure. All data line connections to the RS232 connector are filtered with pi-section low pass filters.

The Z90's RS232 port is configured as DCE (data communications equipment) so that it may be connected to a PC's 9-pin RS232 port with a straight-through or "modem" cable. A modem cable has pin 2 at one end connected to pin 2 at the other end, pin 3 to pin 3, and so on.

In addition to the normal transmit and receive connections, the DTR (data terminal ready) line is active and is used to provide an automatic reset for the microcontroller when the user installs updated firmware via the boot loader. Automatic reset, primarily used during software development, may be disabled by the user via jumper JP501, because it is incompatible with some USB-to-serial port adapters. Because of these difficulties, I recommend not installing the DTR related parts. In this case, the necessary microcontroller reset prior to loading an updated program is easily provided by briefly cycling the power switch to off, or via simultaneously pressing the top and bottom soft keys on the Z90.

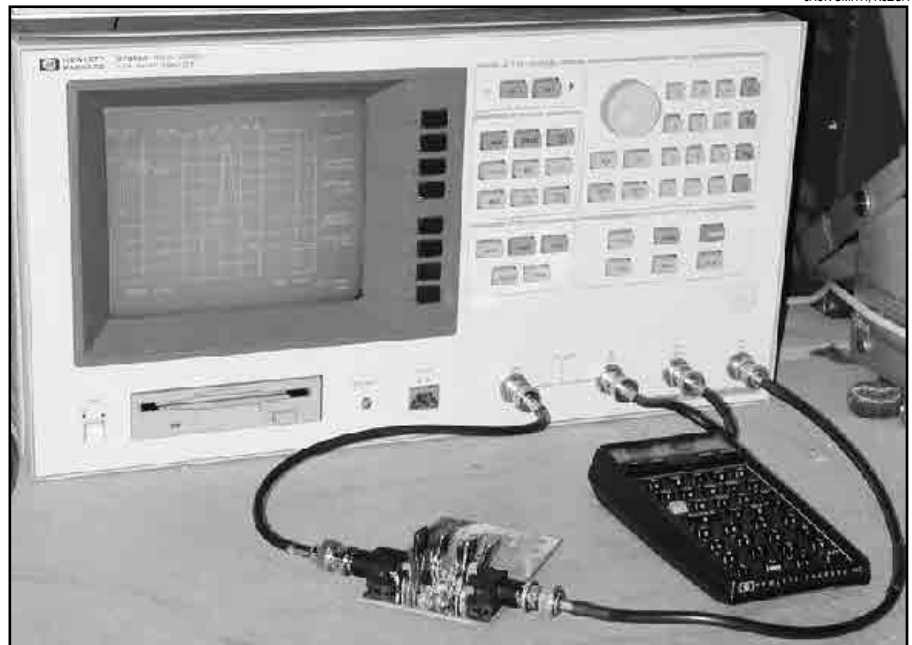
The microcontroller also communicates, via an 8-bit parallel bus, with the GLCD controller. The CFAG320240C0-FMI-T GLCD

has a resolution of  $240 \times 320$  dots ("quarter VGA") and is illuminated by a cold-cathode fluorescent lamp. The CFAG320240C0-FMI-T consists of both a GLCD and a controller board with 32 K display memory. For simplicity, I've referred to the combination as a GLCD. The CCFL's high voltage inverter (the CCFL requires about 600 V) is a modular unit, supplied by the GLCD manufacturer, and is powered by

a dedicated 7805 voltage regulator.

The GLCD controller is memory mapped only and has no drawing commands so the 18F4620 firmware provides routines to draw lines, write pixels and text to controller memory and the like. I found writing the GLCD library to be the single most difficult firmware programming task of this project.

The BASIC language compiler I used,



JACK SMITH, K8ZOA

Figure 4 — Measuring the response of a prototype crystal filter with an HP87510A VNA.

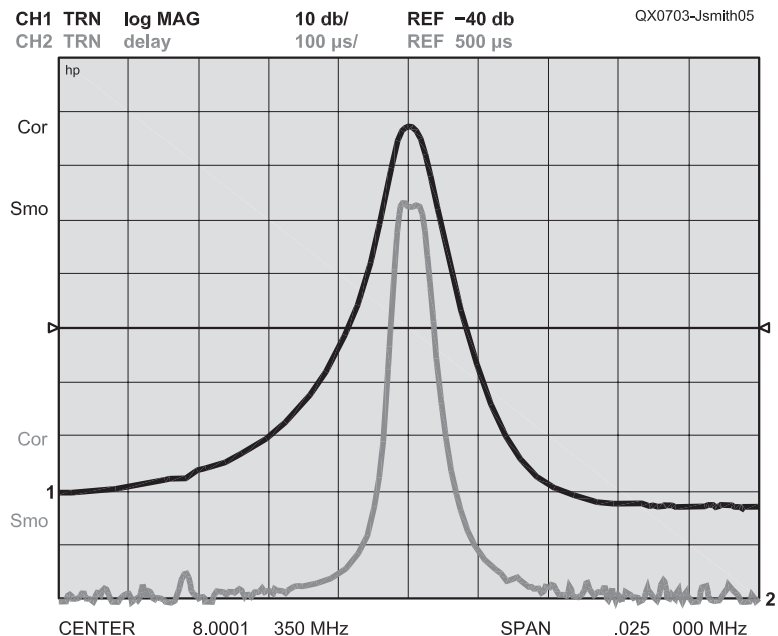


Figure 5 — Measured amplitude and group delay response of the Z90's 1 kHz filter.



*Swordfish*, now includes a graphics library with common drawing commands compatible with 320 × 240 GLCDs using the Epson S1D13700 controller such as the CFAG320240CX-FMI-T (but not the CFAG320240C0-FMI-T which uses an S1D13305-compatible controller), but neither this display nor the library were available until some months after completing the Z90's firmware.

The power supply for the Z90 is straightforward. The positive supply voltage is filtered and distributed to several integrated +5 V regulators. Multiple independent regulators permit better noise decoupling and balance out the heat load. Devices needing higher voltage are supplied from the main positive supply bus, through decoupling networks. As mentioned in connection with Module 200, the positive supply voltage should be between 13.5 and 14.5 V and should not exceed 15 V under normal operating conditions.

### Module 600 — Soft Keys

When open, the six front-panel switches are pulled high by resistors on the main board. Pressing a switch takes the associated pin of the PIC18F4620 low. This board is used only with the Z90.

### Construction and Check-Out

All Z90 and Z91 parts mount on double-sided printed circuit boards. Both the Z90 and Z91 have identical main boards and DDS daughter boards, the Z90 has a third PCB for the soft keys. Although the Z90 and Z91 boards are identical, the GLCD and soft key related parts are omitted from the Z91. The 18F4620 firmware is identical, so a Z91 can be converted to a Z90 at any time by adding the omitted components. Figure 8 shows the completed Z90 boards installed in a cabinet, together with the GLCD and its controller. The soft key board connects to the main board with a 10-pin ribbon cable, with connectors at both ends, and the GLCD connects to the main board with a 20-pin ribbon cable with connectors at both ends.

Based upon early interest in the Z90 and Z91 panadapters, a complete kit, consisting of solder-masked, silk-screened, printed circuit boards, all parts, and an enclosure with laser-cut, silk-screened panels were produced and made available via my Web site ([www.cliffonlaboratories.com](http://www.cliffonlaboratories.com)) for those wishing to replicate this project. If sufficient interest develops, a second run of the kits will be made available.

The main PCB mounts with threaded aluminum standoffs to the chassis pan in standard Ten-Tec enclosures: a BK959 for the Z90 and a BK929 for the Z91. The GLCD and soft key switch mount to the BK959 front panel via two Delrin struts, so that no mounting screw holes were necessary in the Z90 front panel.

Ten-Tec's BK-series cabinets are high-quality units, with excellent fit and finish, but they carry a high price tag. The cabinet and laser cut front and rear panels represent the single largest expense item in the project and kits.

It's important to treat the GLCD gently while mounting, as it must not be twisted or bent. My prototype used a shrouded 20-pin header that required bending the tabs holding the liquid crystal part of the GLCD to the

controller board, which proved troublesome as the tabs provide pressure for the GLCD elastomer connectors. I have since shifted to an unshrouded header that fits without bending the GLCD tabs.

The Z90 and Z91 boards are assembled and tested in a modular fashion in the following sequence:

- 1) Install the power supply components and verify that all voltages are correct.

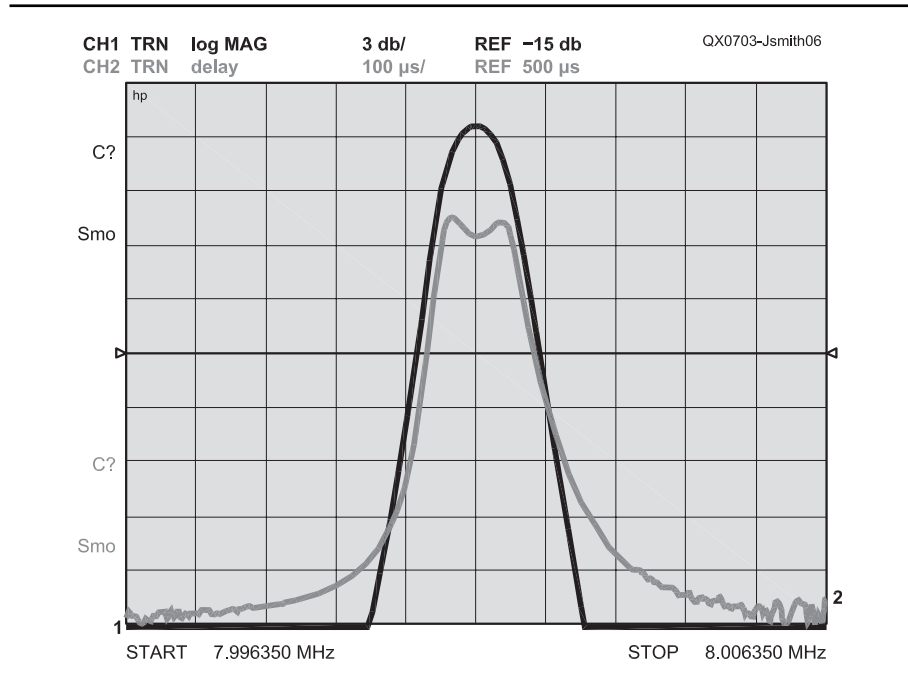


Figure 6 — Expanded view of 1 kHz filter response shows typical Gaussian rounded response and flat group delay characteristics.

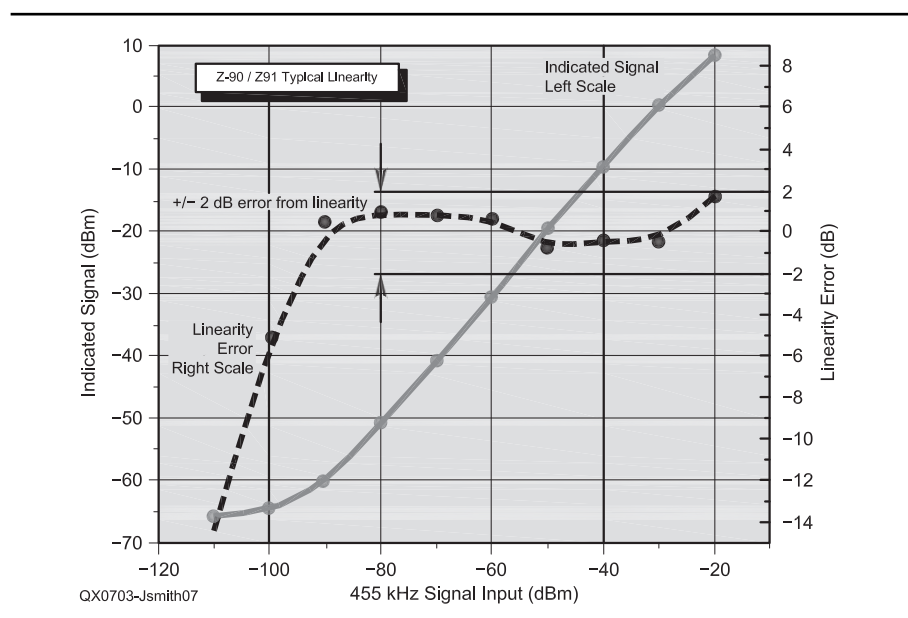


Figure 7 — Typical log detector linearity.

2) Install PIC-related components, soft key parts, and the RS232 interface parts. Communicate with the PIC using a serial terminal program such as *Terminal* or the *Z90 Control* program.<sup>13</sup> The PIC should accept all commands and return responses, although some responses will be incorrect. The Z90 should also respond to soft key commands and those responses should be reflected in the responses sent over the RS232 port. If these tests are successful, the Z90's GLCD may be attached. Upon power up, it should display a graticule and the microcontroller should accept and respond to soft key commands, although some response will be wrong until the remaining parts are installed.

3) Assemble and install the DDS. Using *Terminal* or *Z90 Control* or the soft keys, enter signal generation mode and input a test frequency. Verify that the DDS correctly generates the test frequency with a suitable receiver, spectrum analyzer or oscilloscope. Measure the auxiliary signal generator output level with an oscilloscope or spectrum analyzer, or a voltmeter with an RF detector probe.

4) Install the switchable attenuator, Gali-74 input amplifier, mixer and post-mixer amplifier. Verify their operation with an oscilloscope or spectrum analyzer and signal generator.

5) Install the log amplifier and ADC voltage reference. Using *Terminal*, read the ADC values to verify proper operation.

6) Install the crystal filter components. At this point, construction is finished and the PCB is ready for final checkout and use.

The only traditional screwdriver calibration required is to adjust R509 so that the ADC voltage reference is 2.94 V, using an accurate digital voltmeter. This value should provide reasonable vertical linearity for most AD8307s. An alternative calibration process is to adjust the ADC reference voltage so that a signal changes one full division when the internal 10 dB attenuator is switched in and out.

To adjust screen contrast, R515, the GLCD contrast potentiometer, should be placed at mid-range and the negative voltage adjustment potentiometer on the GLCD board adjusted so that the display can be seen. Fine contrast adjustments can then be made with R515. The crystal time base and filter center frequency offsets are calibrated via setup firmware.

### Z90 Operation

The firmware has three modes of operation: setup, utility and normal operation. Each mode's functions are controllable by three methods — front panel soft keys in the Z90, user commands via a terminal program connected to the RS-232 port, or through the *Z90 Control* software. The three modes and associated functions are:

#### Setup Functions:

- Calibrate the crystal time base.

- Calibrate the 200 Hz and 1 kHz filter center frequency via the “auto-cal” function, whereby the firmware sweeps the filters and determines their as-built center frequencies and saves the information to nonvolatile EEPROM memory.
- Enter up to three custom IFs, with 1 Hz resolution.
- Enter up to three custom span widths.
- Enable/disable RS232 data flow.
- Set the default “skip” factor (how many data

points per horizontal sweep) and default dwell speed (automatically computed or a manual value ranging from 1 to 5 ms per data point).

#### Utility Function:

- Select signal generator mode and enter the desired frequency, with 1 Hz resolution.

#### Operational Mode:

- Select the IF to be used.

MICHAEL WARDEN, W2PY



Figure 8 — Z90 Interior.

JACK SMITH, K8ZOA

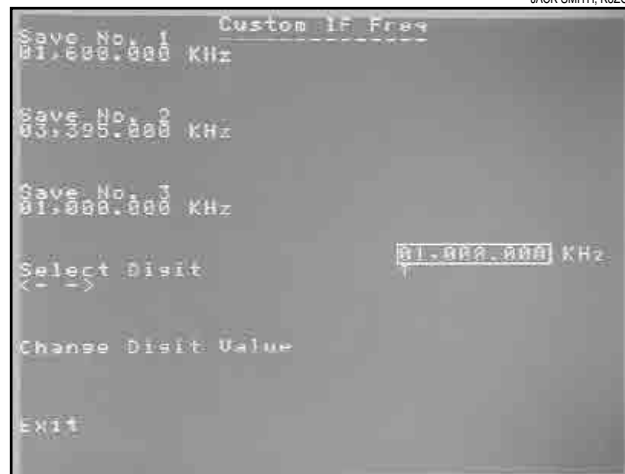


Figure 9 — Typical Z90 User Interaction Screen, defining a “custom IF.”

- Select the span width.
- Select the resolution bandwidth, and RBW mode (manual or automatic selection by firmware, based on selected span).
- Adjust the vertical position of the trace.
- Select vertical gain of 10 dB/div or 2 dB/div and turn the graticule on or off.
- Select vertical averaging (similar to video bandwidth in a spectrum analyzer) factor ranging from one to 64 samples per display point.
- Override the default skip and dwell settings.

All parameter settings are saved in non-volatile EEPROM memory and are retained while power is turned off. When it is next powered on, the Z90 returns to the last entered settings.

Space does not permit a detailed discussion of these functions, but Figure 9 shows



Figure 10 — Z90 Front panel showing soft keys and display graticule.

**Table 1**  
**Command and Control**

Command	Parameters	Min	Max	Comments
<i>General</i>				
?	None			Current parameter report is generated
G*	nnnnnnnn	0	60000000	Generate RF frequency, switch to sig gen mode — frequency in Hz.
P	None			Stop RS-232 data output
Z	None			Start RS-232 data output
X	none			Exit and return to scanning
<i>IF Center Frequency, Span and Resolution Bandwidth</i>				
I*	nn	1		Select a defined (indexed) IF. N is the index number
F*	nnnnnnnn	0	60000000	Center frequency in Hz. This is a temporary entry and will be replaced by a saved index value if other parameters are changed. To preserve the entered span, save it as a custom span with the T command.
T	n	1	3	Store current IF as Custom n
B*	n	0	1	Bandwidth 0 = narrow, 1 = wide
N*	nn	1	9	Select a defined (indexed) span. N is the index number
S*	nnnnnn	5	250	Span in kHz. This is a temporary entry and will be replaced by a saved index value if other parameters are changed. To preserve the entered span, save it as a custom span with the C command.
C	n	1	3	Store current Span as Custom n
<i>Display Related</i>				
A*	nn	1	64	Video average, legal values 1,2,4,,8,16,32,64. Entered value will be converted to maximum legal value <= entered value
D*	n	0	1	Graticule 0 = Off, 1 = On
E*	n	1	6	Time in ms between successive frequency steps. Value = 6 is "automatic" mode where the minimum usable time is selected automatically depending upon bandwidth
K*	n	0	3	Skip factor, 0 to 3 pre-programmed only. Skip jumps in coarser steps for a faster sweep. The larger the skip factor, the greater the frequency jump between steps.
V	n	0	1	Vertical gain. 0 = 10 dB/div, 1 = 2 dB/div
R*	nn	0	80	Reference position - the vertical position of the display.
<i>Calibration</i>				
L	none			Calibrate filter. Starts automatic filter calibration sequence. For best results, disconnect any signal input from the panadapter.
O	none			Saves the current frequency as 10 MHz calibration. To calibrate the time base, go to generation mode (G) and enter 10000000. Adjust the entered frequency until the measured output is exactly 10000000. For example, it might be necessary to enter 10000050 to measure 10000000 at the output. When the output measures 10000000 use the O command to enter this value into the frequency calibration EEPROM.

\*Command letters identified with \* followed by ? returns the current value of that parameter.



the “Custom IF” setup screen, typical of other setup screens. To enter a new IF, the digit to be changed is selected by pressing the soft key across from the “Select Digit” line. The up-arrow symbol moves to below the digit to be edited. Pressing the soft key across from the “Change Digit Value” line cycles the digit through all possible values from 0 through 9.

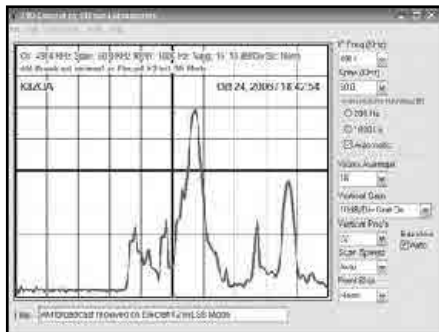


Figure 11 — Z90-Control display software showing normal operating mode.

When finished with editing the new IF value, it may be saved to one of three memory locations by pressing the soft key adjacent to the three “Save” lines.

Figure 10 shows the normal operational mode screen, and the six soft keys. Pressing any soft key cycles the associated parameter through all possible values. The Span function deserves additional discussion because of the two status characters following the word “span.” The first character identifies the skip factor, with “s” being “standard” skip. The actual number of points taken is determined by the firmware based upon the selected span and RBW, but “standard” skip is the least aggressive and will normally sample 120 points per scan. (Skip off mode always takes 240 points per scan, regardless of span and RBW. The most aggressive skip mode results in 60 data points per sweep. However, the firmware implements the user’s skip setting only to the extent reasonable, based upon the selected RBW and span. For example, if the user selects the most aggressive skip,

200 kHz span and 1 kHz RBW, the firmware will instead use skip-off mode and take 240 data points.) The second character, a “\*” in the figure, indicates that the dwell time (the time the firmware pauses before taking an ADC reading after jumping to a new scan frequency) is set automatically by the firmware. Pressing a two soft key combination overrides the span and dwell factors entered during setup.

### Serial Control via Terminal

Both the Z90 and Z91 have RS-232 ports allowing software control and display of data. The standard command syntax consists of a single letter, followed by a numerical value or a question mark. The data speed and mode is fixed at 115,200 b/s, 8 bits, no parity, 1 stop bit, as any slower speed is incompatible with acceptable GLCD refresh time.

Entering the command, for example, “A4” sets the video averaging factor to 4. The command “A?” causes the firmware to respond by reporting the current video averaging factor.



Figure 12 — Setting up custom intermediate frequencies via Z90-Control software.

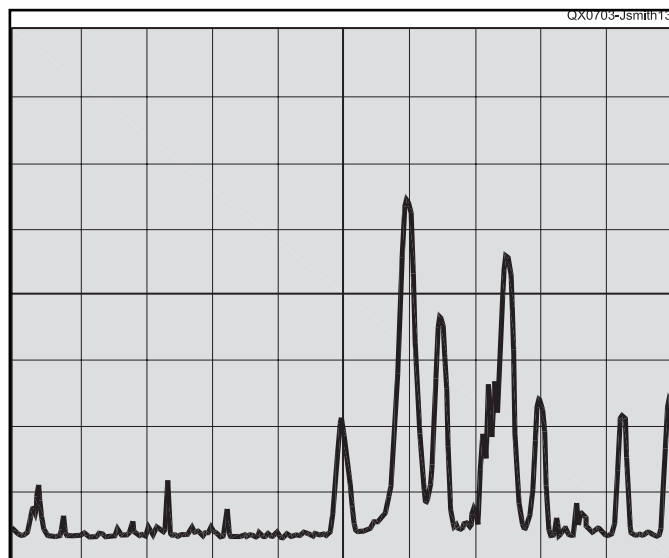


Figure 13 — 10 MHz as seen when connected to Kenwood TS-940 8830 kHz IF Out shows wide range of signals.

**Table 2**  
**Receivers Tested for Operation with the Z90**

Receiver	IF	Comment
Racal RA6790/GM	455 kHz	Output is at nominal -20 dBm and at least 10 dB attenuation should be used to avoid overloading the Z90. The output is sampled after the IF filter, so the usable scan bandwidth depends on the selected bandwidth, maximum usable scan is approximately 20 kHz.
Watkins-Johnson HF-1000	455 kHz	Output sampled before IF selectivity, but bandwidth is limited by 45 MHz roofing filter to approximately 20 kHz.
Cubic R3030	40.455 MHz 455 kHz	40.455 MHz is broadband (approximately 1 MHz bandwidth) 455 kHz is narrowband; 10 dB attenuation may be required.
Kenwood TS-940	8830 kHz	Wideband output. The output signal is subject to gain variations when the receiver’s AGC operates on the RF amplifier and hence the displayed signals will vary in amplitude with the strength of the signal to which the TS-940 is tuned.
Kenwood TS-870	8830 kHz	Specifications match the TS940, but to be tested in the future as the IF output port on my 870 is defective.
Elecraft K2	4415 kHz	Connect to noise blanker port with a buffer amplifier. Requires an extra connector to be installed.

The current syntax has 20 command letters, with additional commands under consideration. See Table 1.

Enabling data output results in the Z90 sending operating parameter status and raw ADC readings over the RS-232 port with every sweep. This data can be used for debugging and maintenance purposes, but is primarily to be used with the Z90 Control program.

### Control and Display Software

I have written a control and display program, Z90 Control, for computers running either the Windows 2000 or Windows XP operating systems. Figure 11 shows the program's main window, displaying an AM shortwave broadcast signal in the 7 MHz band when connected to my Elecraft K2 transceiver.

The Z90 Control software performs the same setup, utility and operational functions described earlier, through Windows-traditional menus and dialog boxes. For example, Figure 12 illustrates how a custom IF is entered into the Z90.

Z90 Control allows the screen image to be copied to the clipboard, or printed on a printer, or saved as a bitmap or JPG format file. Also, incoming data may be saved as a text file for later study. Included with Z90 Control is a boot loader utility permitting updated firmware to be loaded into the 18F4620 flash program memory over the RS232 connection.

### Connecting the Z90 to a Receiver

#### Compatible Receivers

In the easiest case, your receiver or transceiver will have an IF output jack to which the Z90 can be connected. I've tested the Z90 with the receivers listed in Table 2.

The effect of receiver bandwidth restriction ahead of the IF output port is easily seen if we compare data from a Z90 connected to the Kenwood TS-940 (Figure 13) and the Watkins Johnson HF-1000, Figure 14. The two figures show WWV at 10 MHz, and are taken within a few minutes of each other. The Z90 is set, in both cases, at 100 kHz span and 1 kHz RBW. Many signals are seen in Figure 13; Figure 14, in contrast, shows no appreciable signal outside a range of about 25 kHz. This is because the Watkins Johnson HF-1000's IF bandwidth is restricted to about 25 kHz by a "roofing" filter in the 45 MHz first IF. Figure 13 shows signals across the entire 100 kHz span, because the TS-940's 8830 kHz IF output port has a bandwidth of several hundred kHz. If you look carefully, the carrier in Figure 14 does not quite align with the center graticule. In single sideband mode, the HF-1000 offsets the IF by half the selected bandwidth, approximately 1500 Hz in this case.

### Inversion

Some receivers invert their IF output sample. In other words, a signal higher in frequency than the one to which the receiver is tuned appears lower in frequency in the IF output port. This is a consequence of the conversion scheme used by the receiver designer. I'm considering revised software that has an "invert" option to compensate for the receiver's inversion.

Older receivers may require you to make an IF sample connection. Normally, the connection will be made to the mixer stage, ahead of the receiver selective IF filters. The Z90 has a low impedance (50 Ω) input impedance, so it will usually be necessary to find a low impedance point from which to couple the IF sample. This might be at the cathode of a tube-type mixer, or at an emitter resistor for a discrete transistor mixer. The degree of coupling can be controlled by a small value

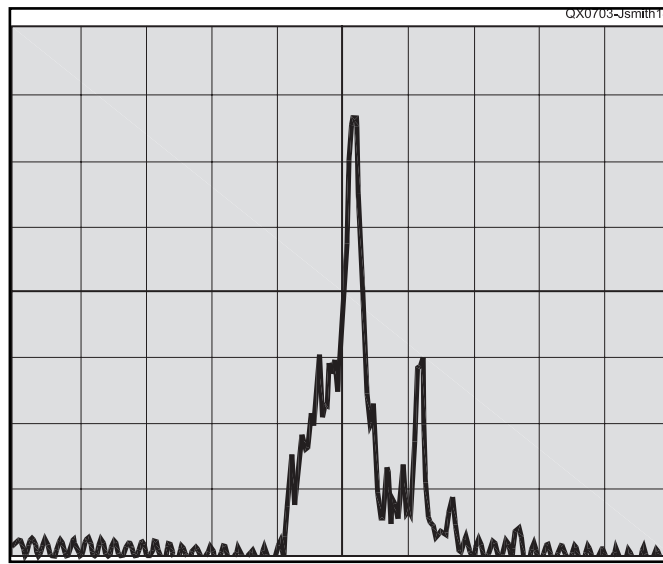


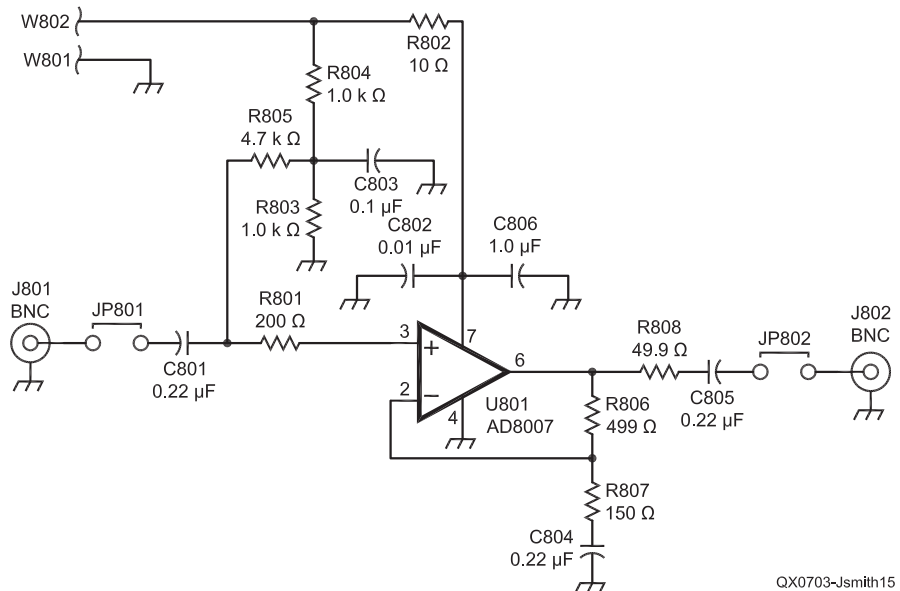
Figure 14 — 10 MHz as seen when connected to Watkins-Johnson HF-1000 shows usable span is limited to about 25 kHz by the HF-1000's roofing filter.

Net Gain in dB measured at J802 into 50 Ω load =  $20 \log_{10}((R806 + R807) / R807) - 6.03$

Change R807 to alter gain:

49.9 Ω = 14.8 dB net  
 100 Ω = 9.6 dB net  
 150 Ω = 6.7 dB net  
 220 Ω = 4.3 dB net  
 499 Ω = 0.0 dB net

R808 is safety resistor to protect against short circuit on output and to ensure stability in driving 50 Ω cables  
 It reduces gain by 6 dB and is considered in the R807 vs gain table



QX0703-Jsmith15

Figure 15 — Buffer amplifier for signal pickoff in receivers without an IF Out port.

series capacitor between the sample point and the lead to the Z90. I've also designed a buffer amplifier shown at Figure 15 and Figure 17. The buffer amplifier's gain is programmable from 0 dB to 15 dB by selection of R807 and offers an input impedance ranging from 4.7 k $\Omega$  at 300 kHz to 1 k $\Omega$  at 30 MHz, as reflected at Figure 16. Of course, the IF sample should be taken from a point ahead of selective elements, in so far as possible.

### Project Status and Future Plans

I've designed, constructed and tested two "Manhattan style" prototypes, two full prototype PCB layouts and several stand-alone PCBs with individual modules and I regard most of the circuitry as satisfactory. The current silk-screend and solder-masked PCBs are identical with the last prototype boards. However, there's always room for software tinkering. I will update my Web page to reflect changes in the circuit and associated firmware and software.

### Acknowledgments

The Z90 microcontroller firmware is written in Mecanique's *Swordfish* programming language, originally using an alpha test version of the *Swordfish* compiler, now a completed commercial product.<sup>14</sup> David Barker, *Swordfish* chief developer, has provided invaluable assistance supporting the compiler during alpha and beta testing, including fixing more than a few of my programming errors. I also wish to thank Larry Phipps, N8LP, for testing a prototype Z90 with his K2 transceiver and for displaying the Z90 and Z91 prototypes at his 2006 Dayton Hamvention table.

### Notes

<sup>1</sup>A brief history of the early days of the pan-adaptor has been assembled by Chuck McGregor, N7RHU, and can be found at [home.comcast.net/~cbmcg/Panadaptors.html](http://home.comcast.net/~cbmcg/Panadaptors.html).

<sup>2</sup>Unsupported frequency ranges include 7.9-8.1 MHz (near the Z90's 8 MHz IF) and 3.95 MHz-4.05 MHz (half-IF). The vast majority of popular IFs tested are spurious free, or, in the case of 10.7 MHz, have one spur at reduced signal levels. With slightly reduced performance, IFs up to 70 MHz can be used, as well as frequencies below 50 kHz.

<sup>3</sup>The switches are called "soft keys" not because their texture is physically soft, but rather because their function depends on firmware status and is thus not fixed. Pressing a switch performs the function identified next to it on the GLCD.

<sup>4</sup>For an excellent introduction to DDS, see Analog Devices "A Technical Tutorial on Direct Digital Synthesis" (1999), at [www.analog.com/UploadedFiles/Tutorials/450968421DDS\\_Tutorial\\_rev12-2-99.pdf](http://www.analog.com/UploadedFiles/Tutorials/450968421DDS_Tutorial_rev12-2-99.pdf).

<sup>5</sup>Description at [www.analog.com/en/prod/0,,770\\_843\\_AD9851,00.html](http://www.analog.com/en/prod/0,,770_843_AD9851,00.html).

<sup>6</sup>See [users.adelphia.net/~n2pk/](http://users.adelphia.net/~n2pk/) for links to Paul's innovative vector network analyzer,

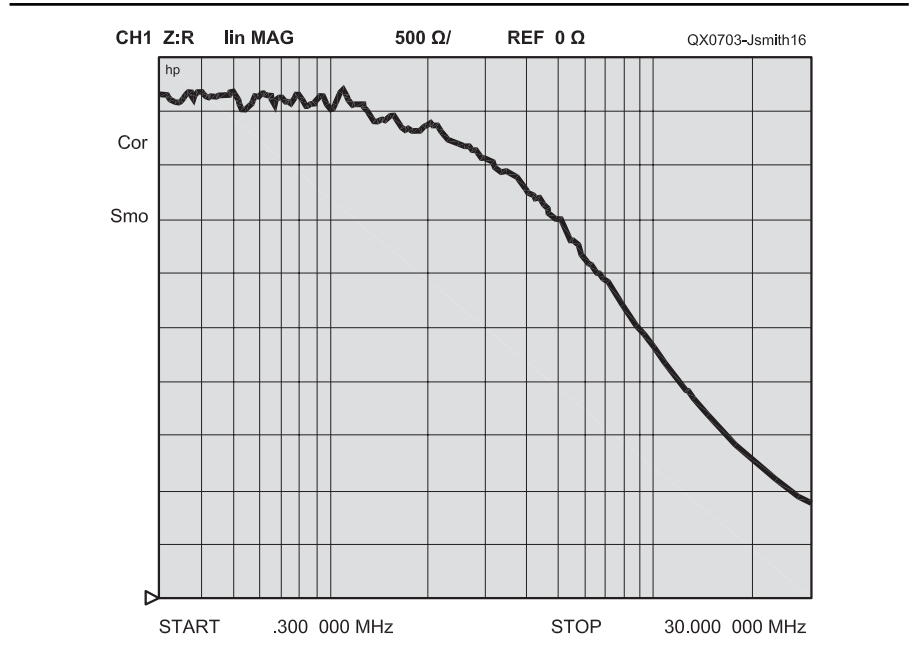


Figure 16 — Input impedance of buffer amplifier as a function of frequency.

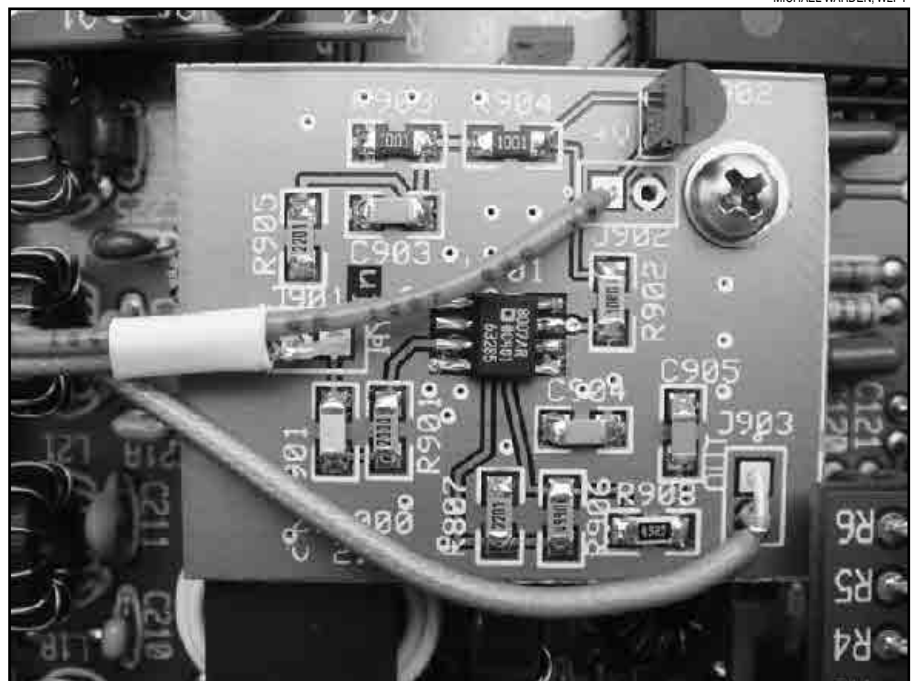


Figure 17 — Photo of buffer amplifier PCB installed in an Elecraft K2 transceiver.

built around a pair of AD9851 DDS chips.  
<sup>7</sup>See [www.amqrp.org/kits/dds60/](http://www.amqrp.org/kits/dds60/) for detailed information on the DDS-60 synthesizer kit.  
<sup>8</sup>In particular, the so-called "inverted alias" frequencies can be troublesome. For example, if the DDS is set to 59 MHz, the 3<sup>rd</sup> harmonic frequency, 177 MHz, interacts with the DAC's 180 MHz clock rate and produces an output at 3 MHz that passes through FL101 unattenuated.  
<sup>9</sup>Wes Hayward, et al, *Experimental Methods*

*in RF Design*, 2003, American Radio Relay League, Newington CT.  
<sup>10</sup>H.W. Batten, et al, "The Response of a Panoramic Receiver to CW and Pulse Signals, Technical Report No. 3," (1952) Electronic Defense Group, Department of Electrical Engineering, University of Michigan, available for download at [hdl.handle.net/2027.42/3473](http://hdl.handle.net/2027.42/3473).  
<sup>11</sup>For example, the holder capacitance can be cancelled with parallel inductance, as de-

scribed by Hayward *supra*. I built an experimental filter following Hayward's idea and found that while symmetry was improved, the number of adjustments, and their touchiness outweighed the benefits for a 1 kHz filter. The balance between complexity and filter performance would likely shift in favor of holder capacitance cancellation for wider bandwidth filters.


<sup>12</sup>More information on the PICflash2 programmer is available at [www.mikroelektronika.co.yu/english/product/tools/picflash2.htm](http://www.mikroelektronika.co.yu/english/product/tools/picflash2.htm)

<sup>13</sup>The program supplied with *Windows, Hyperterm*, should not be used, as it holds the DTR line in reset state and thus the Z90 will

not function. A much superior replacement, without the DTR problem is the freeware program *Terminal*, available for download at [bray.velenje.cx/avr/terminal/](http://bray.velenje.cx/avr/terminal/). However, all *Windows* terminal programs briefly "flash" the DTR line when they initially connect. This seems to be a "feature" in the *Windows* API.

<sup>14</sup>More information on *Swordfish* is available at [www.mecanique.co.uk/swordfish/](http://www.mecanique.co.uk/swordfish/).

*Jack Smith, K8ZOA, has been licensed since 1961, first as KN8ZOA, and has held an Amateur Extra Class license since 1963. He received a BSEE degree from Wayne*

*State University in Detroit in 1968 and a JD degree magna cum laude from Wayne State University School of Law in 1976. Presently retired, he has enjoyed a career involving both engineering and telecommunications law. He is a co-founder of the telecommunications consulting firm TeleworX and is the author of Programming the PIC Microcontroller with MBasic (Newnes Publishing, 2005), as well as many articles published in 73 Amateur Radio magazine. His Web site is [www.cliftonlaboratories.com](http://www.cliftonlaboratories.com).* 



# CARRL EP

Certification and Continuing Education Program

## The all NEW Technician License Course... **Online!**

### The fast, easy way to get your friends and family on-the-air!

#### Get it All!

Technician License Course – EC-010

The goal of this course is to prepare students to take, *and pass*, the entry-level Amateur Radio license exam. This course includes;

- "The ARRL Ham Radio License Manual"
- One year ARRL membership including *QST* every month
- An online graduate support group

**Package Price \$69.00**





#### Other Courses to Sharpen Your Skills

- Antenna Design & Construction – EC-009
- Antenna Modeling – EC-004
- HF Digital Communications – EC-005
- Amateur Radio Emergency Communications
  - Level 1 – EC-001
  - Level 2 – EC-002
  - Level 3 – EC-003R2
- Radio Frequency Propagation – EC-011
- VHF/UHF – Life Beyond the Repeater – EC-008
- Radio Frequency Interference – EC-006
- Analog Electronics – EC-012
- Digital Electronics – EC-013



**ARRL** The national association for AMATEUR RADIO

On Line courses for each class begin every month – Register at [www.arrl.org/cce](http://www.arrl.org/cce) and sharpen your skills.

## Register Online!

# www.arrl.org/cce

QEX 3/2007



# IsoCat: USB Transceiver Control and Sound Card Interface

*Is your new computer missing the old standard serial port? Build the IsoCat and begin enjoying digital mode operation and computer control of your transceiver through the USB port.*

**William Buoy, N5BIA**

## Introduction

Before starting this project, I looked at the many excellent interfaces available on the market. No single interface had the com-

16214 Hollow Rock Dr  
Houston, TX 77070  
n5bia@arrl.net

bination of features I was looking for. These features include the following:

1. The interface had to have both a sound card interface and transceiver control in a compact package.
2. The transceiver and computer had to be isolated from each other through transformers or opto isolators.
3. The transceiver or computer (or both)

had to provide all power to operate the interface.

## Design Goals

In addition to the features I was looking for in an interface, I set a number of design goals when I started this project. These design goals include the following:

1. All components and connectors had

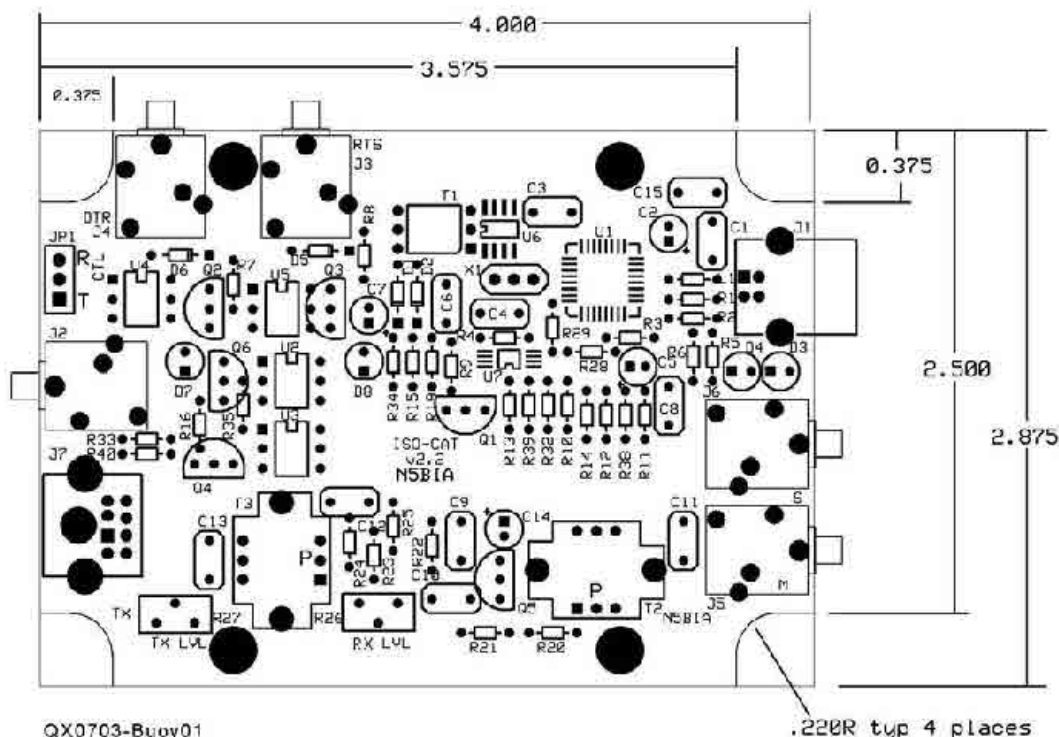


Figure 1 — This parts-placement diagram also serves as a template for cutting holes in the project box for connectors and LED indicators.

to mount on a single circuit board to reduce costs and assembly time.

2. The completed board had to fit inside an inexpensive, easy to work enclosure that was readily available.

3. All cables to the transceiver and the computer had to be detachable for easier storage, simple repair or replacement if a cable was damaged, and to enable connection to transceivers with different connectors.

I believe all of the goals are met in this design.

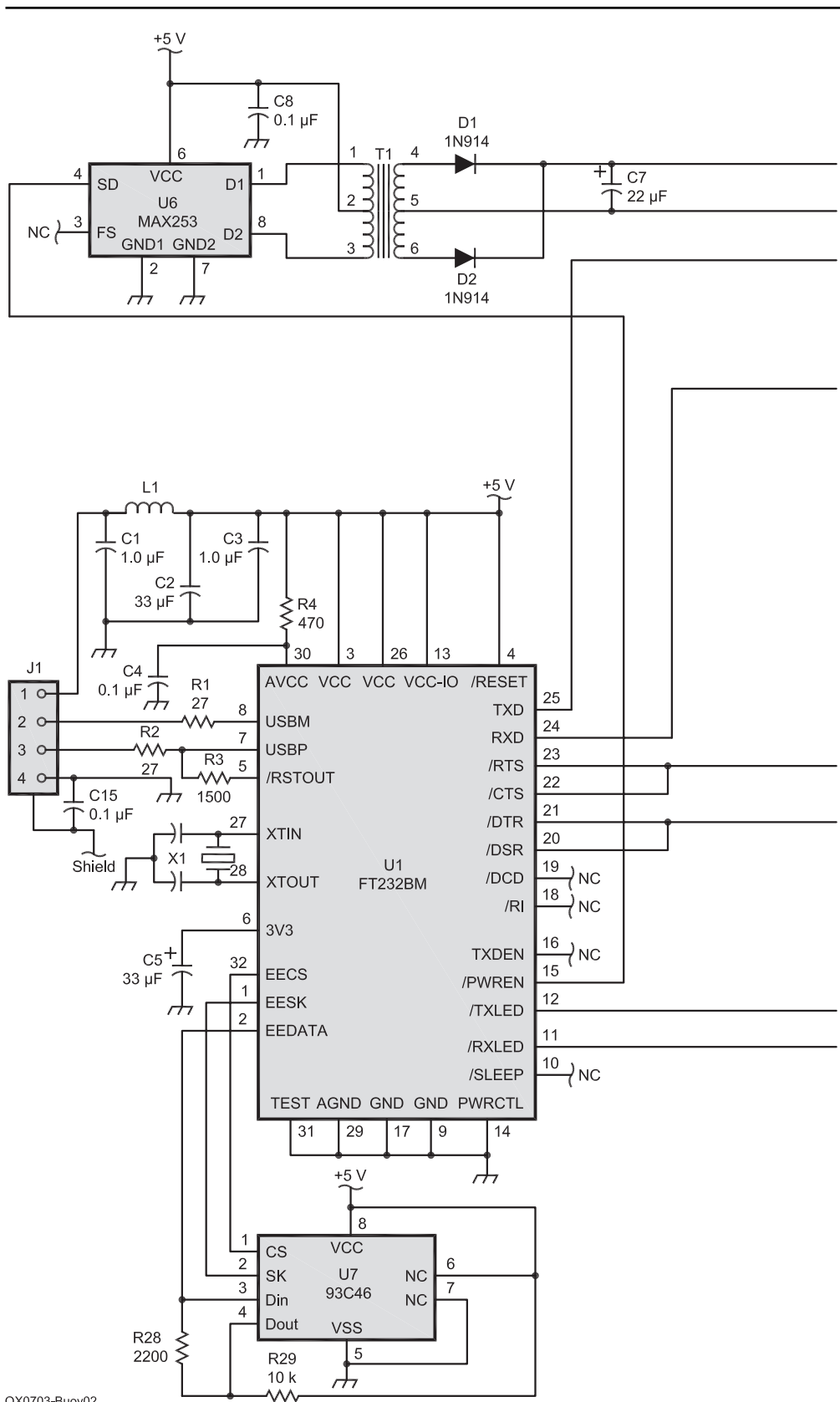
Having never worked with the design aspects of the USB interface, I did not know what to expect. Future Technology Devices International, a company specializing in USB interfacing, came to the rescue! Among their products, I found a basic USB-serial interface chip that seemed a very straightforward way to get started. Offered in a 32-pin LQFP (leaded quad flat pack) surface-mount chip, the IC is available from Digikey.

One of the first challenges was prototyping because the USB interface IC was only available in a surface-mount package. I decided the best approach was to lay out a circuit board instead of building the circuit on a breadboard and transferring the design to a PC board later. Thanks to ExpressPCB ([www.expresspcb.com](http://www.expresspcb.com)), this is a very practical way to prototype, especially if all the parts fit on a 2.5 x 3.8 inch board. They offer three prototype boards (without solder mask or silkscreen) for a very reasonable price with 10-day turnaround. Both the schematic capture and PC layout software is free, and the quality of the software and the boards is excellent. Having used quite a number of far more costly and difficult to use software tools for both schematic capture and PC layout, I highly recommend ExpressPCB.

### Circuit Description

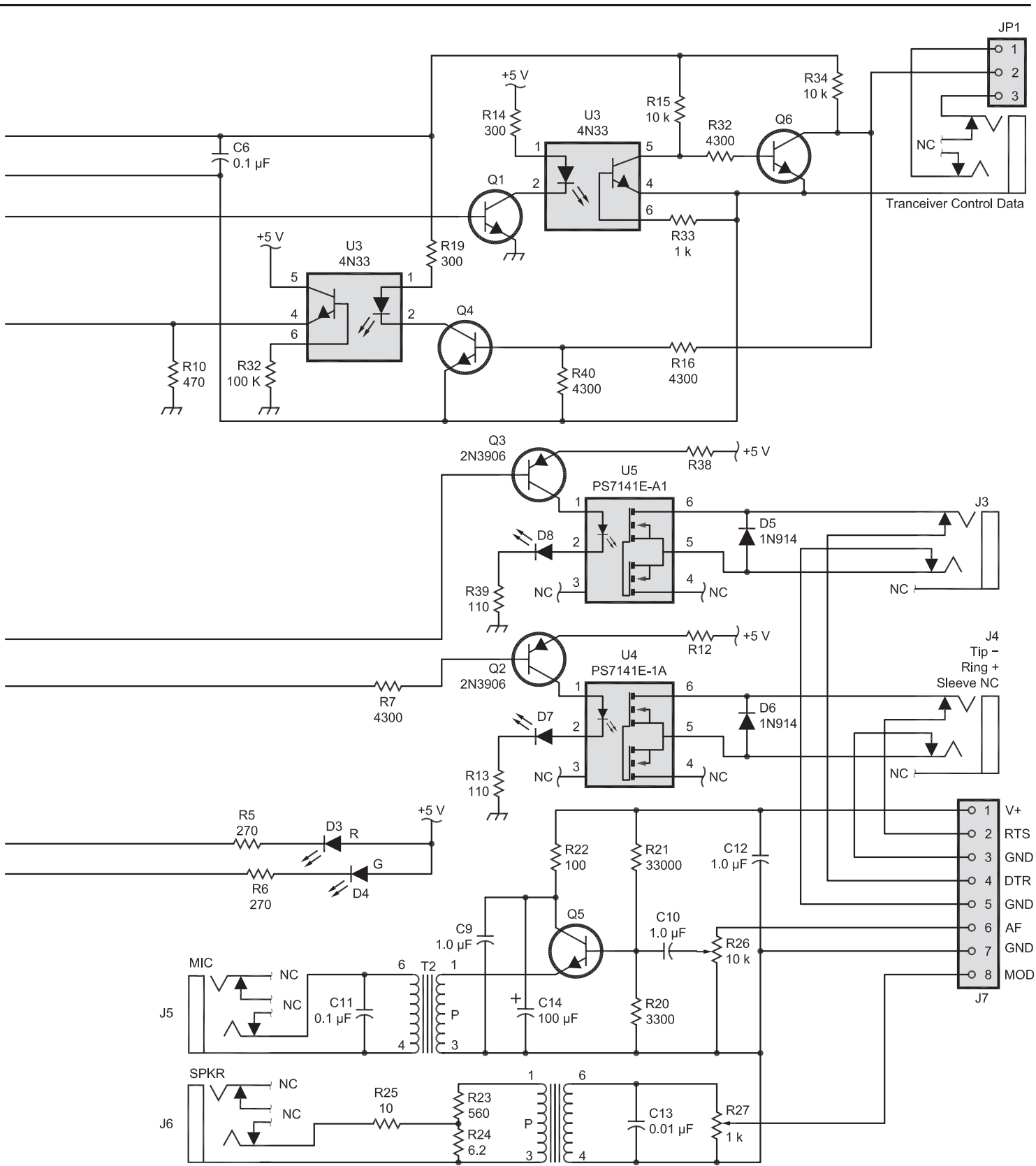
The two subsystems comprising IsoCat are built on a 2.875 x 3.875 inch circuit board. (I built two of the interfaces on the 2.5 x 3.8 inch prototype boards, but packaging was an issue, so I changed to a larger layout. I also paid for the solder mask and silk screening on the final boards.)<sup>1</sup> See Figure 1. Each subsystem can be operated independently of the other. The USB subsystem presents a standard USB interface to the computer and provides a data path to and from the transceiver control ports. The audio subsystem couples the transceiver audio to and from the computer sound card. Each subsystem provides complete isolation between the transceiver and the computer, as well as isolation from each other. Figure 2 shows the IsoCat schematic diagram. Table 1 is a parts list.

<sup>1</sup>Notes appear on page 26.



QX0703-Buoy02

Figure 2 — The IsoCat schematic diagram is shown here.



QX0703-Buoy02

Table 1

Qty	Title	Detail	Reference(m)	Vendor	Vendor P/N	Mfr	Mfr P/N
2	Resistor	1/2 W, 5% 27 Ω, axial lead	R1, R2	Digi-Key	27EBK-ND	Yaego	
1	Resistor	1/2 W, 5%, 1.5 kΩ, axial lead	R3	Digi-Key	1.5KEBK-ND	Yaego	
1	Resistor	1/2 W, 5%, 2.2 kΩ, axial lead	R28	Digi-Key	2.2KEBK-ND	Yaego	
2	Resistor	1/2 W, 5%, 270 Ω, axial lead	R5, R6	Digi-Key	270EBK-ND	Yaego	
1	Resistor	1/2 W, 5%, 300 Ω, axial lead	R14, R19	Digi-Key	300EBK-ND	Yaego	
7	Resistor	1/2 W, 5%, 3.3 kΩ, axial lead	R20	Digi-Key	3.3KEBK-ND	Yaego	
1	Resistor	1/2 W, 5%, 4.3 kΩ, axial lead	R7, R8, R9, R15, R16, R35, R40	Digi-Key	4.3KEBK-ND	Yaego	
1	Resistor	1/2 W, 5%, 47 Ω, axial lead	R11	Digi-Key	47.0EBK-ND	Yaego	
2	Resistor	1/2 W, 5%, 470 Ω, axial lead	R4, R10	Digi-Key	470EBK-ND	Yaego	
1	Resistor	1/2 W, 5%, 100 Ω, axial lead	R22	Digi-Key	100EBK-ND	Yaego	
1	Resistor	1/2 W, 5%, 33 kΩ, axial lead	R21	Digi-Key	33KEBK-ND	Yaego	
3	Resistor	1/2 W, 5%, 10 kΩ, axial lead	R15, R29, R34	Digi-Key	10KEBK-ND	Yaego	
1	Resistor	1/2 W, 5%, 560 Ω, axial lead	R23	Digi-Key	560EBK-ND	Yaego	
1	Resistor	1/2 W, 5%, 6.2 Ω, axial lead	R24	Digi-Key	6.2EBK-ND	Yaego	
2	Diode, light emitting, yellow, diffused	T-1 3/4, 50° viewing angle	D7, D8	Digi-Key	160-1703-ND	LiteOn	LTL-307Y
1	Potentiometer	12-turn, 10 kΩ	R26	Digi-Key	490-2970-ND	Murata	
1	Potentiometer	12-turn, 1 kΩ	R27	Digi-Key	490-2969-ND	Murata	
2	Capacitor, polyester	0.01 μF, 50 V, radial lead, 0.200 spacing	C11, C13	Digi-Key	P4582-ND	Panasonic	ECQ-B1H103JF
4	Capacitor, polyester	0.1 μF, 50 V, radial lead, 0.200 spacing	C4, C6, C8, C15	Digi-Key	P4593-ND	Panasonic	ECQ-B1H104JF
5	Capacitor, stacked metal film	1 μF, 50 V, radial lead, 0.200 spacing	C1, C3, C9, C10, C12	Digi-Key	P4675-ND	Panasonic	ECQ-V1H105JL
1	Capacitor, electrolytic,	100 μF, 16 V, 2 mm LS, 5 mm dia	C14	Digi-Key	P5138-ND	Panasonic	ECA-1CM101
1	Capacitor, electrolytic,	22 μF, 16 V, 2 mm LS, 5 mm dia	C7	Digi-Key	P5135-ND	Panasonic	ECA-1CM220
2	Capacitor, electrolytic,	33 μF, 16 V, 2 mm LS, 5 mm dia	C2, C5	Digi-Key	P5136-ND	Panasonic	ECA-1CM330
1	Inductor, ferrite bead	axial lead	L1	Digi-Key	240-1035-1	Steward	M10805K400R-00
2	Transformer, audio	600 Ω:600 Ω	T2, T3	Mouser Electronics	42TLO16	XICON	
1	Transformer, power, switching	T1	Mouser Electronics	580-7825355	C&D Technologies	78253/55	
1	Crystal, oscillator, 6-MHz	3-lead, w/capacitors	X1	Digi-Key	490-1222-ND	Murata	CSTLS6M00G53Z-B0
4	Diode, small signal, 1N914		D1, D2, D5, D6	Digi-Key	1N914BCT-ND	Fairchild	1N914BTR
1	Diode, light emitting, red, diffused	T-1 3/4, 50° viewing angle	D3	Digi-Key	160-1707-ND	LiteOn	LTL-307P
1	Diode, light emitting, green, diffused	T-1 3/4, 50° viewing angle	D4	Digi-Key	160-1706-ND	LiteOn	LTL-307G
4	Transistor, NPN, 2N3904, TO-92	HS switch, 60 V, 200 mA	Q1, Q4, Q5, Q6	Digi-Key	2N3904FS-ND	Fairchild	2N3904BU
1	IC, dc-dc converter, surface mount	MAX253	U6	Digi-Key	MAX253CSA-ND	Maxim	MAX253CSA
1	IC, USB-serial converter	FT232BL	U1	Mouser Electronics	619-604-00031	Parallax	FT-232-BL LQFP32
2	IC, optoisolator	6-pin DIP	U2, U3	Digi-Key	4N33-ND	Fairchild	4N33
1	Connector, USB	Type B, PC mount, RA	J1	Mouser Electronics	571-7877801	AMP	787780-1
2	Resistor, 1/2 W, 5%, 110 Ω	axial lead	R13, R39	Digi-Key	110EBK-ND	Yaego	
3	Resistor, 1/2 W, 5%, 10 Ω	axial lead	R12, R25, R38	Digi-Key	10EBK-ND	Yaego	
1	Connector, DIN	8-pin, circular, pcb, receptacle	J7	Digi-Key	CP-2280-ND	CUJ	MD-80SM
1	IC, memory	93C46, SSOP	U7	Digi-Key	AT93C46A-10T1-2.7-ND	Atmel	AT93C46A-10T1-2.7
1	Board, printed circuit	ExpressPCB	U7	Digi-Key	AT93C46A-10T1-2.7-ND	Atmel	
5	Connector, 1/8" phone,	PC mount, RA	J2, J3, J4, J5, J6	Mouser Electronics	161-3508	Kobiconn	161-3508
1	Resistor, 1/2 W, 5%, 100 kΩ	axial lead	R32	Digi-Key	100KEBK-ND	Yaego	
1	Resistor, 1/2 W, 5%, 1000 Ω	axial lead	R33	Digi-Key	1KEBK-ND	Yaego	
2	Transistor, PNP, 2N3906, TO-92	axial lead	Q2, Q3	Digi-Key	2N3906FS-ND	Fairchild	2N3906BU
2	Relay, solid state, 400 V, 0.15 A	DIP6	U4, U5	Mouser Electronics	551-PS7141E-1A-A	NEC	PS7141E-1A-A



## USB Interface

The heart of the USB interface is the FTDI FT232BL USB-serial IC. This IC presents a complete USB hardware interface to the computer. The output consists of RS232 serial input, output, and control signals at TTL levels. Before devices such as the FT232, USB interfacing was much more difficult. First generation USB peripherals frequently dedicated a portion of an embedded microprocessor to handling the USB interface. This required extensive knowledge of the USB signal conventions and timing, as well as debugging and development resources. Construction of an interface such as this was beyond the time budget and knowledge level of many experimenters.

The FT232 is a black box from a design perspective. One set of pins provides the physical USB connection. A second group of pins enables access to limited customization features through an optional EEPROM. A third group of pins comprise the data input, output, and control connections to implement an RS232 interface at TTL levels. No programming of the USB interface is necessary — simply connect the pins as directed in the data sheets and the USB side of the interface is done. Add the isolation circuitry on the transceiver side of the interface, and the design is complete.

The input, output, and control pins of this IC are connected to optical isolators, which couple the signals to and from the transceiver while providing dc isolation. Data is handled by a pair of optoisolators, one for data transmitted to the transceiver and one for data returned from the transceiver. To guarantee higher current switching capability and lower ON voltage drop, a pair of optically isolated solid state relays are connected to the DTR and RTS lines to enable T/R control by toggling RTS or DTR. The appropriate choice for your application depends on the software and mode you choose. DTR and RTS are available on isolated 1/8 inch phone jacks and on the eight pin mini-DIN connector for maximum versatility.

An isolated dc-dc converter using the Maxim MAX253 switching power supply IC provides an isolated dc voltage supply to the transceiver side of the control interface. A miniature power transformer, a full-wave rectifier, and a simple filter complete the dc-dc converter design.

The minimal supply current necessary to operate the FT232 and MAX253 is drawn from the USB port. There is also space on the board for an optional 1 K memory IC to provide a custom “personality” to identify this interface. This feature may be used to identify the USB interface with a specific name in the installed equipment list and to change the default behavior when the operating system recognizes and installs the device

during Plug-N-Play operation.

The availability of royalty-free device drivers was an essential component of this design. Like many of you, I do not have the tools, the expertise, or the time to develop device drivers for even one of the current operating systems, let alone three or four. Fortunately, FTDI supports the FT232 family on recent versions of *Windows*, *Mac OS*, and *Linux* with two different types of drivers. Dynamic Link Library (.dll) drivers provide direct program access to the interface chip and are best suited for use where the USB interface IC is embedded in, and is used to directly control, a device such as a camera or cell phone. Virtual Comm Port (VCP) drivers enable the USB device to be recognized as a standard serial device on the host computer. Because most programs that provide rig control such as Simon Brown’s (HB9DRV) *HRD* and Scott Davis’s (N3FJP) logging programs are written to control the transceiver through a serial port, the Virtual Comm Port (VCP) driver is the appropriate choice for this design. These drivers are available directly from the FTDI Web site, [www.ftdi-chip.com](http://www.ftdi-chip.com).

## Audio Interface

The audio interface is similar to many published designs. Transformers couple the sound card output to the transceiver modulation input and the transceiver detector output to the sound card input.

A couple of improvements were made, however. An attenuator in the sound card output channel presents a typical speaker load to the sound card and reduces the level before it is applied to the transceiver input. This level is appropriate for the modulation input on the

accessory connector of the transceiver. Modulation level adjustment is easier to accomplish if the levels are near optimum to start.

The detector output impedance of the transceivers I researched for this project is approximately 10 k $\Omega$ . Not wanting to load the output excessively with a 600  $\Omega$  transformer primary, I built an emitter-follower stage to drive the isolation transformer. The transceiver provides the operating voltage for this stage through the accessory connector. Typical audio output levels from the transceiver detector output is 100 mV. This is more than adequate to drive the sound card input. On the IC-703, this level is not affected by the transceiver volume control setting.

Any sound card mode is supported, including PSK31, PSK63, RTTY, CW, SSTV, and voice. Potentiometers provide easy adjustment of the transmit and receive signal levels during setup.

## Board Assembly

Assembly is relatively straightforward for an experienced builder. Total assembly time can be as little as four to six hours, but 10 to 12 hours is typical. I highly recommend a lighted magnifier to assist in placing the surface-mount ICs. The leads are closely spaced and solder bridges are easily formed and difficult to locate. The magnifier is invaluable in finding the bridges that do occur. Application of soldering flux using a flux pen minimizes the bridging.

You should also work in a static-grounded workspace. Even in humid climates, most workshops have low enough humidity to generate static charges that could degrade the surface mount ICs.

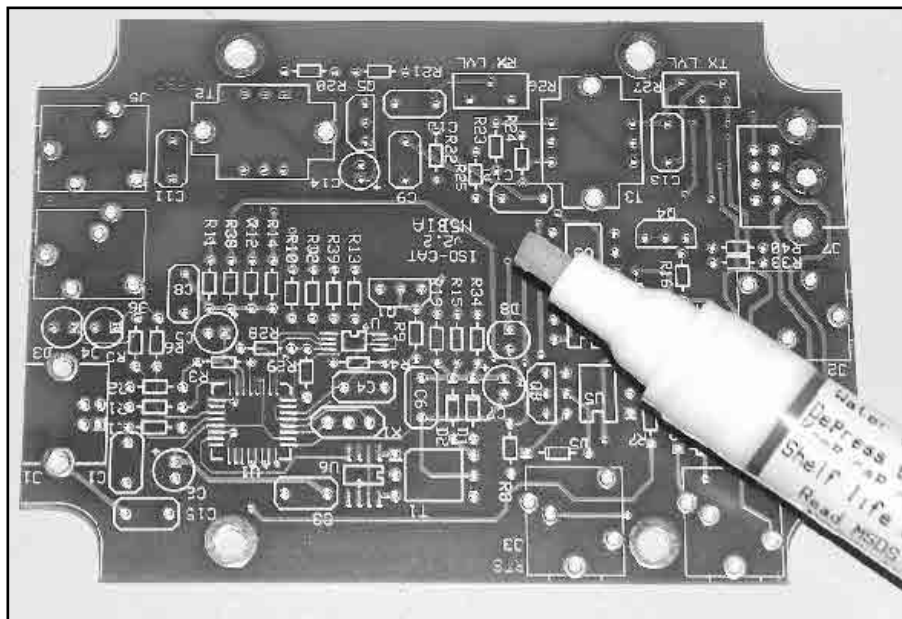


Figure 3 — Apply flux with the flux pen before placing the surface mount ICs on the circuit board.

Working with surface-mount components by hand is tedious and requires a steady hand and concentration. While it would not be practical to place many surface-mount components, two or three are well within the capability of most builders. Just take your time, don't try to rush, and don't decide to do this part of the assembly after a hard day, or late at night.

A few additional tools may be needed, but what ham doesn't enjoy a trip to RadioShack and Sears? You will need a 10 to 15 W soldering iron with a very fine tip. It must be an iron with a three-wire power cord: A static-grounded workspace includes grounded tools. For those fortunate few who have any of several models of Weller or Hakko soldering stations with interchangeable tips and controllable temperature, select a 1/2 inch or finer tip. If your soldering equipment consists of a Weller soldering gun and the 250 W iron that you used to use to solder grounding lugs to the chassis, a trip to RadioShack to pick up a part no. 64-2051 15-W soldering iron is in order. While you are there, pick up a part no. 63-1310 magnifying glass with attached tweezers.

Start with the MAX253. It has the largest solder pads. Start by applying a bit of flux on the contact area. A flux pen makes this an easy operation. Just don't be tempted to use a paste type flux: it will make a big mess and doesn't work well. See Figure 3. Don't be concerned about flux getting between the contacts. Position the IC with pin 1 over the pin 1 mark on the board. Carefully align the remaining pins over the IC footprint. The flux serves as a temporary adhesive during alignment. Check with a magnifying glass, especially if you are over 40!

Solder one of the pins — I like to use a corner pin because they are easiest to reach — then recheck alignment. To do this, heat the exposed area of the contact near the IC pin and touch the junction of the iron and the contact area with the solder. Don't touch the IC because it is very easy to move. Reheat and align as necessary. This is very critical, because misalignment of the pins increases the probability of solder bridges.

Recheck alignment and correct any alignment issues before continuing. When all the pins line up with the footprint, solder the pin on the diagonally opposite corner from the first to hold the IC in position. Recheck the alignment and reheat and adjust as necessary. When the pins are aligned with the pads, solder each pin to the associated pad. See Figure 4. Work quickly, apply solder sparingly, and don't worry too much about shorts at this point. Clean the iron frequently — every two or three joints.

When you have soldered the remaining pins, inspect and clear any shorts before proceeding. This is where the magnifier really pays off. Use solder wick and a light, wiping

touch to clear the shorts as needed. Mount the remaining surface-mount ICs before starting on the through-hole components. I suggest the 93C46 as the next component to install. The pins are the same spacing as the FT232, but here are only eight of them. See Figure 5. Finish up with the FT232, using the same technique. Figure 6 shows all three surface mount ICs soldered in place.

Mount the resistors and diodes next, working out from the center of the board. Next, mount opto-isolators, potentiometers, LEDs, and capacitors. Finish the assembly steps by mounting the connectors and transformers.

The recommended sequence is available in the documentation package available on the ARRL Web site.<sup>2</sup> After all components are soldered in place, clean the flux from the board. Digi-Key and Mouser both list flux removers in their catalog, and if you happen to live near a Fry's, they have an entire display of various electronic cleaners.

### Mechanical Assembly

Begin mechanical assembly by mounting the completed board to the enclosure bottom plate. Use short (1/8 inch) no. 6 machine screws. Use the template to locate the posi-

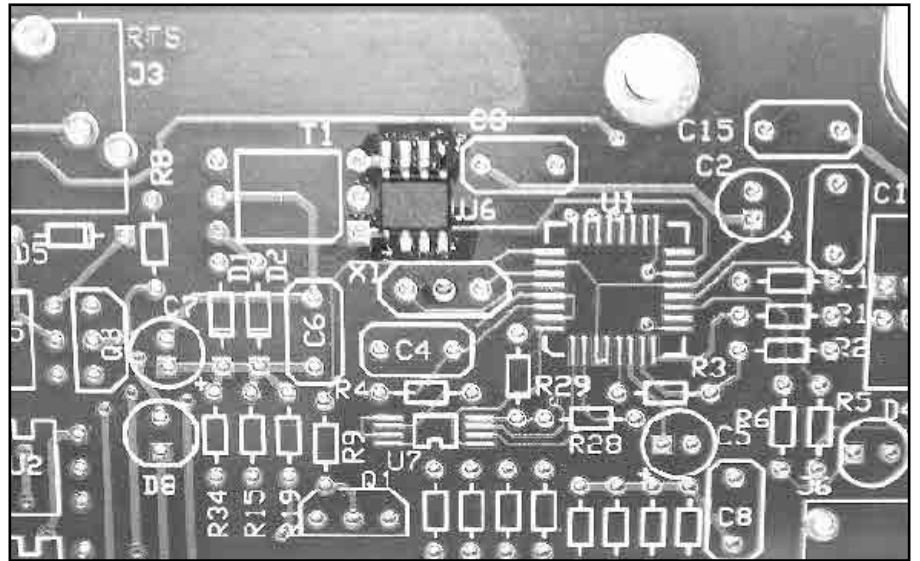


Figure 4 — Place the MAX253 switching power supply IC, U6, on the circuit board first.

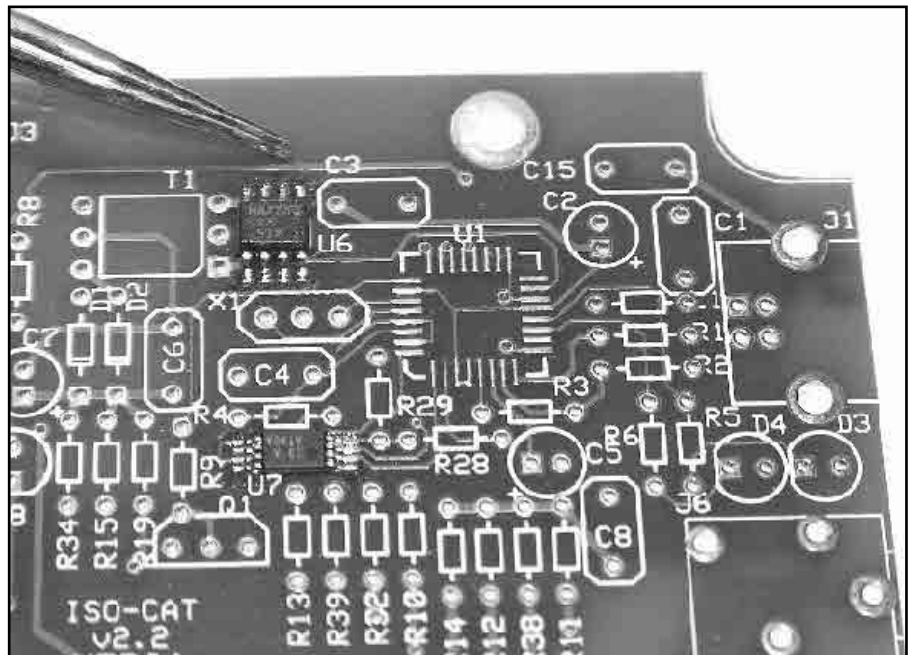


Figure 5 — Mount the 93C46 memory IC, U7, second.

tion of the four holes for the LEDs in the top of the case. Drill these holes, then de-burr all the edges.

Use the templates to mark the locations of the connector openings on each end and on the side of the enclosure. Be sure the connector locations on the enclosure line up with the connectors on the board. Remember the old carpenter's adage: Measure twice, cut once. Using a Dremel tool or an X-Acto saw, cut the sides of the rectangular openings for the connectors. Using an X-Acto knife, carefully score the top portion of the rectangular openings. Bend the tab back and forth to break it off. Smooth the rough edges with a file.

Drill a  $\frac{3}{16}$  inch diameter hole at each phone plug location. Cut the slots from each connector to the edge of the enclosure with a Dremel tool or X-Acto saw. Smooth the edges with a file and test fit the enclosure. Use a file to make any final adjustments to the fit.

Cut out the label and trim it to fit. Partially separate the backing from a sheet of clear laminating film and position the label between the backing and the laminating sheet. Firmly press the backing and the label onto the laminating film. Work out any air bubbles between the label and the film. Trim the film so that a  $\frac{1}{16}$  inch border remains around the label.

Remove the backing material and apply strips of double-sided tape to the back of the label. Be sure the strips do not overlap or come closer than  $\frac{1}{16}$  inch to the edge of the label. Carefully align the label with the enclosure and press it down. Work out any air bubbles. Use a sharp pointed X-Acto blade to trim the LED openings. Test fit the enclosure halves together and trim any obstructions, then set it aside until the testing and alignment is complete. Figure 7 shows the completed top cover and Figure 8 shows the completed IsoCat.

### Testing

I have installed the IsoCat on computers running *Windows 98, 2000, XP and Linux*. I do not have access to a Mac to test those systems. There are drivers available on the FTDI site for all of these operating systems, along

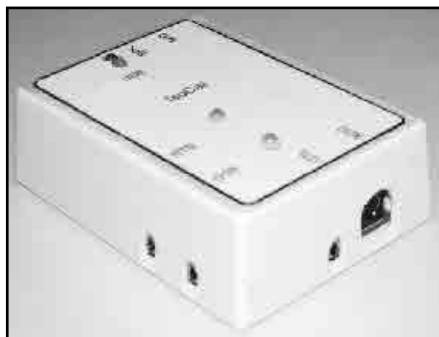


Figure 7 — This photo shows the completed project box, with labels attached.

with instructions for installing on each OS.

The test procedure outlined below is deliberately generic because of the slight differences in each OS and OS version. I am documenting only the PSK31 procedure, but other modes follow similar setup and alignment procedures. The goal is to drive the transmitter with as high a level signal as possible without overdriving it. The same is true of the signal

from the transceiver to the sound card — you want as high a signal level as possible without distortion from the transceiver and without overdriving the sound card input.

### Preparation

Before starting testing, connect the transceiver output to a dummy load and turn the power down. Digital modes place high duty

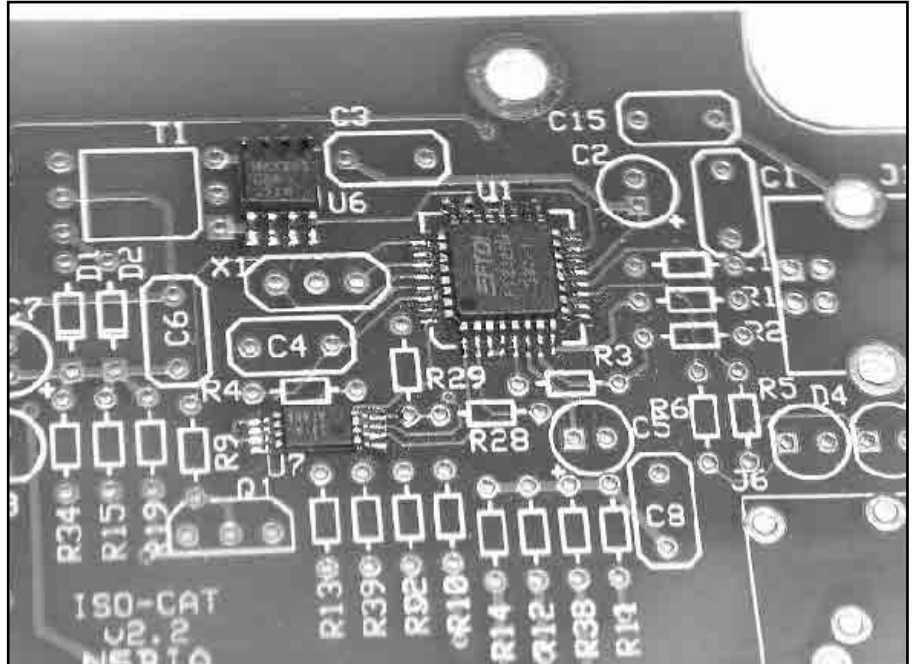


Figure 6 — Complete the surface mount IC installation with U1, the FT232BL USB-serial IC.

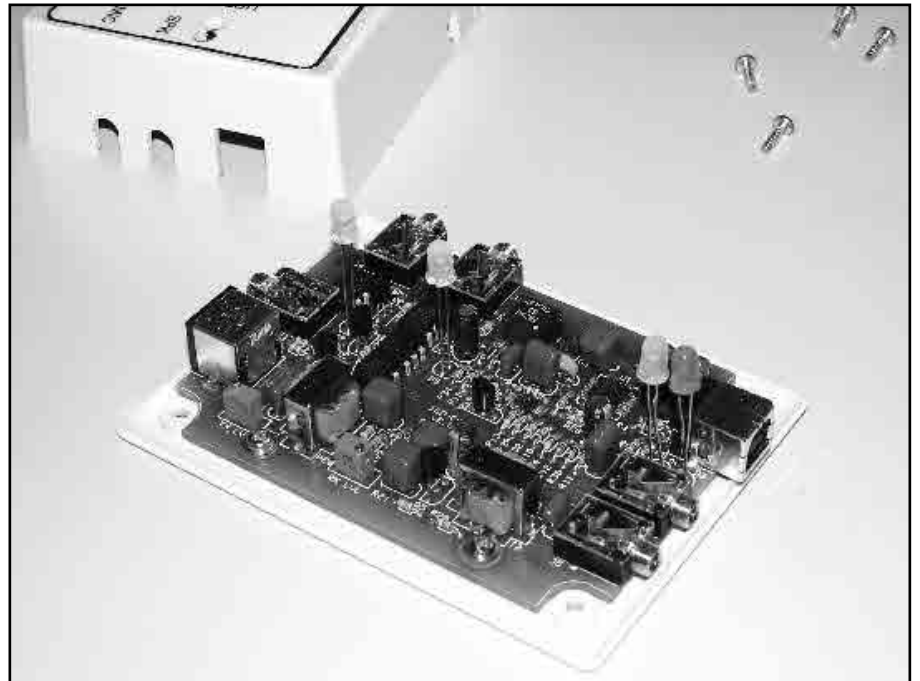


Figure 8 — The completed IsoCat circuit board has been mounted to the project box base.

cycle loads on the transmitter. There is no point stressing the transceiver while testing.

### Transceiver Control

To begin testing, connect the IsoCat to your system and install the appropriate drivers. Do not connect the interface to the transceiver. For *Windows* systems, you should have the VCP driver install package on the hard drive or on a diskette. Be sure you are using the drivers found on the ARRL/qxfiles Web site or included with the kit. (See Notes 1 and 2.)

After the IsoCat is installed, connect the control port on the radio to the control connector. Set the jumper near the output connector to match your transceiver — some expect the control signal on the tip, others expect it on the ring contact. Launch your rig control program and configure appropriately for the transceiver and control port you found previously. Accept the changes and let the program establish a connection with the transceiver. I have used this interface with Scott Davis' (N3FJP) programs, with Simon Brown's (HB9DRV) programs, as well as several free-ware RTTY programs, all with equal success. The only issue that may cause consternation is if there are a large number of serial ports on the station computer. Most programs expect the serial port to be numbered between COM1 and COM8, especially if you are using hardware keying. A possible workaround on Microsoft *Windows XP* systems may be to change the comm port number using the driver properties dialog in the VCP driver. See the FTDI documentation for details.

Verify that the control program responds to changes initiated at the transceiver. Verify that the transceiver reliably switches from receive to transmit and back.

### Sound Card Interface

When the transceiver and computer are communicating reliably, continue with the sound card testing and calibration. Complete the following additional connections:

1. Connect the sound card headphone or speaker output to the modulation input connector on the interface with a 1/8 inch stereo audio cable.
2. Connect the sound card microphone input to the modulation output connector on the interface with a 1/8 inch stereo audio cable.
3. Connect the control signal cable from the interface to the control data input connector on the transceiver with the data cable.
4. Connect the signal connector to the transceiver accessory connector with the accessory cable.

Figure 9 shows the IsoCat connected to the appropriate cables, ready for testing.

### Adjustment

1. Turn the TX level and RX level pots on the circuit board fully counterclockwise.

2. Start the computer.
3. Set the sound card microphone gain and the audio level to about 75% using the control panel.
4. Connect the transceiver to a dummy load.
5. Power up the transceiver. NOTE: During computer startup, be sure the transceiver is off — some operating systems may toggle the control lines, keying the transceiver. This is not good!
6. Launch the digital mode application of choice.
7. Set the transmitter for 50% or less of its rated power output.
8. Initiate a test transmission.
9. Turn the TX level clockwise until the ALC level begins to increase, then counterclockwise until the ALC level is 0.
10. Unkey the transceiver.
11. Connect an antenna to the transceiver. Locate a station that is transmitting a signal using the desired mode.

12. Slowly turn the RX level clockwise until the signal is at about 75% to 80% of maximum. In most cases, this will be optimum and still allow a bit of headroom.

Congratulations, now you are ready for some operating time! As a former teacher was prone to saying, "This I will leave as an exercise for the student." I hope to hear you on the air.

### Cables

Four cables and one adapter are required to connect the IsoCat to the computer and transceiver. Standard lengths (2, 3, 4 or 6 foot) may

be selected to suit your station requirements. I have a couple of sets made up so that I can place the components in optimum locations in a variety of locations and not have to compromise on the cables. The cable set includes:

Standard 1/8 inch stereo audio cables to connect the computer and transceiver audio.

USB type B connector for the interface to computer connection.

Two custom cables are required. Connectors and pinouts are transceiver-dependent.

A miniature DIN connector to transceiver accessory connector.

An adapter cable from the transceiver control port to an 1/8 inch stereo phone plug. On many transceivers, this is simply a 1/8 inch stereo patch cable. Be sure to set the jumper on the IsoCat board for your transceiver. Some transceivers expect the signal on the ring, while most expect it on the tip.

### Conclusion

This is an interesting and educational project. It opens the door to experimenting with sound card modes, such as PACTOR, TTY, Hellschreiber, and SSTV. It is also useful for recording QSOs to your computer and recording voice contest exchanges. I have spent many enjoyable hours building and operating with this interface.

### Notes

<sup>1</sup>The author is offering two kits: A bare-bones kit consisting of the circuit board with surface mount components down and all remaining components to build the board is \$70. The builder provides all cables and enclosure;

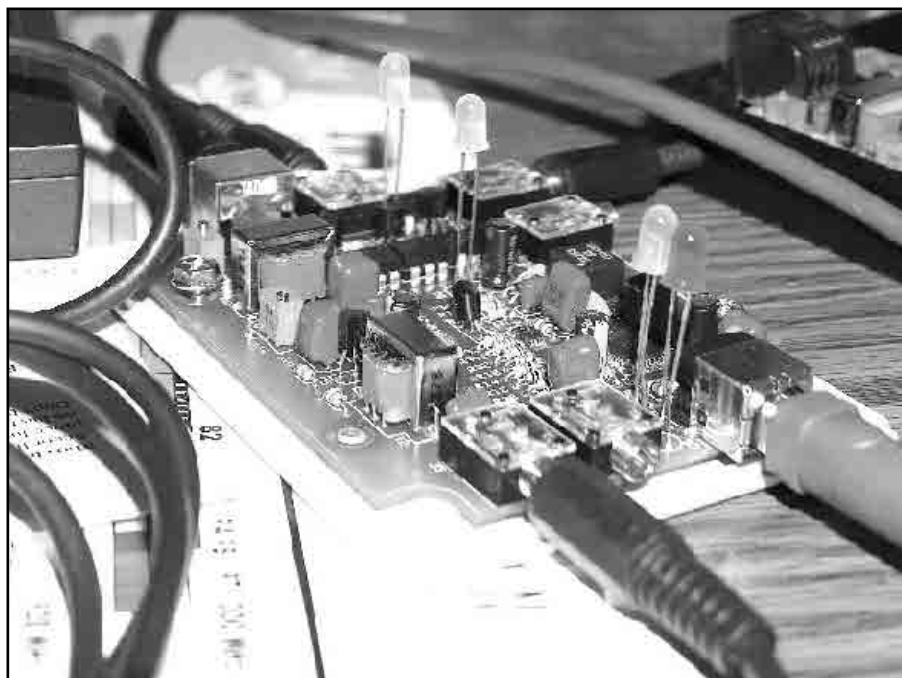


Figure 9 — Final testing and adjustment is completed by connecting the appropriate cables to the transceiver and computer.



A deluxe kit for \$80 consisting of the bare bones kit plus three 1/8 inch cables, one USB cable, the enclosure, and connectors and cable to build the accessory-connector-to-interface cable. He will also sell just the bare board for \$10. For those who want instant gratification, completed units are \$95. They are supplied with all cables and the printed guide. Shipping is estimated at under \$10 via USPS to any US location. There are additional support files and documentation on the author's Web site, [n5bia.com/isocat](http://n5bia.com/isocat).

<sup>2</sup>Additional information is available on the QEX Web site. Go to [www.arrl.org/qexfiles](http://www.arrl.org/qexfiles) and look for the file **3x07\_Buoy.zip**.

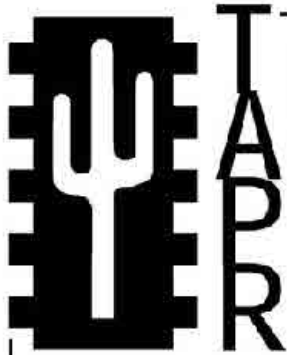
*Bill Buoy, N5BIA was first licensed as a Technician Plus in 1979. Bill upgraded to General in 1983 at the FCC offices in Houston, Texas, and passed his Extra class exam on the first try at HamCom in Arlington, Texas in 2003. At his home in Houston, he operates an IC-7000 and an IC-703 with wire antennas strung in his back yard.*

*Besides the weak-signal sound card digital modes, Bill is working to increase his CW speed. He is also learning Linux, because he believes it is a viable option for low cost, reliable, and versatile Amateur*

*Radio computer support.*

*A member of Northwest Amateur Radio Society (NARS), Bill maintains the club Web site, [www.w5nc.org](http://www.w5nc.org) and the Texas QSO Party Web site, [www.txqp.org](http://www.txqp.org) in addition to his own Web site, [www.n5bia.com](http://www.n5bia.com). Bill is also a private pilot and plans to earn his instrument rating this year.*

*Bill worked as an electronic engineer for over 15 years in the oil patch service industry. He is currently a technical writer working for a subcontractor to a large computer manufacturer in Houston.*



**Join the effort in developing Spread Spectrum Communications for the amateur radio service. Join TAPR and become part of the largest packet radio group in the world. TAPR is a non-profit amateur radio organization that develops new communications technology, provides useful/affordable kits, and promotes the advancement of the amateur art through publications, meetings, and standards. Membership includes a subscription to the *TAPR Packet Status Register* quarterly newsletter, which provides up-to-date news and user/technical information. Annual membership \$20 worldwide.**



**TAPR CD-ROM**

Over 600 Megs of Data in ISO 9660 format. TAPR Software Library: 40 megs of software on BBSs, Satellites, Switches, TNCs, Terminals, TCP/IP, and more! 150Megs of APRS Software and Maps. RealAudio Files. Quicktime Movies. Mail Archives from TAPR's SIGs, and much, much more!

**Wireless Digital Communications: Design and Theory**

Finally a book covering a broad spectrum of wireless digital subjects in one place, written by Tom McDermott, N5EG. Topics include: DSP-based modem filters, forward-error-correcting codes, carrier transmission types, data codes, data slicers, clock recovery, matched filters, carrier recovery, propagation channel models, and much more! Includes a disk!



**Tucson Amateur Packet Radio**

8987-309 E Tanque Verde Rd #337 • Tucson, Arizona • 85749-9399  
 Office: (972) 671-8277 • Fax (972) 671-8716 • Internet: [tapr@tapr.org](mailto:tapr@tapr.org) [www.tapr.org](http://www.tapr.org)  
 Non-Profit Research and Development Corporation

# In Search of New Receiver-Performance Paradigms, Part 3

*We've had a critical look at areas of receiver performance that need testing. To conclude the series, here's more about related instrumentation, procedures and reporting formats.*

**Doug Smith, KF6DX**

**In** the first two parts of this article series, I wrote about the limitations of receiver performance that need testing.<sup>1, 2</sup> Now let's get to the nitty-gritty

<sup>1</sup>Notes appear on page 34.

225 Main St  
Newington, CT 06111-1494  
kf6dx@arrl.org

by examining test instrumentation and procedures. I suggest — and in some cases, insist on — changes to currently accepted procedures. Other procedures are routinely performed by receiver manufacturers but not by independent test labs. Still others aren't getting enough attention from any quarter.

## Summary of Extended Test Battery

Table 1 shows what I propose in this

series. Each entry is a measurement of a specific receiver trait, an associated unit of measure, what the measurement indicates and some notes about how to do the testing.

I call for certain instrumental and procedural changes. They are intended to ensure that every measurement measures what it's supposed to measure, exclusive of other effects.

**Table 1**  
**Critical Receiver Test Outline**

<i>Parameter</i>	<i>Unit of Measure</i>	<i>Indication</i>	<i>Notes</i>
Noise figure	dB	SNR degradation by receiver	Bandwidth-independent
Noise floor	dBm/Hz	Normalized receiver noise	Needed for DR calculations
Bandwidth 1	Hz	Passband width and shape	Ripple included
Bandwidth 2	Hz	Stopband shape, shape factor	Include equiv. square BW
Birdies	Hz & dBm	Equivalent signal strength	Freqs. of offenders found
Signal leakage	dBm	Conducted to antenna	FCC, CE limits, labels
Radiated emiss.	μV/m	Signal strength of radiation	FCC, CE limits, labels
Conducted emiss.	μV	Power-line induced	FCC, CE limits, labels
Control sys. 1	subjective	Does what it says it will do	Doesn't misbehave or crash
Control sys. 2	various	Notch depth, response time, etc	Manual and automatic cntrl's
Control sys. 3	subjective	Control placement, ergonomics	Menu systems incl.
Documentation	subjective	Slope of learning curve	Schematics, circuit. descr. incl?
Reliability	MTBF in hours	How long between failures	From manufacturer
Serviceability	MTTR in hours	How long to repair	From manufacturer
Warranty	months	What's covered, limitations	From manufacturer
EMI/RFI	V/m, A/m	Susceptibility to external fields	DC to daylight
Vibration	5 G	FM under vibe	50-15,000 Hz shake test
Shock	50 G	No damage as shipped	Drop test
Temperature	various	Freq. stability, display, other	Over range of manuf'r specs
Waterproofing	check for leaks	Chk. for bubbles, int. air press.	Manufacturer does this?
Power supply	V, Hz	Op. over voltage, freq. range	50, 60 Hz under, over-volt'g
RF harm. dist.	dB	2 <sup>nd</sup> & 3 <sup>rd</sup> harm. rejection at RF	For every octave of RX cov'g
IMD3DR	dB	IMD3DR at fixed QRM levels	Use at least 3 ref. levels
IMD2DR	dB	IMD2DR at fixed QRM levels	Use at least 3 ref. levels
IP3E	dBm	IP3 equiv. at fixed QRM levels	Use at least 3 ref. levels
IP2E	dBm	IP2 equiv. at fixed QRM levels	Use at least 3 ref. levels
½IF, IF, image	dB	Rejection in dB	Standard
Other spurious	dB	Rejection in dB	Predict and search for them
PNDR	dB	Phase-noise dynamic range	Existing blocking DR test
AGC times	ms	Attack, decay, hold	Over & undershoot, pumping
Audio quality	THD %, IMD levels	In-band distortion, AGC slow	Both acoustic and electrical

## Instrumentational and Procedural Changes

Based on results to date, certain changes in measurement methods and their instrumentation are mandated to accompany updated procedures for use by both manufacturers and independent test labs. They are described below.

While I acknowledge that more than one way to measure any particular receiver trait may exist, manufacturers and independent testers ideally would agree on common procedures. In fact, experience in manufacturing is largely what should drive a desire for uniformity. Measurements must be repeatable within known margins of uncertainty.

### Noise Figure, Noise Floor Power

Noise figure is bandwidth independent but noise-floor power is not. Since we want to measure passband shape anyway, one way to go is to integrate that shape to find its equivalent rectangular bandwidth, then simply measure the noise power. It's not enough to simply measure the  $-6$ -dB points and assume that all's square. Passband ripple, stopband attenuation and shape factor all come into play.

As an example, refer to the rugged filter shape of Figure 1. Its nominal bandwidth is 500 Hz. We can compute its equivalent rectangular bandwidth using Simpson's Rule.<sup>3</sup> (Rectangular means a filter with zero ripple and a shape factor of unity.) We break the filter shape into 50-Hz segments and measure the response at the center point of each segment. An integration measures the area under the filter response curve in units of amplitude  $\times$  frequency. Since the individual segments are added, we cannot express amplitude in dB; we must use linear units expressed in terms of a fraction of  $A$ , the nominal 0-dB passband level. The selection of where  $A$  lies is arbitrary, so we take it to be the passband response peak.

Perform integration by Simpson's rule as a sum of discrete terms:

$$A' = 50 \sum_{k=-\frac{N}{2}}^{\frac{N}{2}} 10^{\frac{p_k}{10}} \quad (\text{Eq 1})$$

where  $N$ , an even natural number, is the number of segments taken and  $p_k$  is the  $k^{\text{th}}$  segment measurement in dB.  $A'$  is the equivalent rectangular bandwidth in Hz. Obviously,  $N$  must be large enough to encompass the filter stopband response to at least 60 dB below  $A$ .

Our sample filter has a nominal bandwidth of 500 Hz and its  $-6$  dB points are that far apart. Its passband ripple is 3 dB but its equivalent rectangular bandwidth is barely 280 Hz. Increasing the number of segments  $N$  would give a more accurate answer, but you get the idea. An error of almost 3 dB would have been introduced in noise-floor power and dynamic-

range calculations had we not measured the equivalent rectangular bandwidth.

For the example, we can compute a normalized noise-floor power density in dBm/Hz by measuring the total noise-floor power and subtracting  $10 \log(280 \text{ Hz})$ . If the total noise power measured were  $-128$  dBm, then the average noise-floor power density would be  $-128 - 10 \log(280) \approx -152.5$  dBm/Hz. By comparison with the theoretical noise-floor limit of  $-174$  dBm/Hz at room temperature, we'd conclude that the receiver's noise figure (NF) is  $-152.5 - (-174) \text{ dBm} = 21.5$  dB (plus or minus measurement uncertainties). NF is a commonly accepted, bandwidth-independent figure of merit for receivers. Let's start using it.

### Birdies

Predict and search for birdies over the entire operating range. For all birdies found, record the order of the birdie and its signal-to-noise ratio. Computer control of receivers and test equipment make exhaustive searches practical.

### Unwanted Emissions

Search for and measure signal leakage to the antenna using a spectrum analyzer. Examine units for CE and FCC compliance by checking for proper labeling.

### Control System, Documentation

Adopt systematic procedures to test control systems to see that they do what they claim to do. Report anomalies and crashes.

Try to "break" things. Subjectively evaluate manuals and other documentation for correctness and completeness.

### Reliability, Serviceability, Warranty

I suggest we measure and report these things but we must at least solicit information about them from manufacturers. Anything less is neglectful. Having completed nondestructive testing of a receiver, should we go out of our way to try to break the unit? The answer is yes, but only to a reasonable extent.

Obviously, some of the tests previously described may be destructive and must come last in the test battery. Those include:

- A search for fatal "bugs" in the control system;
- Shock, vibration and temperature testing ("shake and bake");
- Overvoltage and reverse-polarity testing at the power supply, and
- RF reverse-power, electromagnetic-pulse (lightning) and general electrical safety testing.

Some basic measurements must be repeated after those possibly destructive tests to evaluate survival. Although I haven't mentioned the last item in the list before in this article series, it deserves a few words here.

Sometimes destructive testing is unintentional. I recall shipping a transceiver to a customer who, as it turns out, intended to write a review of it in a major magazine. During the normal course of letting several users play with the unit, someone (who shall be forever anonymous) inadvertently pumped 1500 W

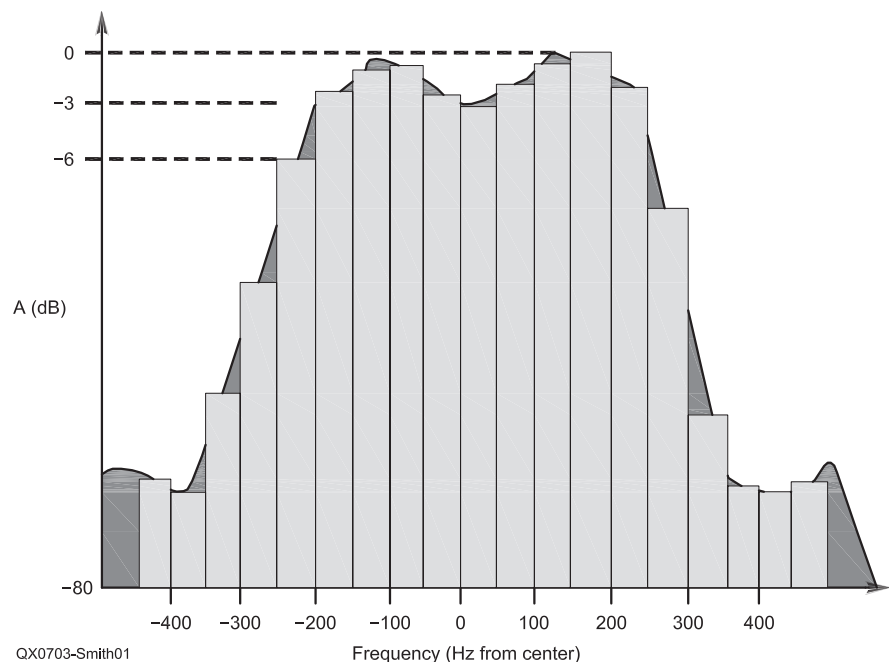


Figure 1 — A rough-as-guts bandpass filter showing Simpson's-Rule integration parameters.

into the antenna port of the receiver. When the customer returned the unit to our lab for repairs, we discovered a very charred RF input/output module (the circuit board had burned), a destroyed first mixer and a lot of soot around the insides of the enclosure. We replaced the burnt module and first mixer, cleaned the enclosure as best we could, retested everything and had the transceiver on a UPS truck back to the customer within 48 hours. The report of that incident in the formal review was a testament both to the reviewer's honesty and to the manufacturer's service department.<sup>4</sup>

The point is that destructive testing can be a good opportunity to evaluate the time and cost of repair. In this era of modular design, some repairs might be possible in the field by users; others might require a return to the factory or to an authorized service center. At initial contact, good service representatives try to evaluate the problem and discover if a return can be avoided. If so, they may issue instructions and even authorize shipment of replacement parts to the customer. All that takes time, especially with customers who aren't so technically oriented. Service representatives are trying to minimize time and cost. Still, they know that their treatment of the customer reflects on the company's reputation. Taking extra time on the telephone and in written correspondence are almost always an advantage.

Electrical safety is of great concern to equipment manufacturers. Product liability lawsuits are their bane. Users must be well-informed about the proper installation, operation and maintenance of electrical equipment. Absent a user's negligence, situations still arise in which it's difficult to determine the proximate cause of damage or injury. Antenna manufacturers have known about that from the dawn of radio time because too many of their products have contacted electrical power-distribution lines, with devastating results. The same has been true for makers of antenna towers, high-voltage amplifiers, power supplies and so forth.

A receiver is a relatively benign thing from that standpoint but lightning and ac power are still threats to life and property. Let's say a receiver is connected to its antenna during a local thunderstorm (it shouldn't be!) and suffers a nearby, but indirect, lightning event. Sensitivity degrades considerably and the unit must be returned for factory service. To make his disposition, the service representative depends on the customer's honest answer about whether lightning was in the area around the time of failure and on the service technician's findings of component failure or failures. It's not always easy to determine circumstances after the fact, but sometimes it is.

Two outstanding examples are permanently engraved in my mind. The first involved one gentleman who didn't understand

that his radio was dc-powered. He wired its +13.8 V dc cable to a 120 V ac plug and —*pow!* That rig wasn't a total loss but before it was returned to him, you can be sure the correct power plug for his installation had been fitted (normally it wouldn't be) and he was charged for everything.

In another case, a family's steel-hulled yacht went for a day cruise with its new HF rig and 23-foot vertical antenna aboard. The antenna had been installed by some brave lad atop the boat's 75-foot mainmast. What the crew didn't know was that overhanging 25-kV power lines lay dead ahead only 89 feet above the harbor channel — *kablooey!* Although service personnel definitively determined what components needed to be replaced to return to specifications, we declared the rig a total loss because we strongly suspected that other components had been "winged" (small but significant changes in sensitivity, power output and other areas).

#### **EMI/RFI**

A 100-W audio amplifier coupled to a suitable solenoid or transformer is the way we test for mains-frequency EM susceptibility. Magnetic field strength, in A/m, can readily be calibrated. At power-line frequencies, a PM detector should be used to quantify effects.

I think we know how to blast receivers with RF fields (!) and that's a normal part of CE testing. It should be a regular part of every manufacturers' and independent labs' testing, too.

#### **Vibration and Shock**

A PM detector should be used to detect any frequency instability during vibration testing. An acceleration of 5 G over the audio frequency range is sufficient.

We should also look for mechanical resonances that could ultimately cause failures or annoyance. During a frequency sweep, such resonances are normally obvious because the unit under test makes a big racket.

Do a drop test if the shipping company hasn't already done one for you. Examine and report manufacturers' packing methods. Query them about their experiences and report what they'll allow.

Simple drop tests using low-cost, resettable, calibrated sensors are practical. A controlled vibration test is a little tougher since ideally, it should be conducted over a range of frequencies at a constant G level. The idea is to find frequencies at which a receiver is particularly susceptible to vibration resonances. A high-Q resonance in a receiver multiplies physical displacement of resonant parts by the quality factor or Q.

Acceleration (G force) during sinusoidal vibration is directly proportional to the squares of both frequency and displacement. Appendix A derives those relationships,

which dictate that during a constant-G, swept-frequency vibration test, displacement be reduced inversely to frequency as frequency is increased. Such a vibration table is beyond the means of many receiver manufacturers, but competent test laboratories have them and generally make them available for a fee. A crude approximation to the test can be made with an electric motor rotating an eccentric cam, coupled to a flat surface by way of a flexible rubber damper. Frequency can be varied by changing the power to the motor.

A constant acceleration of 5 G RMS and a frequency range of 50-5000 Hz are good test levels. Note that peak-to-peak displacement at 5 G and 50 Hz is almost two inches!

#### **Temperature**

Thorough temperature testing should be done on all units selected for extended tests, whether they are intended for mobile use or not. cursory temperature tests should be done on all units. In emergency situations, we often rely on receivers to perform in temperature extremes. With so much emphasis placed on the phrase, "When all else fails..." we should be stressing this aspect of reliability. Frequency stability, noise figure and other critical parameters deserve checking over a manufacturer's declared temperature range.

Even lacking a calibrated temperature chamber, it wouldn't be hard to pop a receiver in the freezer or in the oven for a while until the desired test temperature were reached. Users want to know what happens to their rigs on cold mornings and in direct sunshine on hot desert days. Frequency stability is the main concern, but general functionality should be explored with particular attention paid to physical controls and displays.

#### **Waterproofing**

Nondestructive water testing is done by applying greater than atmospheric pressure to the interior of a receiver via some kind of opening to the interior of the unit. The unit is submerged to the specified depth in water and the engineer looks for air bubbles emanating from the unit. Typically, designers include a threaded hole for that purpose. The hole is plugged with a screw and rubber O-ring after the test. Lack of such a facility on a receiver (we're mainly talking about handhelds and scanners) indicates that positive testing hasn't been done. Check for it.

#### **Power Supply**

Units should be checked for both under-voltage and overvoltage operation. Supply voltage, whether it be ac or dc, should be lowered until the unit stops functioning and that voltage level reported. Supply voltage should be increased above the nominal to the manufacturer's specified limit or by 15%, whichever is greater. In addition, reverse-



polarity protection must be assessed.

AC-powered units need a 50-Hz test. A 50-Hz sinusoidal source may either be bought, built or rented for the purpose. Some manufacturers let their overseas distributors do this testing for them.

Overvoltage and reverse-polarity testing ought to be among the last tests performed because they might be destructive. Many well-designed rigs employ a “crowbar” circuit that permanently shorts the power supply input to ground when an overvoltage or reverse-polarity situation is encountered.

### **RF Harmonic Distortion**

Measure and report second- and third-harmonic rejection levels on all bands, especially harmonics of AM broadcast-band signals. With a reference at the noise floor, the measurements could be called harmonic dynamic ranges.

### **Linearity Measurements**

One very important thing here is to get away from using analog meters to measure output responses of receivers. Use an audio spectrum analyzer instead. No measurement in this category ever need be declared noise-limited because that just says that the measurement didn't measure what it was supposed to measure. In combination with phase-noise dynamic range (PNDR), we can still get the whole picture. The change goes for IMD DR, notch-depth measurements and so forth.

An audio spectrum analyzer allows an engineer to measure the level of a discrete IMD product regardless of the noise level. A voltmeter cannot do that.

Another necessary change is to measure the various dynamic ranges of a receiver under realistic conditions. By that I mean that receiver noise figure has to be monitored during dynamic range testing to detect any changes in the presence of strong, off-channel signals. Two-tone IMD tests therefore become three-tone tests.

The traditional two-tone test procedure measures the noise floor under pristine, single-signal conditions. As demonstrated in Part 2, however, front-end and digital AGC systems can and do degrade a receiver's noise performance when strong adjacent-channel signals are present. The three-tone setup simply adds another input generator to the mix and solves the problem.

In the revised IMD procedure, one generator inputs an on-channel signal at some reference power. Three reference levels were suggested in Part 2. (See Note 2.) The other two generators input the interfering tones. Their frequencies are selected for the proper spacing and to place the in-band IMD product adjacent to the on-channel signal being monitored. The on-channel signal is checked while increasing the level of the interference

until the IMD product is equal in amplitude to the on-channel signal as seen on the spectrum analyzer. IMD DR and IPE (intercept point equivalent) are then computed.

That step is where bandwidth dependence can be eliminated. For example, IMD3DR is expressed as the ratio of the equal power of each of two off-channel tones input to a receiver to the IMD3 product they produce at the noise-floor power. Normalizing the noise-floor power to a 1-Hz bandwidth leads to an IMD3DRE expressed in dB/Hz and an IP3E in dBm. In Part 2, I described how to measure, compute and report the equivalent rectangular bandwidth of odd passband shapes.

Such expressions might seem strange at first, but they're not nearly as strange as trying to compute IMD3DRs and IP3s at disparate or unknown bandwidths and reference levels. To summarize: IMD3DR should be declared with respect to the reference level and so should IP3E. If IMD3 is measured at a reference level of 50  $\mu$ V (S-9), then declare the S-9 IMD3DR and S-9 IP3E. If you aren't concerned with anything below S-9, just call it what it is. We've seen that receivers don't necessarily allow extrapolation of IP3 measurements made at high reference levels to the noise-floor power.

The new procedure and reporting format eliminate bandwidth dependency by accounting for passband and stopband shapes. Yes, it's a bit of extra work; but in this case, it's worth the effort.

The combiners used in linearity testing are crucial to good results. Poor isolation between signal generators often causes IMD to appear in the output stages of the generators themselves. That's especially true during attempts to measure increasingly higher IMD-DRs these days. I therefore offer Appendix B, which describes a combiner/splitter topology that makes it possible to achieve high broadband port-to-port isolation through enhanced passive signal cancellation.

### **Phase-Noise Dynamic Range (PNDR)**

Existing blocking dynamic range (BDR) measurements measure phase noise in a receiver because in virtually all modern, robust designs, phase noise takes over before saturation of any stage can occur. It's a good test to retain because although phase noise ought to be the same in a transceiver's receiver as in its transmitter, the transmitter might include AM noise that doesn't appear in the receiver. Let's call it what it is: PNDR.

A swept measurement over a large range of offsets is necessary. A low-noise crystal oscillator, or a heavily frequency-divided signal source, must be used as the interfering signal.<sup>5</sup> Depending on architecture, tuning a receiver over the range of offsets may or may not reveal the true PNDR curve. Some receivers have two or more synthesizers that move

in piecemeal fashion during tuning. That may force the use of a tunable interference source. Phase noise in receivers is getting so low these days that it can be difficult to find an interference source that's 10 dB better than the receiver, but it can and must be done.

### **Automatic Gain Control (AGC)**

Since a differential AGC system similar to that described in Part 2 is likely operating in most DSP-based receivers, there's a danger of AGC pumping from large, off-channel transient signals. Large amounts of digital gain compensation degrade SNRs in receivers. The dynamic responses of *all* AGC systems should be checked. Measure and report attack, decay and hold times and overshoot.

IF-DSP receivers have the option of putting notch filters, noise reduction and other subsystems inside the AGC loop so that the S meter shows their effects. When the results of such signal processing aren't reflected on the S meter, you really don't have IF-DSP but AF-DSP. That difference is important to many users and should be ascertained during tests, and reported.

### **Audio Quality**

In keeping with the idea of measuring both electrical and acoustic performance, two sets of measurements are necessary here. One is conducted by direct electrical connection to headphone, external-speaker and auxiliary-audio output jacks of a receiver; the other is performed by closely coupling a microphone to the internal loudspeaker. The former method is well-understood; the latter has not seen much use outside of audiophile circles.

We must dispense with certain qualitative evaluations of a receiver's sound, which commonly include vague terms like thin, warm, full and tinny. Audio output power and frequency response measurements should indicate what's put into the air, not just into the loudspeaker terminals. The scientific way to go about acoustic measurements is to measure sound pressure level or SPL. A calibrated, low-distortion microphone is what's needed. Let's face it: You can design a receiver with very low total harmonic distortion (THD), but its loudspeaker is going to add significantly to that unless it's a rather expensive type. Efficiencies of small loudspeakers can be quite low.

The highest wavelength audible to human beings is about 2 cm. Therefore, the test microphone should be placed within about 10 wavelengths — 20 cm — of the unit under test. It should be pointed straight at the loudspeaker and have a unidirectional pattern so as not to pick up room echoes. Along with measurement of THD, IMD and frequency response, we should be looking for resonances of the receiver enclosure that create buzzing noises and the like. SPL should be the criterion in determining output power. It's easy enough

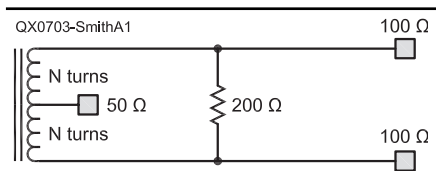


Figure A1 — The Magic T.

to hook the microphone to an audio spectrum analyzer to see everything that needs seeing.

### Reporting the Data

Report numerical data with only as many significant figures as the margin of uncertainty supports. Compute and declare margins of uncertainty using standard statistical methods.<sup>6</sup> Correct previously published data when errors are found in them.

To neglect those rules, as so many testers have done and still do, is actually a disservice to readers. Inform your favorite reviewers and manufacturers that you want the additional data, measured and presented in the scientific way.

### Conclusion

To conclude, let me restate my main premises:

- The main goal of receiver testing is to discover a unit's limitations.
- Tests must convey everything that matters to a user or potential buyer.
- Tests must measure the parameter of interest to the exclusion of other effects.
- Test data must allow useful comparisons among units.
- Instrumentation must be traceable to standards of known precision.
- Procedures must allow others to precisely reproduce tests.
- Margins of uncertainty must be declared for all measurements.
- In no way should a test procedure affect the definition of what is measured.
- Previously published data need to be corrected when errors are discovered.

Okay, we won't be *Consumer Reports* but I find that in almost every category, we're not making the best grade in Amateur Radio from a scientific standpoint. That's not to state that I haven't made some of the mistakes I've illustrated — I have. But I will correct them and I won't make them again. I hope you don't, either.

### Acknowledgements

Thanks to L.B. Cebik, W4RNL, for editing this manuscript. For fruitful discussions and extraordinary work, I also thank Leif Åsbrink, SM5BSZ, Jack Burchfield, K4JU, Cornell Drentea, KW7CD, Ed Hare, W1RF1, Ulrich Rohde, N1UL, H. Paul Shuch, N6TX, Joe Taylor, K1JT, and Mike Tracy, KC1SX, for invaluable discussions and support.

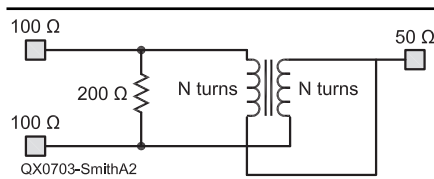


Figure A2 — Alternate representation of the Magic T.

### Appendix A: Vibration and Shock Calculations

During uniform harmonic vibration, displacement,  $p$ , is sinusoidal:

$$p = A \sin(2\pi ft) \quad (\text{Eq A1})$$

where  $A$  is peak displacement in meters,  $f$  is frequency in hertz, and  $t$  is time in seconds. Velocity,  $v$ , is the first derivative of displacement with respect to time:

$$v = \frac{dp}{dt} = 2\pi fA \cos(2\pi ft) \quad (\text{Eq A2})$$

where  $v$  is in m/s.

Acceleration,  $a$ , in  $\text{m/s}^2$  is the first derivative of velocity with respect to time and the second derivative of displacement:

$$a = \frac{dv}{dt} = \frac{d^2p}{dt^2} = -(2\pi f)^2 A \sin(2\pi ft) \quad (\text{Eq A3})$$

G force may be obtained by dividing  $a$  by the acceleration due to gravitation, about  $10 \text{ m/s}^2$ . Maximum G force occurs at peak instantaneous displacement, but at zero instantaneous velocity, as the shake table is changing direction.

During a drop (shock) test, assume linear deceleration and estimate a velocity at impact and a time between initial impact and zero velocity. Deceleration is again computed as  $dv/dt$  — in this case, as the slope of the line of velocity versus time:

$$a = \frac{dv}{dt} \quad (\text{Eq A4})$$

Mass is not a factor in the equation.

The energy of impact in a shock test may be computed as the force applied to an object times the distance over which it was applied. In linear deceleration, the distance is simply  $vt/2$ . The force is  $F = ma$ , so the energy is  $W = Fvt = m(v/t)(vt/2) = mv^2/2$ , or exactly the device's kinetic energy before impact. Note that time is not a factor. The energy is the same no matter the time taken, but G forces are time-dependent — the longer the deceleration time, the softer the impact. Where does the energy go?

In fact, all of an object's kinetic energy is transferred to the thing it hits in a non-elastic impact in a vacuum. But, we can expect both the object and the thing it hits to exhibit some elasticity, so maybe the object bounces a couple of times and the impact certainly produces

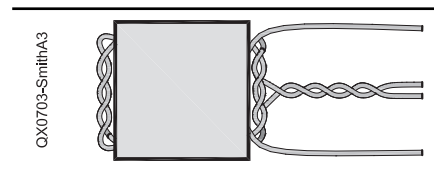


Figure A3 — Physical construction.

a sound in air. It may not be an enjoyable sequence for radio designers to experience, but some of us have wanted to pitch a radio over the eaves from time to time!

### Appendix B: A High-Isolation Hybrid Combiner/Splitter<sup>7</sup>

A typical hybrid combiner/splitter has four ports. Whether splitting or combining, the goal is to provide isolation between two of the ports and little isolation between those two ports and at least one of the other ports.

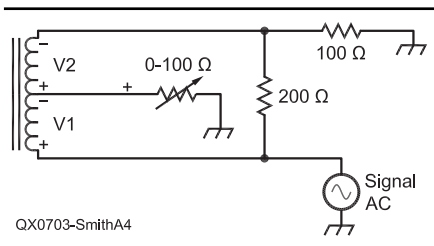
Begin with a basic  $0^\circ$  combiner/splitter — the so-called "Magic T." Refer to Figure A1. The Magic T is a very simple thing.<sup>8</sup> It may be just a center-tapped winding on a binocular bead. Designing the split winding as a transmission line enhances performance. See Figure A2. Physical construction is illustrated in Figure A3. Because it has only three ports, it's really a sort of half-hybrid or half-bridge circuit. It provides reasonable port-to-port isolation when termination resistances are close to optimal. When the common port is terminated in  $50 \Omega$ , the ideal termination resistance for each of the two mutually isolated ports is  $100 \Omega$ . The ballast resistor is  $200 \Omega$ .

To use the Magic T as a splitter, drive the common port and get two in-phase signals at the mutually isolated ports. Input power is split equally, yielding a minimum 3-dB loss between the input port and each output port. As a combiner, apply two signals to the isolated ports and obtain a two-tone at the common port. Loss is again at least 3 dB for each signal through the combiner. Figure A4 reveals that the flux induced in the core material (if any) is theoretically zero when the two signals being combined are equal in amplitude and phase *and* when all termination impedances are ideal.

Details of how the Magic T achieves its isolation deserve explanation here, since they expose the key to the improved isolation of my final circuit. When everything is perfect, isolation is theoretically infinite; but what happens when things are imperfect? Moreover, what's the relative phase of the signal appearing at one isolated port when the other is driven in combiner operation?

### How It Works

Refer to Figure A4. In it, the Magic T is a three-port network and the common port is terminated with a  $100 \Omega$  variable resistor.



QX0703-SmithA4

Figure A4 — Magic-T voltage diagram.

Assume that the source impedances of the generator and the termination at the other port are exactly  $100 + j0 \Omega$ . When the variable resistor is exactly  $50 \Omega$  and the transformer is ideal, isolation is perfect.

In the figure, voltage  $V1$  induced onto the bottom side of the winding is equal to voltage  $V2$  across the top side of the winding. Polarities of those voltages are indicated by the plus and minus signs. It's not easy to see at first, but analysis shows that the voltage across the variable resistor (set to  $50 \Omega$ ) is half the generator's output voltage. The power appearing there is one half of the input power because of the impedance transformation. Because the  $200 \Omega$  resistor is connected across both windings, it's effectively transformed to  $50 \Omega$  on both halves of the winding. The voltage across the variable resistor is therefore equal to  $V1$  and in phase with the generator. The voltage at the undriven port is zero because the voltage contribution caused by the  $200 \Omega$  resistor (in-phase) precisely cancels voltage  $V2$  (out of phase).

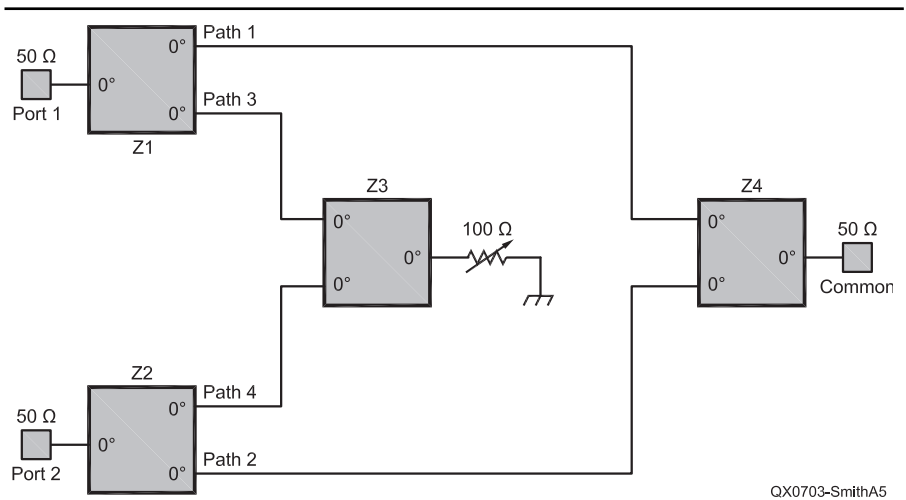
The  $200 \Omega$  resistor dissipates half the power and the variable resistor dissipates the other half. Power in the variable resistor is  $V1^2/50$  and power in the  $200 \Omega$  resistor is the same:  $(2V1)^2/200$ .

Now consider what happens when the variable resistor is set to less than  $50 \Omega$ . Voltage  $V1$  is still equal to voltage  $V2$ , but the voltage across the variable resistor is less than that. Voltage  $V2$  dominates at the undriven port over the contribution from the  $200 \Omega$  resistor. The voltage at the undriven port is nonzero and  $180^\circ$  out of phase with respect to the generator. I haven't solved for that voltage in terms of the variable resistor, but I suppose it would be easy enough to do.

Finally, adjust the variable resistor to some value greater than  $50 \Omega$ . Again,  $V1 = V2$ , but the voltage across the variable resistor is higher than that. Voltage  $V2$  is less than the contribution from the  $200 \Omega$  resistor and the voltage at the undriven port is nonzero and in phase with the generator. Those properties of the Magic T lead directly to my idea.

### Improving Port Isolation

The port-to-port isolation of the Magic T is theoretically infinite when everything is perfect; but leakage inductance, inter-winding



QX0703-SmithA5

Figure A5 — Block diagram of hybrid combiner-splitter.

capacitance, imperfect terminations and other effects tend to diminish it. Broadband values of 30 to 40 dB are typical. Armed with four Magic Ts, however, we can do a lot better.

While my hybrid works just as well as a splitter, I'll use terms relating to combiner operation to explain it. Refer to Figure A5. Each isolated port signal (Port 1 or Port 2) is split using a Magic T. Those Ts are labeled Z1 and Z2. A pair of outputs from Z1 and Z2 is combined in Z4, another Magic T. The other pair of outputs is combined in Z3. All hybrids are identical except for the variable resistor on Z3. Imagine that the termination at the final output of Z4 and the source impedances at Ports 1 and 2 are exactly  $50 + j0 \Omega$ .

As you read this, remember that isolation between Port 1 and Port 2 is what matters. Here's what happens in the circuit. A signal applied at Port 1 appears at the outputs of Z1. One of the outputs of Z1 goes through Z4 to the final Common output port along Path 1. That signal has passed through two Magic Ts, incurring a 6-dB attenuation. The other Z1 output goes along Path 3, through Z3 to the variable resistor.

Because of imperfect isolation, a small amount of the signal on Path 1 leaks across Z4 to Path 2. As demonstrated, the leaked signal may have phase  $0^\circ$  or  $180^\circ$  with respect to the generator, depending on the load. The leaked signal appears at a port of Z2 and propagates to Port 2 through that T with an additional loss of 3 dB. At the same time, a small amount of the signal on Path 3 leaks across Z3 to Path 4, where it appears at a port of Z2 and propagates to Port 2 with an additional 3-dB loss.

The Path 4 leaked signal may have phase  $0^\circ$  or  $180^\circ$  with respect to the leaked signal on Path 2. Its amplitude and phase may be adjusted using the  $100 \Omega$  variable resistor until the leaked Path 2 and Path 4 signals cancel

at Port 2. Note that Z2 acts as a combiner for those two signals.

Of course, Z2 also acts as a splitter for signals applied to Port 2, and a similar thing to what I described above occurs in the other direction toward Port 1. Thus, isolation between Port 1 and Port 2 may be greatly improved over what a single Magic T would achieve alone.

### Empirical Results

With careful construction and shielding, I built some of these units that exhibit 90 dB or more of isolation. Transmission-line techniques are necessary in the windings to obtain good broadband performance, but the ability to adjust the variable resistor on Z3 tends to compensate for imperfections there. I believe the optimal line impedance would be about  $70 \Omega$  for  $50\text{-}\Omega$  systems.<sup>9</sup>

Even with relatively few turns, the transformer tends to be overcompensated as frequency is increased. I used seven twists per inch of 24 AWG enamel wire as a good approximation to  $70\text{-}\Omega$  transmission line. Mini-Circuits ADTL-4-75 units may be used.<sup>10</sup>

I obtained isolation of  $>>60$  dB over several octaves in the HF range. Adjusting the variable resistor made the isolation "sweet spot" go up and down the spectrum. With fingernail-sized binocular beads (Fair-Rite 43 or 61 material) and two turns, units showed 40 to 50 dB isolation even at 300 MHz. The lower frequency limit with Fair-Rite 43 material is about 2 MHz. Matching of the hybrids among the four units seems critical for best results. Each must resemble the other as closely as possible. Fixed resistors used in the hybrids were 1%, 1206-type surface-mount components.

Test equipment available to me lacked sufficient third-order IMD dynamic range to accurately measure third-order input IP3, but I found a lower limit of  $+60$  dBm  $\pm 2$  dBm. That was a surprising result given

the small size of the beads. Since I also could not measure the units' second-order distortion, I established a lower limit for IP2 of +90 dBm  $\pm$  5 dBm. I measured insertion loss of 6.5 dB  $\pm$  1 dB over the range 2 to 300 MHz.

When reaching for 90-dB isolation numbers, shielding and other construction details are critical. My unit was constructed on regular fiberglass circuit board, 0.062 inch thick, using microstrip lines where appropriate.

#### Future Possibilities

Note that in splitter operation when the input signals have identical amplitude and phase, no flux is produced in the ferrite cores. When combining signals at different frequencies and amplitudes, though, core flux is not zero and IMD effects should become evident. I'm tempted to postulate that some cancellation of even those effects is occurring but further analysis would be required before I'd put my neck out.

With some additional work, the technique

would be applicable to microwave frequencies using microstrip or stripline layouts. It could also be expanded to accommodate more than two mutually isolated ports or to increase isolation even further, but the growth of complexity and insertion loss seems to limit those possibilities. This type of combiner/splitter is now a standard part of ARRL IMD procedures.

#### Notes

- <sup>1</sup>D. Smith, KF6DX, "In Search of New Receiver Performance Paradigms, Part 1," *QEX*, Nov/Dec 2006, pp 23-30.
- <sup>2</sup>D. Smith, "In Search of New Receiver Performance Paradigms, Part 2," *QEX*, Jan/Feb 2007, pp 23-30.
- <sup>3</sup>G. Thomas, Jr and R. Finney, *Calculus and Analytic Geometry*, 1992, Addison-Wesley, ISBN: 0-20152-929-7.
- <sup>4</sup>L. Wolfgang, WR1B, "Product Review," *QST*, May 1998, pp 63-69.
- <sup>5</sup>B. Pontius, N0ADL, "Measurement of Signal-Source Phase Noise with Low-Cost Equip-

ment," *QEX*, May/June 1998, pp 38-49; also see D. Stockton, GM4GNX, "Chapter 10 — Oscillators and Synthesizers," *ARRL Handbook*, 2007, ISBN: 0-87259-976-0; J. van der List, PA0JOZ, "Experiments with Phase-Noise Measurement," *QEX*, Jan/Feb 1999, pp 31-41; K. Karlsen, LA2NI, "A Method of Measuring Phase Noise in Oscillators," *QEX*, Nov/Dec 2004, pp 55-61.

- <sup>6</sup>D. Smith, "Tech Notes — Quantifying Measurement Uncertainty," *QEX*, Jan/Feb 2006, pp 54-56.
- <sup>7</sup>D. Smith, "A High-Isolation Hybrid Combiner/Splitter," *Proceedings of the Southeastern VHF Society*, April 2006, ARRL, ISBN 0-87259-967-1. This is an improvement on the discovery I made several years ago.
- <sup>8</sup>A good description of Magic T operation written by Mike Ellis may be found on the Web at [members.tripod.com/michaelgellis/magict.html](http://members.tripod.com/michaelgellis/magict.html).
- <sup>9</sup>H. Granberg, "Broadband Transformers and Power Combining Techniques for RF," *Motorola AN749*, Rev. 1993.
- <sup>10</sup>Visit [www.minicircuits.com/dg03-240.pdf](http://www.minicircuits.com/dg03-240.pdf).

Doug Smith, KF6DX, has edited *QEX* since 1998.



**We Design And Manufacture To Meet Your Requirements**

\*Prototype or Production Quantities

**800-522-2253**

**This Number May Not Save Your Life...**

But it could make it a lot easier! Especially when it comes to ordering non-standard connectors.

#### RF/MICROWAVE CONNECTORS, CABLES AND ASSEMBLIES

- Specials our specialty. Virtually any SMA, N, TNC, HN, LC, RP, BNC, SMB, or SMC delivered in 2-4 weeks.
- Cross reference library to all major manufacturers.
- Experts in supplying "hard to get" RF connectors.
- Our adapters can satisfy virtually any combination of requirements between series.
- Extensive inventory of passive RF/Microwave components including attenuators, terminations and dividers.
- No minimum order.



NEMAL ELECTRONICS INTERNATIONAL, INC.  
12240 N.E. 14TH AVENUE  
NORTH MIAMI, FL 33161  
TEL: 305-899-0900 • FAX: 305-895-8178  
E-MAIL: [INFO@NEMAL.COM](mailto:INFO@NEMAL.COM)  
BRASIL: (011) 5535-2368

URL: [WWW.NEMAL.COM](http://WWW.NEMAL.COM)

## NEW! from Klingenfuss Radio Monitoring and available from ARRL

### 2007 Super Frequency List on CD-ROM

More than 39,000 entries cover all broadcast and utility stations on shortwave—from 0 to 30 MHz! Hundreds of fascinating new digital data decoder screenshots!

ARRL Order No. 1002 — **ONLY \$34.95\***

\*shipping \$6 US (ground)/\$11 International

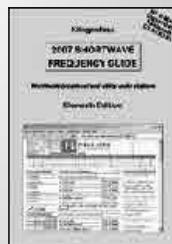


### 2007 Shortwave Frequency Guide—Eleventh Edition

Clearly arranged frequency and schedule tables for worldwide broadcast and utility radio stations.

ARRL Order No. 1014 — **ONLY \$44.95\***

\*shipping \$10 US (ground)/\$15 International

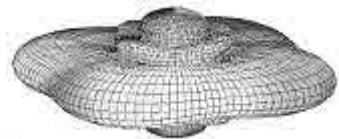


**ARRL** The national association for AMATEUR RADIO

SHOP DIRECT or call for a dealer near you.  
ONLINE [WWW.ARRL.ORG/SHOP](http://WWW.ARRL.ORG/SHOP)  
ORDER TOLL-FREE 888/277-5289 (US)

QEX 3/2007

A picture is worth a thousand words...



With the

## ANTENNA MODEL™

wire antenna analysis program for Windows you get true 3D far field patterns that are far more informative than conventional 2D patterns or wire-frame pseudo-3D patterns.

Describe the antenna to the program in an easy-to-use spreadsheet-style format, and then with one mouse-click the program shows you the antenna pattern, front/back ratio, front/rear ratio, input impedance, efficiency, SWR, and more.

An optional **Symbols** window with formula evaluation capability can do your computations for you. A **Match Wizard** designs Gamma, T, or Hairpin matches for Yagi antennas. A **Clamp Wizard** calculates the equivalent diameter of Yagi element clamps. **Yagi Optimization** finds Yagi dimensions that satisfy performance objectives you specify. Major antenna properties can be graphed as a function of frequency.

There is **no built-in segment limit**. Your models can be as large and complicated as your system permits.

**ANTENNA MODEL** is only \$90US. This includes a Web site download and a permanent backup copy on CD-ROM. Visit our Web site for more information about **ANTENNA MODEL**.

Teri Software  
P.O. Box 277  
Lincoln, TX 78948

[www.antennamodel.com](http://www.antennamodel.com)

e-mail [sales@antennamodel.com](mailto:sales@antennamodel.com)  
phone 979-542-7952

# On the Crossed Field Antenna Performance, Part 2

*In Part 2 of this article, the authors analyze a variety of factors affecting the performance of a crossed-field antenna.*

**Valentino Trainotti, Senior Member, IEEE, and Luis A. Dorado, Student Member, IEEE**

TABLE I  
CFA DIMENSIONS IN METERS.

Monopole 1 height	$H_1$	10
Barrel diameter	$D_1$	3.0
Monopole 1 top-load length	$L_1$	0.0
Barrel base height	$\delta_1$	1.5
Monopole 1 wire radius	$a_1$	$6 \cdot 10^{-3}$
Monopole 2 (disk) height	$H_2$	1.0
Disk radius (monopole 2 top-load length)	$L_2$	2.5
Disk hole radius	$r_h$	0.05
Monopole 2 wire radius	$a_2$	$6 \cdot 10^{-3}$
Artificial ground plane radius	$R_0$	5.0

TABLE II  
CFA EQUIVALENT NETWORK MATRIX.

METHOD	$Z_{11}$	$Z_{12}$	$Z_{22}$
TLM	$2.18 - j410$	$0.11 - j124$	$0.09 - j856$
MoM	$2.13 - j430$	$0.20 - j117$	$0.13 - j844$

## VII. EXAMPLES

Having the available theory expressed previously, the Crossed Field Antenna analysis can be made by means of numerical examples.

---

University of Buenos Aires,  
Argentina  
[vtrainotti@ieee.org](mailto:vtrainotti@ieee.org)  
[luis\\_dorado@ieee.org](mailto:luis_dorado@ieee.org)

### A. CFA Operating Windows

As a first example, a CFA model is analyzed at the frequency of 1 MHz, with the antenna dimensions indicated in Table I and over average soil ( $\sigma = 10^{-2} \text{ S/m}$ ,  $\epsilon_r = 10$ ).

The CFA equivalent network impedance matrix can be calculated using the Transmission Line Method (TLM) and by means of the Method of Moments (MoM) [33] (wire grid model [25]). Both methods produce practically the same result, as can be seen in Table II for 1 MHz and average ground.

In this example, monopole 1 is a barrel build up by twenty four copper wires ( $\sigma_c = 5.8 \cdot 10^7 \text{ S/m}$ ) of radius  $a_1$ , as shown in Fig. 4. Barrel diameter,  $D_1$ , wire radius,  $a_1$ , and barrel base height,  $\delta_1$ , are taken into account in the calculation of the monopole 1 equivalent transmission line average characteristic impedance  $Z_{0m1}$  [1].

As a first analysis, input impedances of both antenna ports are calculated as functions of voltage phase difference  $\phi_2$  for  $K = 1$  and over average ground, and can be seen in Figs. 11 and 12.

In Fig. 11, negative input resistances  $R_1$  and  $R_2$  can be seen for some ranges of  $\phi_2$ , while in Fig. 12 the input reactances  $X_1$  and  $X_2$  are always negative. There exist two small windows, difficult to appreciate in Fig. 11, where both input resistances are positive, permitting the antenna operation. One window is located in the neighborhood of  $\phi_2 = 180^\circ$  and the other near  $\phi_2 = 360^\circ$ .

Input impedances are shown in both windows in Tables III and IV. It is interesting to see that the input reactances are practically constant in both windows, where the antenna can operate.



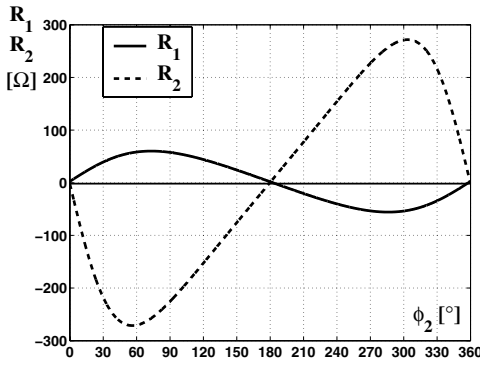


Fig. 11. CFA input resistances  $R_1$  and  $R_2$  as functions of  $\phi_2$  for  $K = 1$  and over average ground.

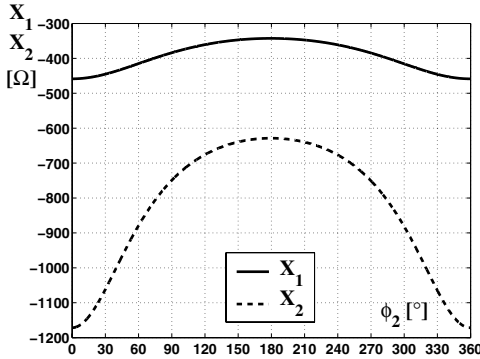


Fig. 12. CFA input reactances  $X_1$  and  $X_2$  as functions of  $\phi_2$  for  $K = 1$  and over average ground.

TABLE III

CFA INPUT IMPEDANCES IN 180°-WINDOW.

$\phi_2$	$R_1$	$X_1$	$R_2$	$X_2$
deg	$\Omega$	$\Omega$	$\Omega$	$\Omega$
179.4	2.30	-343	-0.71	-629
179.8	2.00	-343	0.31	-629
180.2	1.70	-343	1.32	-629
180.6	1.39	-343	2.34	-629
181.0	1.09	-343	3.36	-629
181.4	0.79	-343	4.37	-629
181.8	0.49	-343	5.39	-629
182.2	0.19	-343	6.41	-629
182.6	-0.12	-343	7.42	-629

TABLE IV

CFA INPUT IMPEDANCES IN 360°-WINDOW.

$\phi_2$	$R_1$	$X_1$	$R_2$	$X_2$
deg	$\Omega$	$\Omega$	$\Omega$	$\Omega$
358.0	-0.12	-459	15.7	-1171
358.2	0.15	-459	14.0	-1171
358.4	0.42	-459	12.2	-1171
358.6	0.69	-459	10.4	-1172
358.8	0.96	-459	8.67	-1172
359.0	1.23	-459	6.90	-1172
359.2	1.50	-459	5.14	-1172
359.4	1.77	-459	3.37	-1172
359.6	2.04	-459	1.61	-1172
359.8	2.31	-459	-0.16	-1172

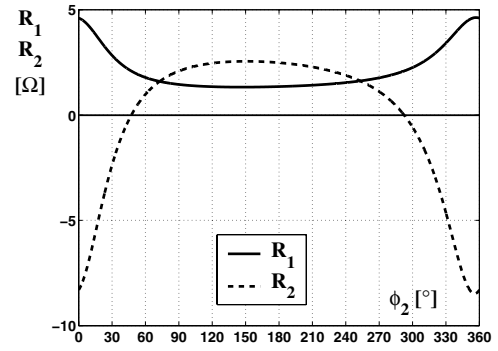


Fig. 13. Tuned CFA input resistances  $R_1$  and  $R_2$  as functions of  $\phi_2$  for  $K = 1$ . The 180°-window can clearly be seen where  $R_1$  and  $R_2$  are positive.

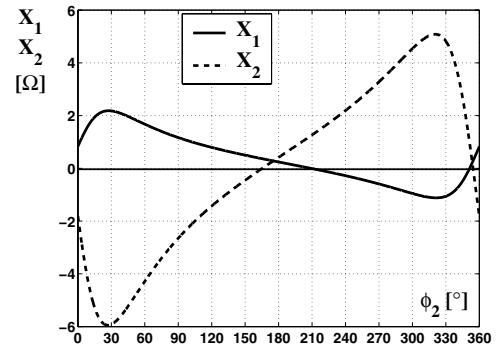


Fig. 14. Tuned CFA input reactances  $X_1$  and  $X_2$  as functions of  $\phi_2$  for  $K = 1$  and in the 180°-window.

In order to tune the antenna, opposite reactances are connected in series to both ports. If the 180°-window is chosen, the reactance to be connected in series with port 1 is  $X_{L1} = 343$  and with port 2 is  $X_{L2} = 629$ . Under this condition, the input resistances and reactances of both ports are shown in Figs. 13 and 14, where they have a very small variation as functions of  $\phi_2$ , also the input impedances of both ports are practically real close to  $\phi_2 = 180^\circ$ . In this example, only the antenna losses are taken into account and the tuning coils are supposed to be of infinite merit factor  $Q_L = Q_{L1} = Q_{L2}$ , permitting to know the antenna operation without any other effect.

In the 180°-window, when the generators have the same voltage amplitude ( $K = 1$ ), the antenna is operational because the input powers on both ports are positive for  $\phi_2$  between 50° and 290°, where both input resistances are positive. In this case, the equivalent network mutual conductance is negative,  $G_{12} = -0.253$  S, and the antenna operates as in Fig. 7.

If the 360°-window is chosen, the reactance to be connected in series with port 1 is  $X_{L1} = 459$  and with port 2 is  $X_{L2} = 1172$ . Under this condition, the input resistances and reactances of both ports are shown in Figs. 15 and 16, where they also have a very small variation as functions of  $\phi_2$ . The input impedances of both ports are practically real for  $\phi_2$  between 0° and 100° and between 240° and 360°. In this case, the antenna is operational too, because the input powers in both ports are positive. Also, because the equivalent network mutual conductance is positive,  $G_{12} = 0.165$  S, the

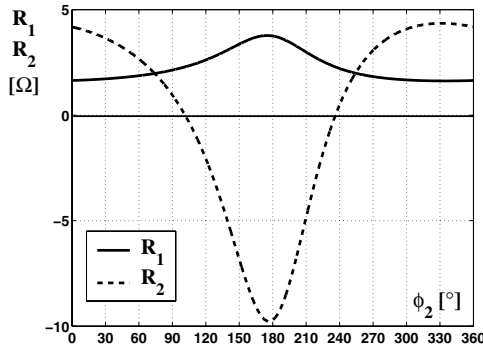


Fig. 15. Tuned CFA input resistances  $R_1$  and  $R_2$  as functions of  $\phi_2$  for  $K = 1$ . The  $360^\circ$ -window can clearly be seen where  $R_1$  and  $R_2$  are positive.

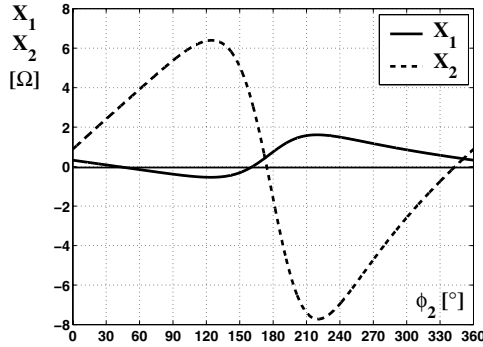


Fig. 16. Tuned CFA input reactances  $X_1$  and  $X_2$  as functions of  $\phi_2$  for  $K = 1$  and in the  $360^\circ$ -window.

antenna operates as in Fig. 6.

From this analysis, the range of the voltage phase difference  $\phi_2$  was obtained under antenna resonance condition, when the input impedances of both ports are practically real or resistive.

The  $\phi_2$  value of interest in these ranges or windows is that which permits to have the input powers,  $W_1$  and  $W_2$ , under control, with a given relationship  $K_w = W_2/W_1$ .

In some cases, it is possible to find values of  $K$ ,  $\phi_2$  and  $V_1$ , which permit to get a given total input power,  $W_{in} = W_1 + W_2$ , and a given power ratio  $K_w = W_2/W_1$ , under the conditions  $W_1 > 0$  and  $W_2 > 0$ . In other words, generator voltages  $V_1$  and  $V_2$  can be adjusted to give a specified total input power and power ratio, but this is not always possible. In Appendix B, it is found that if  $\phi_2$  is written as a function of  $K$ , and  $K$  satisfies a certain condition, then a solution is possible.

### B. CFA Performance

Knowing the CFA operation in both windows, input impedances, near field, wave impedance, radiation resistance, efficiency, gain and far field strength at 1 km for 1 kW input power can be calculated.

In Tables V and VI, the results of the CFA  $180^\circ$  and  $360^\circ$ -windows can be seen.

A monopole with the same height ( $H_1/\lambda = 0.0333$ ), taken as reference, has a radiation resistance  $R_{rad} = 0.71 \Omega$ , a gain  $G = -0.12$  dBi and the corresponding field strength at 1 km for 1 kW of input power is  $E = 171$  V/m. The CFA has

TABLE V  
CFA PERFORMANCE IN  $180^\circ$ -WINDOW.

K	$\phi_2$	$R_1$	$X_1$	$R_2$	$X_2$	$R_{rad}$
—	deg	$\Omega$	$\Omega$	$\Omega$	$\Omega$	$\Omega$
1.6	130.6	1.04	0.68	3.47	-1.08	0.59
1.7	155.3	1.04	0.42	3.50	-0.22	0.59
1.8	174.4	1.04	0.24	3.52	0.40	0.59
1.9	191.9	1.04	0.07	3.54	0.95	0.60
2.0	209.6	1.05	-0.10	3.55	1.53	0.60
2.1	230.3	1.05	-0.32	3.58	2.28	0.60

K	$V_1$	$ V_2 $	$ I_1 $	$ I_2 $	G	E
—	V	V	A	A	dBi	mV/m
1.6	27.3	43.6	21.9	12.0	-0.69	160
1.7	24.7	41.9	21.9	12.0	-0.69	160
1.8	23.4	42.2	21.9	11.9	-0.69	160
1.9	22.9	43.5	21.9	11.9	-0.68	160
2.0	23.0	45.9	21.9	11.9	-0.68	160
2.1	23.9	50.2	21.9	11.8	-0.68	160

TABLE VI  
CFA PERFORMANCE IN  $360^\circ$ -WINDOW.

K	$\phi_2$	$R_1$	$X_1$	$R_2$	$X_2$	$R_{rad}$
—	deg	$\Omega$	$\Omega$	$\Omega$	$\Omega$	$\Omega$
2.2	310.1	1.14	0.77	7.57	-1.96	0.79
2.4	341.3	1.14	0.42	7.46	0.37	0.79
2.6	4.873	1.14	0.18	7.39	1.96	0.80
2.8	27.48	1.14	-0.06	7.32	3.50	0.80
3.0	54.52	1.14	-0.38	7.22	5.51	0.80

K	$V_1$	$ V_2 $	$ I_1 $	$ I_2 $	G	E
—	V	V	A	A	dBi	mV/m
2.2	28.9	63.5	20.9	8.13	0.18	177
2.4	25.5	61.1	20.9	8.19	0.19	177
2.6	24.2	62.9	20.9	8.23	0.19	177
2.8	23.9	67.0	20.9	8.27	0.19	177
3.0	25.2	75.6	20.9	8.32	0.19	177

the same 1 kW input power with 500 W applied to each port ( $K_w = 1$  and  $W_1 = W_2 = 500$  W).

From the two CFA operating windows, in Tables V and VI, a small loss (0.57 dB) and a small gain (0.31 dB) can be seen with respect to the gain of the reference monopole.

The CFA and reference monopole VSWR have been calculated for average ground at the center frequency of 1 MHz, for a metallic ground plane 5 m in radius, for  $K = 1.8$  and  $\phi_2 = 174.4^\circ$  ( $180^\circ$ -window) in Fig. 17 and for  $K = 2.4$  and  $\phi_2 = 341.3^\circ$  ( $360^\circ$ -window) in Fig. 18. The VSWR sharp behavior is due to a very low antenna height in both cases ( $H_1/\lambda = 0.0333$ ).

At the center frequency of 1 MHz, the input power in each port is exactly 500 W, then the total input power is 1 kW. As frequency is increased or decreased, the input powers in both ports are not exactly equal and this difference is higher at the minimum and maximum frequencies of the useful bandwidth.

It can be noticed from these calculations that the CFA bandwidth is a little bit better in the  $180^\circ$ -window, but the

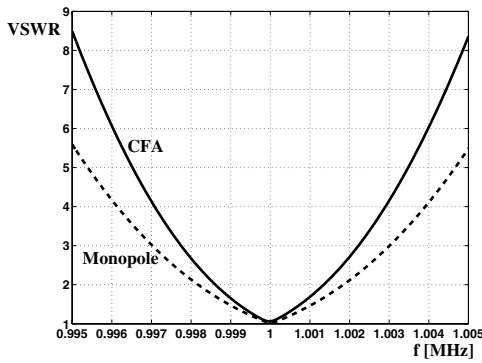


Fig. 17. CFA and monopole VSWR as a function of frequency for  $K = 1.8$  and  $\phi_2 = 174.4^\circ$ .

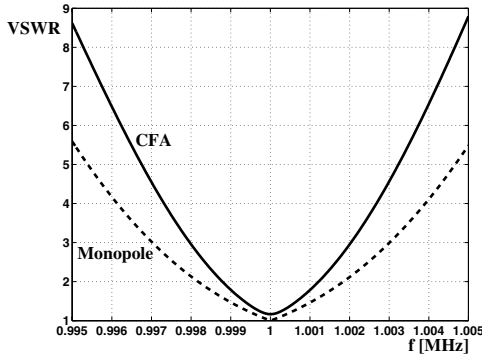


Fig. 18. CFA and monopole VSWR as a function of frequency for  $K = 2.4$  and  $\phi_2 = 341.3^\circ$ .

antenna gain is a little bit lower. This difference is theoretically noticeable but it is not really significant from the engineering point of view. Furthermore, a monopole of the same height has a similar gain and more bandwidth as calculations indicate, but it is more convenient in practice due to an easier system to be tuned.

### C. Tuning Coil Losses

Tuning coil losses are included for several merit factors  $Q_L = Q_{L1} = Q_{L2}$ , in order to know their effects on the antenna performance. These losses are also included in the reference monopole of height  $H_1/\lambda = 0.0333$ .

In Table VII, the effect of the tuning coil merit factor  $Q_L$  is clearly seen in the monopole behavior when it is placed on an average ground. Antenna bandwidth has been calculated for  $VSWR = 2$  and electric field strength at 1 km corresponds to an input power of 1 kW.

The same effect is seen in Tables VIII and IX for the CFA when it is operating in the  $180^\circ$ - and  $360^\circ$ -windows.

When losses are increased, a corresponding increase in the antenna bandwidth is clearly obtained. Nevertheless, a decrease in gain occurs for the monopole and CFA in both windows.

### D. Near Field

With the tuning coil losses taken into account, for a merit factor  $Q_L = 200$ , near electric and magnetic fields have been

TABLE VII  
SHORT MONOPOLE TUNING COIL EFFECT.

$Q_L$	$\pm\Delta f$	$\eta$	G	E	E
—	kHz	—	dBi	mV/m	dB $\mu$ V/m
$\infty$	1.8	0.32	-0.12	171	104.65
400	2.7	0.22	-1.80	141	102.98
200	3.5	0.17	-3.00	123	101.77
100	5.2	0.11	-4.71	101	100.06
50	8.7	0.07	-6.90	78.3	97.88

TABLE VIII  
 $180^\circ$ -WINDOW CFA TUNING COIL EFFECT.

$Q_L$	$\pm\Delta f$	$\eta$	G	E	E
—	kHz	—	dBi	mV/m	dB $\mu$ V/m
$\infty$	1.4	0.28	-0.69	160	104.09
400	2.2	0.17	-2.82	125	101.95
200	3.1	0.13	-4.24	106	100.53
100	4.8	0.08	-6.18	85.1	98.59
50	8.2	0.05	-8.54	64.8	96.24

calculated for both windows and, specifically, for  $K = 1.8$  and  $\phi_2 = 174.4^\circ$  (Table V) and for  $K = 2.4$  and  $\phi_2 = 341.3^\circ$  (Table VI). In Fig. 19, the near electric field for the CFA and the reference monopole over average ground can be seen as a function of distance, for an input power of 1 kW.

The ratio between the near electric and magnetic fields is the wave impedance  $Z_0$  as a function of distance  $\rho/\lambda$  and it can be seen in Fig. 20. This wave impedance is practically the same for both CFA windows, so only one curve for magnitude and one for phase are presented in Fig. 20.

In Table X, wave impedances are calculated for the CFA and a reference monopole of the same height ( $H_1/\lambda = 0.0333$ ), at a frequency of 1 MHz and over average ground. The Moment Method solution is very close to the values given here.

**It can be noticed that the CFA wave impedance is very close to that of the reference monopole. Furthermore, no Poynting Vector Synthesis (PVS) [34] can be seen, because the wave impedance is reactive close to the antenna and real at distances greater than half-wavelength ( $Z_0 \cong 377$ ). Therefore, the CFA behaves like any short monopole, because a reactive near field zone exists close to the antenna structure and the radiated field starts at a distance near to half-wavelength.**

TABLE IX  
 $360^\circ$ -WINDOW CFA TUNING COIL EFFECT.

$Q_L$	$\pm\Delta f$	$\eta$	G	E	E
—	kHz	—	dBi	mV/m	dB $\mu$ V/m
$\infty$	1.2	0.35	0.19	177	104.96
400	2.1	0.20	-2.11	136	102.66
200	2.9	0.15	-3.61	114	101.16
100	4.7	0.09	-5.59	91.0	99.18
50	8.1	0.05	-7.98	69.1	96.79

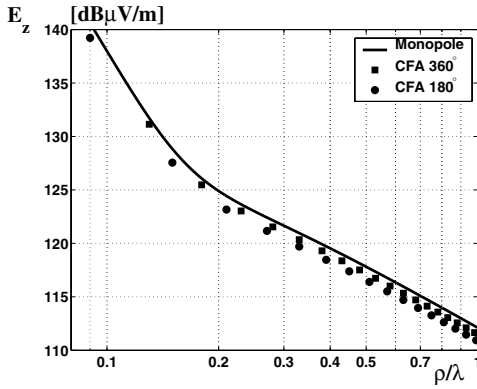


Fig. 19. CFA near electric field  $E_z$  as a function of distance  $\rho/\lambda$  at 1 MHz for average ground ( $\sigma = 10^{-2}$  S/m,  $\epsilon_r = 10$ ) and an input power of 1 kW.

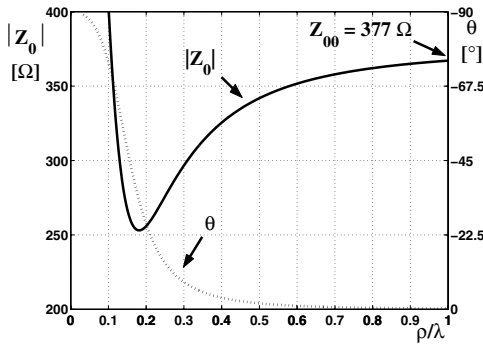


Fig. 20. CFA wave impedance as a function of distance  $\rho/\lambda$  at 1 MHz.

TABLE X  
CFA AND SHORT MONOPOLE WAVE IMPEDANCES.

$\rho/\lambda$	$ Z_{0\text{CFA}} $ Ω	$\theta_{\text{CFA}}$ °	$ Z_{0\text{MON}} $ Ω	$\theta_{\text{MON}}$ °
0.1	387.7	-73.9	385.5	-73.8
0.2	254.9	-25.4	254.8	-25.3
0.3	296.5	-8.14	296.4	-8.12
0.4	325.4	-3.47	325.3	-3.47
0.5	341.8	-1.79	341.8	-1.78
0.6	351.6	-1.04	351.6	-1.03
0.7	357.9	-0.65	357.9	-0.65
0.8	362.1	-0.44	362.1	-0.44
0.9	365.0	-0.31	365.0	-0.31
1.0	367.1	-0.22	367.1	-0.22
2.0	374.1	-0.03	374.1	-0.03
3.0	375.4	-0.01	375.4	-0.01
4.0	375.9	-0.00	375.9	-0.00
5.0	376.1	-0.00	376.1	-0.00

TABLE XI  
SHORT MONOPOLE OVER WET SOIL.

$Q_L$	$\pm\Delta f$	$\eta$	G	E	E
—	kHz	—	dBi	mV/m	dBμV/m
$\infty$	1.3	0.46	1.36	202	106.13
400	2.2	0.27	-0.85	157	103.93
200	3.0	0.20	-2.30	133	102.47
100	4.7	0.13	-4.25	106	100.52
50	8.1	0.07	-6.62	80.8	98.15

TABLE XII  
180°-WINDOW CFA OVER WET SOIL.

$Q_L$	$\pm\Delta f$	$\eta$	G	E	E
—	kHz	—	dBi	mV/m	dBμV/m
$\infty$	1.0	0.41	0.90	192	105.67
400	1.8	0.21	-1.92	139	102.85
200	2.7	0.15	-3.61	114	101.16
100	4.4	0.09	-5.78	89.0	98.99
50	7.8	0.05	-8.31	66.5	96.46

### E. Soil Effect

Antenna performance has been calculated changing the type of soil. In Tables XI, XII and XIII the performance of a short monopole and a CFA of the same height ( $H_1/\lambda = 0.0333$ ) operating in the 180°- and 360°-windows can be seen over wet soil ( $\sigma = 0.03$  S/ and  $\epsilon_r = 20$ ).

In Tables XIV, XV and XVI the performance of a short monopole and a CFA of the same height ( $H_1/\lambda = 0.0333$ ) operating in the 180°- and 360°-windows can be seen over dry soil ( $\sigma = 0.001$  S/ and  $\epsilon_r = 4$ ).

Field strength E at 1 km corresponds to an input power of 1 kW. From these calculations, it can be noticed a better bandwidth for every case in favor of the short monopole. Also, an increase in bandwidth is achieved when tuning coil and

TABLE XIII  
360°-WINDOW CFA OVER WET SOIL.

$Q_L$	$\pm\Delta f$	$\eta$	G	E	E
—	kHz	—	dBi	mV/m	dBμV/m
$\infty$	0.9	0.48	1.60	208	106.37
400	1.7	0.24	-1.34	148	103.43
200	2.6	0.16	-3.07	122	101.70
100	4.3	0.10	-5.26	94.5	99.51
50	7.8	0.06	-7.79	70.6	96.98

TABLE XIV  
SHORT MONOPOLE OVER DRY SOIL.

$Q_L$	$\pm\Delta f$	$\eta$	G	E	E
—	kHz	—	dBi	mV/m	dBμV/m
$\infty$	4.7	0.12	-4.26	106	100.51
400	5.6	0.11	-4.98	97.6	99.79
200	6.4	0.09	-5.60	90.9	99.17
100	8.1	0.07	-6.63	80.8	98.15
50	11.5	0.05	-8.15	67.8	96.62

TABLE XV  
180°-WINDOW CFA OVER DRY SOIL.

$Q_L$	$\pm\Delta f$	$\eta$	G	E	E
—	kHz	—	dBi	mV/m	$\text{dB}\mu\text{V/m}$
$\infty$	3.6	0.11	-4.98	97.6	99.79
400	4.4	0.09	-5.90	87.8	98.87
200	5.3	0.07	-6.66	80.4	98.11
100	6.9	0.05	-7.87	70.0	96.90
50	10.3	0.04	-9.61	57.3	95.17

TABLE XVI  
360°-WINDOW CFA OVER DRY SOIL.

$Q_L$	$\pm\Delta f$	$\eta$	G	E	E
—	kHz	—	dBi	mV/m	$\text{dB}\mu\text{V/m}$
$\infty$	3.2	0.14	-3.85	111	100.92
400	4.1	0.11	-4.91	98.4	99.86
200	5.0	0.09	-5.75	89.3	99.02
100	6.8	0.07	-7.07	76.7	97.70
50	10.0	0.04	-8.89	62.2	95.88

ground losses are increased.

#### F. Artificial Ground Plane Effect

A circular metallic ground plane of radius  $R_0$  and copper conductivity ( $\sigma_m = 5.8 \cdot 10^7 \text{ S/}$ ) is laid down under the monopole and CFA antennas. The effect of this radius  $R_0$  on the antenna performance over average ground is analyzed for tuning coils of merit factor  $Q_L = 200$ .

In Tables XVII, XVIII and XIX the short monopole, 180°- and 360°-window CFA performances are presented as functions of the artificial ground plane radius  $R_0$ , where field strength E at 1 km corresponds to an input power of 1 kW.

It can be appreciated from these results that the greater the ground plane radius  $R_0$  the greater the antenna gain G and the smaller the bandwidth  $\pm f$ , which is a well known effect.

TABLE XVII  
MONOPOLE PERFORMANCE OVER METALLIC GROUND PLANE.

$R_0$	$\pm\Delta f$	$\eta$	G	E	E
m	kHz	—	dBi	mV/m	$\text{dB}\mu\text{V/m}$
5	3.5	0.17	-3.00	123	101.77
10	2.8	0.21	-2.05	137	102.72
20	2.5	0.23	-1.53	145	103.24
30	2.4	0.24	-1.38	148	103.39

TABLE XVIII  
180°-WINDOW CFA PERFORMANCE OVER METALLIC GROUND PLANE.

$R_0$	$\pm\Delta f$	$\eta$	G	E	E
m	kHz	—	dBi	mV/m	$\text{dB}\mu\text{V/m}$
5	3.1	0.13	-4.24	106	100.53
10	2.6	0.15	-3.39	117	101.38
20	2.3	0.17	-2.94	124	101.84
30	2.2	0.17	-2.81	125	101.97

TABLE XIX  
360°-WINDOW CFA PERFORMANCE OVER METALLIC GROUND PLANE.

$R_0$	$\pm\Delta f$	$\eta$	G	E	E
m	kHz	—	dBi	mV/m	$\text{dB}\mu\text{V/m}$
5	2.9	0.15	-3.61	114	101.16
10	2.5	0.17	-2.88	124	101.89
20	2.3	0.19	-2.51	130	102.26
30	2.2	0.19	-2.40	131	102.37

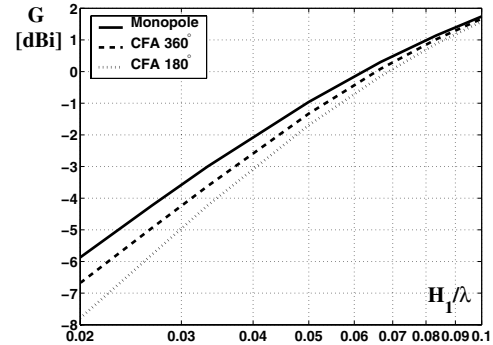


Fig. 21. CFA gain as a function of monopole 1 height  $H_1/\lambda$ , for a disk radius of  $L_2 = 2.5$  m, at the frequency  $f = 1$  MHz and over average ground.

#### G. Height Effect

The CFA antenna performance has been analyzed as a function of the monopole 1 height,  $H_1$ , and with a constant disk radius of  $L_2 = 2.5$  over average ground and with tuning coils of merit factor  $Q_L = 200$ . A reference monopole of the same height has also been calculated.

Figs. 21 and 22 show the antenna gain and bandwidth as functions of height  $H_1/\lambda$ .

With regard to the antenna gain, Fig. 21 shows that the gain difference is smaller for greater antenna heights, this means that the disk has a deleterious effect on the antenna performance. At the same time, Fig. 22 shows a better bandwidth of the monopole compared to the CFA for any height.

#### H. Disk Effect

The CFA antenna performance has been analyzed as a function of the disk radius,  $L_2$ , and with a constant monopole 1

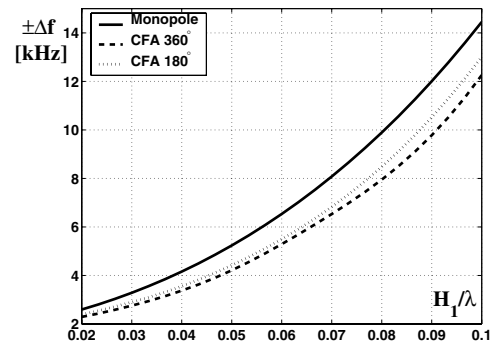


Fig. 22. CFA bandwidth for  $\text{VSWR} = 2$  as a function of monopole 1 height  $H_1/\lambda$ , for a disk radius of  $L_2 = 2.5$  m, at the center frequency  $f = 1$  MHz and over average ground.



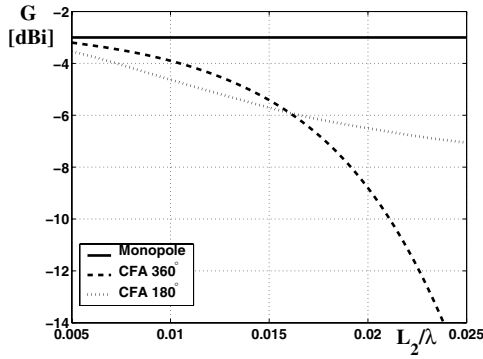


Fig. 23. CFA gain as a function of disk radius  $L_2/\lambda$  for a monopole 1 height of  $H_1 = 10$  m, at the frequency  $f = 1$  MHz and over average ground.

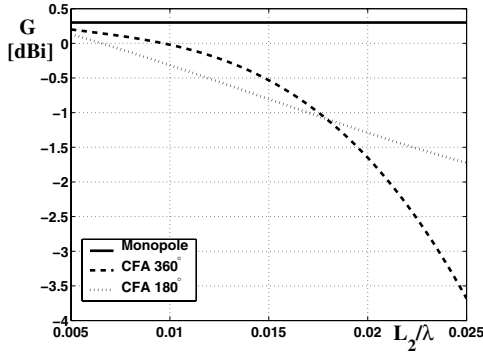


Fig. 24. CFA gain as a function of disk radius  $L_2/\lambda$  for a monopole 1 height of  $H_1 = 20$  m, at the frequency  $f = 1$  MHz and over average ground.

height of  $H_1 = 10$  and 20 m, over average ground and with tuning coils of merit factor  $Q_L = 200$ . A reference monopole of the same height has also been calculated.

Antenna gain is shown in Figs. 23 and 24 as a function of disk radius  $L_2/\lambda$ , where the disk deleterious effect can be clearly appreciated.

Antenna bandwidth is shown in Figs. 25 and 26 as a function of disk radius  $L_2/\lambda$ , where the disk deleterious effect can also be appreciated.

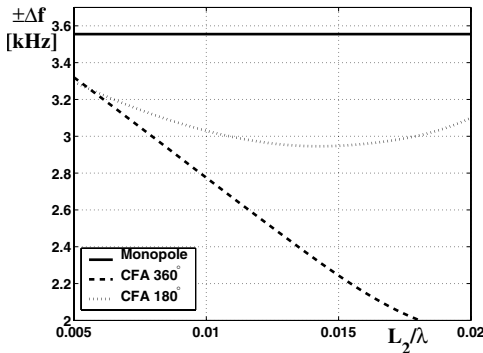


Fig. 25. CFA bandwidth for  $VSWR = 2$  as a function of disk radius  $L_2/\lambda$  for a monopole 1 height of  $H_1 = 10$  m, at the center frequency  $f = 1$  MHz and over average ground.

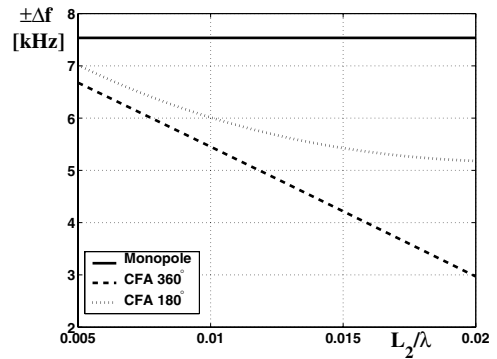


Fig. 26. CFA bandwidth for  $VSWR = 2$  as a function of disk radius  $L_2/\lambda$  for a monopole 1 height of  $H_1 = 20$  m, at the center frequency  $f = 1$  MHz and over average ground.

### I. Top-Load Effect

The CFA antenna performance has been analyzed as a function of the monopole 1 top-load length,  $L_1$ , with  $n = 8$  branches and a constant monopole 1 height of  $H_1 = 10$  over average ground and with tuning coils of merit factor  $Q_L = 200$ . A reference monopole of the same height and top-load has also been calculated.

In Fig. 27, it can be appreciated an increase in gain as the top-load length  $L_1$  is increased for the short monopole and CFA operating in both windows. At the same time, the deleterious effect of the disk is clearly appreciated, because for a larger top-load the monopole and CFA gains are practically the same.

In Fig. 28, the antenna bandwidth is shown, where a better bandwidth for the short monopole can be appreciated in all cases.

It seems this technique of top-load increase was adopted after the previous CFA antenna models. The top-load increase was obtained by means of a conical top-load installed to any CFA, as shown in Fig. 4, in order to improve the input impedance, bandwidth and gain, impossible to be achieved by a short barrel alone used as a vertical monopole. The effect of the top-load cone height  $H_1$  (see Fig. 4) is to increase the antenna effective height, so a similar effect could be achieved increasing the monopole 1 height from  $H_1$  to  $H_1 + H_1$  and maintaining the same top-load length  $L_1$ .

This is a clear demonstration that a very short antenna has always a very sharp frequency behavior and for the CFA antenna this statement is also valid, because it obeys the same antenna theory with no exceptions.

## VIII. MEASUREMENTS

Far field calculations have been carried out for existing CFA antennas, where measurements are available. Papers of measurements have been evaluated and comparisons with theoretical calculations have been performed.

Nile Delta Tanta (Egypt) CFA antenna operates at 1161 kHz. Field strength data have been released and are shown in [13].

This antenna model has been calculated over a flat ground plane with the same available dimensions, in order to compare with the released field strength data.

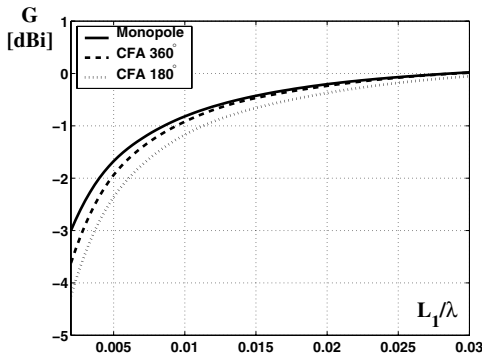


Fig. 27. CFA gain as a function of top-load length  $L_1/\lambda$  for a monopole 1 height of  $H_1 = 10$  m and a disk radius  $L_2 = 2.5$  m, at the center frequency  $f = 1$  MHz and over average ground.

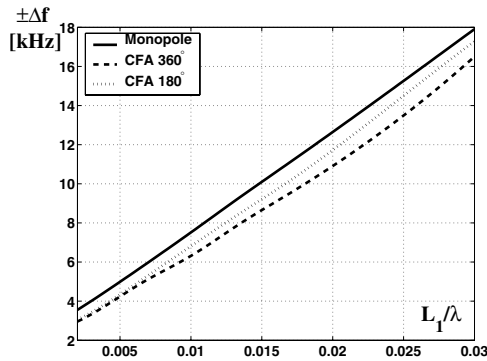


Fig. 28. CFA bandwidth for VSWR = 2 as a function of top-load length  $L_1/\lambda$  for a monopole 1 height of  $H_1 = 10$  m and a disk radius  $L_2 = 2.5$  m, at the center frequency  $f = 1$  MHz and over average ground.

Fig. 29 shows the measured values compared to a theoretical short monopole, placed over a perfectly conducting artificial ground plane, and a CFA model over wet ground. Good agreement can be seen and the Tanta CFA has a field strength according to a short antenna placed over a good artificial ground plane.

It is important to know that this antenna was installed over a building with a metallic ground plane laid down in the roof. Metallic straps along the building walls have been installed, connecting the roof ground plane to the actual ground plane at the soil level. This complex ground plane has the effect of increasing the antenna height  $H$  and, of course, it increases the antenna efficiency and gain, converting this antenna in a kind of skirted monopole [35], as Fig. 30 shows.

However, measured field strength values are not spectacular and they are within the expected values for this kind of short antenna.

Another example where a CFA antenna was used is the San Remo experiment for a frequency of 1188 kHz. This experimental system was made up by *Rai Way* under the direction of Dr. Alberto Fassio, in order to evaluate its performance. Measurements have been made by RAI engineers and technicians under the direction of Luciano Pautasso. They have used well calibrated field strength instrumentation.

In Fig. 31, RAI field strength measurements are compared by means of a similar theoretical CFA model installed over a

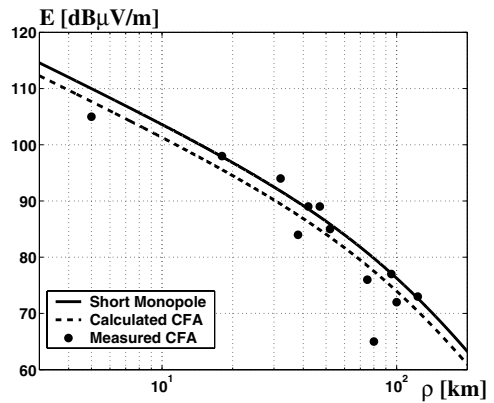


Fig. 29. Measured Tanta CFA field strength as a function of distance  $\rho$  compared to a theoretical short monopole and a calculated CFA, on a ground plane of  $\sigma = 0.05$  S/m and  $\epsilon_r = 20$  for an input power of 30 kW (Tanta CFA was installed on a building roof).

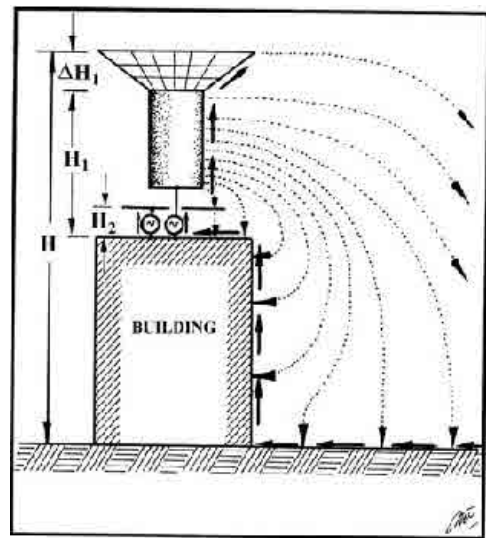


Fig. 30. CFA antenna on a building roof.

flat artificial ground plane and average ground.

San Remo CFA antenna was installed on a transmitting building roof too and a metallic artificial ground plane was laid down over the roof. Building location is close to the Mediterranean sea side, so some measured points are along the sea coast and some others are located inland with different ground constants.

Fig. 31 shows a lower field strength than the theoretical calculations. In some cases, the measured field strength is close to the average ground theoretical curve, but the actual link was performed over sea water.

Due to low measured field strength values, the top-load of this antenna was increased by means of sixteen aluminum tubes, but no increase in field strength was observed due to a very small top-load increase. At the present time, this antenna is not operating because it has been dismantled.

In Brazil, two CFA experimental antennas have been installed in order to determine their performances. One CFA was installed in Sao Paulo by Sylvio Damiani, intended to be used at a frequency of 560 kHz. Personal information

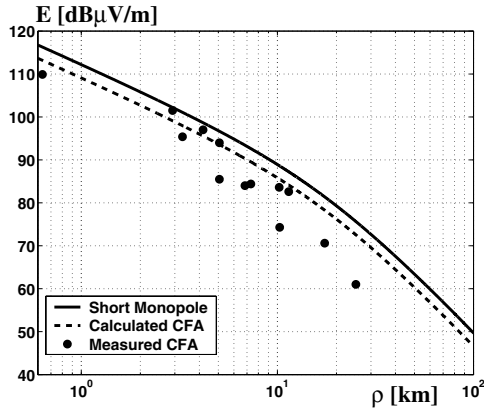


Fig. 31. Measured San Remo CFA field strength as a function of distance  $\rho$  compared to a theoretical short monopole and a calculated CFA, on a ground plane of  $\sigma = 0.01$  S/m and  $\epsilon_r = 10$  for an input power of 2 kW (San Remo CFA was installed on a building roof).

from Mr. Otavio Emmanuel Lima is that this antenna was never operating better than -10 dB compared to a quarter-wave monopole. No more experiments with this antenna were performed after Sylvio passed away.

Another CFA experimental antenna was installed in Goiania by Mr. Lima for a frequency of 1230 kHz. This antenna was installed on a small building roof 4 m in height and a 12 by 12 m metallic ground plane was laid down over the roof. The antenna monopole 1 was 6.5 m in height and the metallic disk was 4 m in diameter. Mr. Lima was making a lot of tests on it during long time. Nevertheless, the better field strengths achieved were always 6 dB below, compared to a quarter-wave monopole.

Finally, it was pointed out that a CFA gain improvement is obtained installing it on a building roof. In the case of very low power installations, as the case of the short time CFA experiment performed in Sidney, Australia, (personal communication), an intended 1 kW operation was mandatory decreased by the authority to 200 W, because of neighbor complaints, due to a lot of interferences and disturbances caused to different systems in a crowded area by the radiated AM signal.

## IX. CONCLUSION

CFA antennas have been exhaustively analyzed. From this analysis, it is pointed out the following:

- A CFA antenna transmission line model has been proposed and its equivalent network has been obtained. At the same time, this model has been validated by means of Moment Method simulations and some available experimental data.
- From this approach, it can be seen three antenna working possibilities according to the sign of the mutual conductance  $G_{12}$ .
- Two operating windows, for values of  $\phi_2$  near  $180^\circ$  or  $360^\circ$ , and some specific values of K permit having a positive input power in each port.
- Antenna tuning has been obtained connecting the appropriated coils including their merit factors.

- Antenna operation for each  $\phi_2$ -window has been compared to a reference monopole of the same height and on the same ground plane and top-loading conditions.
- It can be concluded that the disk presence has always a deleterious effect, decreasing the antenna performance.
- The CFA performance is always a little worst than the reference monopole in gain and bandwidth. The antenna performance increases as either the antenna height or top-loading is increased, in the same way as for any standard short monopole. Also, a simple monopole has a similar or better performance with an easier tuning system.
- CFA antenna has the same radiation pattern and near field distribution as any short monopole, then no Poynting Vector Synthesis (PVS) can be seen close to the CFA antenna.
- A CFA gain improvement is obtained installing it on a building roof, in the same manner as for a standard monopole, as it was pointed out since long time in different parts of the frequency spectrum [35].
- It must be pointed out that moderated or high power operations with short antennas does not mean they can be installed in any place, but in conventionally isolated areas as good engineering practice indicate for standard LF and MF AM stations. Of course, this installation place is matter of the Government Administration, due not only to interference but to non ionized radiation levels too.

## APPENDIX A

### DISK LOSS RESISTANCE

CFA disk surface current density on each face is given by

$$J_s = \frac{1}{2} \frac{I(\rho)}{2\pi\rho} \quad (54)$$

Where  $I(\rho)$  is given by (46).

The power dissipated in both disk faces, due to the finite metallic disk conductivity,  $\sigma_c$ , can be determined by

$$W_d = 2 \int_{r_h}^{L_2} |J_s|^2 \sqrt{\frac{\omega\mu_0}{2\sigma_c}} 2\pi\rho d\rho \quad (55)$$

This integral can be carried out to give

$$W_d = \frac{1}{4\pi} \sqrt{\frac{\omega\mu_0}{2\sigma_c}} \frac{|I_2|^2}{(L_2 - h)^2} \left[ L_2^2 \left( \frac{L_2}{h} \right) - 2L_2(L_2 - h) + \frac{L_2^2 - \frac{2}{h}}{2} \right] \quad (56)$$

Then, the disk loss resistance, summing up the losses of the vertical feed conductor of height  $H_2$ , will be

$$R_{c2} = \frac{W_d}{|I_2|^2} + \frac{H_2}{a_2} \sqrt{\frac{f\mu_0}{4\pi\sigma_c}} \quad (57)$$

## APPENDIX B

### OPERATING WINDOWS

The CFA input power ratio,  $K_w$ , is defined as

$$K_w = \frac{W_2}{W_1} \quad (58)$$

Then

$$K_w = \frac{K^2 G_{22} + K G_{12} c \phi_2 + K B_{12} \phi_2}{G_{11} + K G_{12} c \phi_2 - K B_{12} \phi_2} \quad (59)$$

For a given input power ratio  $K_w$ , the voltage phase difference  $\phi_2$  can be written as a function of  $K$ , that is

$$\begin{aligned} \phi_2(K) = \\ \pm a c c \left[ \frac{K_w G_{11} - K^2 G_{22}}{K \sqrt{(1 - K_w)^2 G_{12}^2 + (1 + K_w)^2 B_{12}^2}} \right] + \\ + a c a \left[ \frac{(1 + K_w) B_{12}}{(1 - K_w) G_{12}} \right] \pm \pi = 0, 1, 2, \dots \quad (60) \end{aligned}$$

The chosen  $K$  must verify the following inequality:

$$\left| \frac{K_w G_{11} - K^2 G_{22}}{K \sqrt{(1 - K_w)^2 G_{12}^2 + (1 + K_w)^2 B_{12}^2}} \right| \leq 1 \quad (61)$$

Once a  $K$  has been chosen, the  $\phi_2(K)$  are calculated and mapped into the  $[0, 2\pi)$  interval, where they cover a neighborhood of  $\pi$ , called the 180°-window, and neighborhoods of 0 and  $2\pi$ , called the 360°-window (or 0°-window).

In the case of equal input powers ( $K_w = 1$ ), it follows that

$$\phi_2(K) = \pm a c 1 \left[ \frac{G_{11} - K^2 G_{22}}{2 K B_{12}} \right] \pm \pi = 0, 1, 2, \dots \quad (62)$$

and

$$\left| \frac{G_{11} - K^2 G_{22}}{2 K B_{12}} \right| \leq 1 \quad (63)$$

Thus, for a given total input power  $W_{in}$  and power ratio  $K_w$ , the values of  $\phi_2$  and  $K$  can be obtained from (60) and (61), then the port 1 input voltage will be

$$V_1 = \sqrt{\frac{W_{in}}{G_{11} + 2 K G_{12} c \phi_2 + K^2 G_{22}}} \quad (64)$$

## APPENDIX C

### GLOSSARY OF SYMBOLS

$a_i$	$i$ -th monopole wire radius [m].
$\beta$	Phase constant or wave number ( $\beta = 2\pi/\lambda$ ) [rad/m].
$B_{12}$	CFA mutual susceptance [S].
$B_{ii}$	$i$ -th monopole self-susceptance [S].
$C_2$	Disk capacitance [F].
$D$	CFA directivity.
$\eta$	CFA efficiency.
$E_\theta$	Electric field $\theta$ -component [V/m].
$\epsilon_r$	Soil relative permittivity.
$G$	CFA gain.
$G_{12}$	CFA mutual conductance [S].
$G_{ii}$	$i$ -th monopole self-conductance [S].
$H_e$	CFA effective height [m].
$H_{ei}$	$i$ -th monopole effective height [m].
$H_i$	$i$ -th monopole height [m].
$H_\phi$	Magnetic field $\phi$ -component [A/m].

$i$	$= 1, 2$ .
$I_i$	$i$ -th monopole effective input current [A].
$I(\rho)$	Disk current distribution [A].
$j$	$\sqrt{-1}$ imaginary unit.
$J_s$	Disk surface current density [A/m].
$K$	Input voltage amplitude ratio.
$K_w$	Input power ratio.
$L_1$	Monopole 1 top-load length [m].
$L_2$	Disk radius (monopole 2 top-load length) [m].
$n$	Monopole 1 top-load branches.
$\phi_2$	Input voltage phase difference.
$Q_{Li}$	$i$ -th monopole coil merit factor.
$\rho$	Radial distance from the antenna base [m].
$\rho_h$	Disk hole radius [m].
$R_0$	Artificial ground plane radius [m].
$R_{12}$	CFA mutual resistance [ ].
$R_i$	$i$ -th monopole input resistance [ ].
$R_{ci}$	$i$ -th monopole conductor resistance [ ].
$R_g$	Artificial ground plane resistance [ ].
$R_{gpi}$	$i$ -th monopole ground plane loss resistance [ ].
$R_{ii}$	$i$ -th monopole self-resistance [ ].
$R_{cLi}$	$i$ -th monopole conductor resistance per unit length [ / ].
$R_{Li}$	$i$ -th monopole tuning coil resistance [ ].
$R_{rad}$	CFA radiation resistance [ ].
$R_{radi}$	$i$ -th monopole radiation resistance [ ].
$R_s$	Soil resistance [ ].
$\sigma$	Soil conductivity [S/m].
$\sigma_c$	Wire conductivity [S/m].
$\sigma_m$	Artificial ground plane (metallic layer) conductivity [S/m].
$V_i$	$i$ -th monopole effective input voltage [V].
$W_d$	Power dissipated in the disk [W].
$W_i$	$i$ -th monopole input power [W].
$W_{in}$	CFA input power [W].
$W_{rad}$	CFA radiated power [W].
$X_{12}$	CFA mutual reactance [ ].
$X_i$	$i$ -th monopole input reactance [ ].
$X_{ii}$	$i$ -th monopole self-reactance [ ].
$X_{ti}$	$i$ -th monopole top-reactance [ ].
$X_{Li}$	$i$ -th monopole tuning coil reactance [ ].
$Y_{12}$	CFA mutual admittance [S].
$Y_{ii}$	$i$ -th monopole self-admittance [S].
$Z_0$	Near field wave impedance [ ].
$Z_{00}$	Free space intrinsic impedance (377 ).
$Z_{0mi}$	Equivalent transmission line average characteristic impedance of the $i$ -th monopole [ ].
$Z_{12}$	CFA mutual impedance [ ].
$Z_i$	$i$ -th monopole input impedance [ ].
$Z_{ii}$	$i$ -th monopole self-impedance [ ].
$Z_g$	Artificial ground plane impedance [ ].
$Z_s$	Soil impedance [ ].

## REFERENCES

- [1] V. Trainotti and L. A. Dorado, *Short Low and Medium Frequency Antenna Performance*, 54th Annual IEEE Broadcast Technology Society Symposium Proceeding, October 2004, Reprinted in QEX May-June 2005.

- [2] A. Djordjevic, *A Review of the Crossed-Field Antenna*, Private Communication, October 1999.
- [3] J. S. Belrose, *The Crossed Field Antenna Analyzed by Simulation and Experiment*, A. P. 2000 Symposium, Davos, Switzerland, April 2000.
- [4] J. S. Belrose, *Characteristics of The CFA Obtained by Numerical and Experimental Modeling*, CFA Panel Presentation, 50th. Annual Broadcast Technology Symposium, Vienna, VA, 27-29, September 2000.
- [5] J. S. Belrose, *Radiation Characteristics of an Electrically Small MF Broadcast Antenna - By Simulation*, Eleventh International Conference on Antennas and Propagation (ICAP 2001). Manchester, UK, 17-20, April 2001.
- [6] V. Trainotti, *Short Medium Frequency AM Antennas*, IEEE Trans. on Broadcasting, vol. 47, no. 3, pp. 263-284, Sept. 2001.
- [7] J. S. Belrose, *A CFA on the Roof of a Building*, Private Communication, March 2001.
- [8] IEEE-BTS, *CFA Forum*, 50th Annual IEEE Broadcast Symposium, Vienna, VA, 27-29, Sept. 2000.
- [9] J. K. Breakall, M. W. Jacobs, A. E. Resnik, G.Y. Eastman, M.D. Machalek, and T. F. King, *A Novel Short AM Monopole Antenna with Low Loss Matching System*, IEEE BTS 52nd. Annual Broadcast Symposium, Oct. 10-11, 2002. Omni Shoreham Hotel, Washington, D.C.
- [10] J. K. Breakall, M. W. Jacobs, T. F. King and A. E. Resnik, *Testing and Results of a New Efficient Low-Profile AM Medium Frequency Antenna System*, NAB 2003 Broadcast Engineering Conference Proceedings, pp. 235-243, April 2003.
- [11] F. M. Kabbary, M. C. Hatley and B. G. Stewart, *Maxwell's Equations and the Crossed Field Antenna*, Electr. World & W. W. 95, pp. 216-218, 1989.
- [12] F. M. Kabbary, M. C. Hatley and B. G. Stewart, *CFA Working Assumptions*, Electr. World & W. W. 96, pp. 1094-1099, Dec. 1992.
- [13] F. M. Kabbary, M. Khattab and M. C. Hatley, *Extremely Small High Power MW Broadcasting Antennas*, IEEE International Broadcasting Conference (IBC), Amsterdam, 10-12th Sep. 1997.
- [14] F. M. Kabbary, M. Khattab, B. G. Stewart, M. C. Hatley and A. Fayoumi, *Four Egyptian MW Broadcast Crossed-Field Antennas*, Proceedings of the NAB Conference, Las Vegas, NV, pp. 235-241, April 1999.
- [15] W. C. Alexander, *Is this AM Antenna for real?*, Radio World, March 31, 1999.
- [16] M. C. Hatley and F. M. Kabbary, 1988, *British Patent Application 2,215,524*.
- [17] W. C. Johnson, *Transmission Lines and Networks*, Mc. Graw Hill, N. Y., 1950.
- [18] J. J. Karakash, *Transmission Lines and Filter Networks*, The Macmillan Company, N. Y., 1950.
- [19] W. L. Everitt, *Communication Engineering*, Mc. Graw Hill, N.Y. 1937.
- [20] E. Laport, *Radio Antenna Engineering*, Mc. Graw Hill, N. Y., 1952.
- [21] J. D. Kraus, *Antennas*, Mc. Graw Hill, N. Y., 1950.
- [22] C. A. Balanis, *Antenna Theory Analysis and Design*, John Wiley & Sons, N. Y., 1982, 1997.
- [23] W. L. Stutzman and G. A. Thiele, *Antenna Theory and Design*, John Wiley & Sons, N. Y., 1982, 1998.
- [24] P. S. Carter, *Circuit Relations in Radiating Systems*, Proc. IRE, vol. 20, no. 6, pp. 1004, June 1932.
- [25] L. A. Dorado, EMMCAP<sup>(R)</sup>, *Electromagnetic Modeling Computation and Analysis Program*, <http://www.emmcap.com.ar/>
- [26] E. C. Jordan, *Electromagnetic Waves and Radiating Systems*, Prentice-Hall Inc., N. Y., 1950.
- [27] S. A. Schelkunoff and H. T. Friis, *Antenna Theory and Practice*, John Wiley & Sons, N. Y., 1952.
- [28] V. Trainotti, *Simplified Calculation of Coverage Area for MF AM Broadcast Station*, IEEE A & P Magazine, pp. 41-44, June 1990.
- [29] V. Trainotti, W. G. Fano and L. A. Dorado, *Ingeniería Electromagnética II*, Nueva Librería, Buenos Aires, Argentina, 2005.
- [30] J. E. Storer, *The Impedance of an Antenna over a Large Circular Screen*, J. of App. Physics, vol. 22, no. 8, pp. 1058-1066, August 1951.
- [31] J. R. Wait and W. J. Surtees, *Impedance of a Top-Loaded Antenna of Arbitrary Length over a Circular Grounded Screen*, J. of App. Physics, vol. 25, no. 5, pp. 553-555, May 1954.
- [32] G. H. Brown, R. F. Lewis and J. Epstein, *Ground System as a Factor in Antenna Efficiency*, Proc. IRE, vol. 25, no. 6, pp. 758-787, June 1937.
- [33] R. Harrington, *Field Computation by Moment Methods*, Macmillan, N. Y., 1968.
- [34] M. C. Hatley, F. M. Kabbary and M. Khattab, *An Operational MF Antenna using Poynting Vector Synthesis*, Proceedings of the Seventh International Conference on Antennas and Propagation, Part 2, IEE Conference Publication No. 333, pp. 645-648, April 1991.
- [35] Radio Research Laboratory Staff, *Very High Frequency Techniques*, Mc Graw Hill, N.Y. 1947, Vol. 1.



**Valentino Trainotti** was born in Trento, Italy, in 1935. He received the Electronic Engineering Degree from the Universidad Tecnológica Nacional, Buenos Aires, Argentina in 1963.

His post-graduate coursework on antenna measurements and geometric theory of diffraction was completed at California State University in 1981 and Ohio State University in 1985.

He has worked from 1963 to 2003 at CITEFA as the Antenna & Propagation Division Chief Engineer.

His work also includes being on the Engineering Faculty at the University of Buenos Aires as a part-time Full Professor of Electromagnetic Radiation and Radiating Systems for graduated students.

He is an IEEE Senior Member, Member of the IEEE Ad-Com BTS Society, IEEE BT Transactions Associate Editor, IEEE BTS Argentina Chapter Chair, URSI Commission B Argentina Chair, and 1993 IEEE Region 9 Eminent Engineer.

He has worked more than thirty years developing and measuring antenna systems for several applications from LF to SHF.



**Luis A. Dorado** was born in Tucuman, Argentina, in 1976. He received the Electronic Engineering Degree from the Universidad Nacional de Tucuman, Tucuman, Argentina, in 2001, and is currently working toward the Ph.D. degree.

He has developed commercial and academic simulation software related to computational electromagnetics, especially moment method algorithms for computing radiation and scattering from wire structures and antennas.

He is currently working on new numerical and analytical analysis tools and techniques for solving problems in these areas. His research interest include computer simulation of EMC problems and antennas over real ground.





# A Low Budget Vector Network Analyzer for AF to UHF

*The author's PC turned his "simple gadget" into a sophisticated piece of test equipment.*

**Professor Dr Thomas C. Baier, DG8SAQ**

## Introduction

After years of professional work with commercial vector network analyzers (VNWA), I did not want to miss this handy kind of test equipment in my shack at home any longer. Looking through the surplus market, I found that the price for a commercial VNWA is still well out of reach for the average hobbyist. At that time, a *QEX* article on a homebrew VNWA caught my attention.<sup>1</sup> Some Internet research revealed another similar project by N2PK.<sup>2</sup> Both projects have in common the use of direct digital synthesizer (DDS) circuits to generate an RF test signal and an LO signal for down-converting the tested component's response signals to zero IF. The dc IF signals are then digitized by appropriate analog-to-digital converters. The digital numbers are fed into a standard personal computer (PC) for further processing and imaging.

I found that concept very attractive; but coming from the analog side of electronics design, I thought about ways to simplify the analog section and cut down as much as possible on the digital components, consisting of A/D converters and a microcontroller at the least. Clearly, there was no reasonable substitute for the DDS oscillators. But I found that all other digital and mixed-signal tasks could be performed by the standard PC. I

<sup>1</sup>Notes appear on page 53.

University of Applied Sciences  
Prittitzstrasse 10  
89075 Ulm, Germany  
baier@hs-ulm.de

intended to tie the DDS oscillators directly to the parallel PC printer interface and to make use of the standard PC stereo sound card for analog signal acquisition. Thus a very simple concept took shape in my mind. All that was needed to build a VNWA were two DDS oscillator chips, an SWR bridge and three mixers (through, reflect and reference). I assembled a first prototype in a cardboard box within a few days. That's where the adventure started.

Had I known beforehand how many software problems I had to solve, I might never have started the project. However, after about a year of heavy learning and coding, the PC has turned my simple little gadget into an accurate piece of RF test equipment.

## Why Vector Network Analysis?

Did you ever want to match a crystal filter systematically to obtain a perfectly flat pass-band? Or did you ever want to know the ca-

pacitance value of that special SMD capacitor or the Q value of your homemade inductor? A vector network analyzer is the perfect choice to solve all these problems. When you analyze an RF component like a filter, or an antenna, you are typically interested in the return loss and/or in the insertion attenuation of the component in a specific frequency range. This information can be obtained with a scalar network analyzer, which basically consists of a signal source, an SWR bridge and an RF detector. The return loss is defined as the power reflected from the device input divided by the input power incident into the device. The insertion attenuation equals the output power of the device divided by the incident input power.

Vector network analyzers do not only measure these signal power ratios but also the phase increments from input signal to reflected and/or transmitted signal. On first sight, these phase values seem uninteresting;

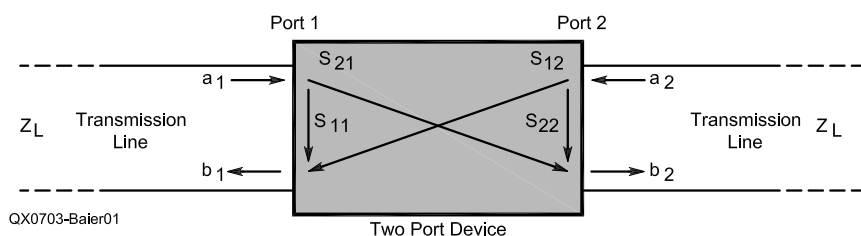


**Figure 1 — Connection between S-parameters and incident and evanescent waves at an electrical two port device.**

but a closer look reveals that it is these phases that enable us to calculate impedance values and use the measurement results in system simulations with software tools like APLAC or ADS,<sup>3,4</sup> to calculate the behavior of the test object at modified termination impedance levels. The theory behind this is the theory of scattering parameters or S parameters. The set of S parameters, also called S matrix, completely describes the linear properties of an RF device. A VNWA is designed to measure these S-parameters.

### Two-Port S Parameters

To completely characterize the linear properties of a two port RF device (like an IF filter) at a given frequency, four S-parameters are required, which are combined to form the two-port S-matrix:

$$\begin{pmatrix} S_{11} & S_{12} \\ S_{21} & S_{22} \end{pmatrix}$$

S-parameters are complex numbers; that is, they consist of a magnitude (=attenuation) and a phase value. As shown in Figure 1, they relate incident wave amplitudes  $a_i$  to reflected and transmitted wave amplitudes  $b_i$ :

$$\begin{aligned} b_1 &= S_{11} \cdot a_1 + S_{12} \cdot a_2 \\ b_2 &= S_{21} \cdot a_1 + S_{22} \cdot a_2 \end{aligned} \quad [\text{Eq 1}]$$

While indices=1 denote waves on the device input, indices=2 denote waves on the device output.

At this point, it becomes clear how to measure S parameters. To measure  $S_{21}$ , make sure that there is only one wave  $a_1$  incident from the left side. Measure it and measure also the wave  $b_2$  transmitted through the de-

vice under test (DUT). Since  $a_2 = 0$  (no wave incident to the output of the DUT from the right hand side)  $S_{21}$  can simply be obtained:  $S_{21} = b_2/a_1$ .

$S_{11}$  can be obtained in a similar manner by additionally measuring the reflected wave from the DUT input  $b_1$ :  $S_{11} = b_1/a_1$ .

$S_{12}$  and  $S_{22}$  can be measured in the very same way by exchanging DUT input and output. Commercial two-port VNWAs achieve this DUT reversal with built-in switches. The simpler homebrew method is to interchange the connectors during the S-parameter acquisition.

Now, the test condition  $a_2 = 0$  needs a little additional consideration. It means that there is no RF power propagating into the DUT output from the right hand side. Of course, we are not about to connect an oscillator to the DUT output while measuring  $S_{21}$ . But there is another source for such a signal, namely the wave reflected from the signal detector at the DUT output. Reflection always takes place when the detector input impedance is unequal to the transmission line impedance  $Z_L$  (usually 50  $\Omega$ ) it connects to. Similarly, care has to be taken that the signal source impedance of the VNWA on the DUT input side is properly matched to the transmission line impedance. Otherwise the wave  $b_1$  reflected from the DUT back to the VNWA will be re-reflected at the oscillator interface back into the DUT and introduce an error on  $a_1$ .

### VNWA Design

Figure 2 shows the basic design of my VNWA. It consists of two digitally tunable DDS oscillators. The RF oscillator generates a wave  $a_1$  which is running through an

SWR bridge to the DUT. The bridge is used to measure the incident wave  $a_1$  (reference signal) and the reflected wave  $b_1$  (reflect signal). The wave  $b_2$  transmitted through the DUT is also measured (through signal). All these test signals are mixed down with a DDS local oscillator to an IF signal in the audio frequency range that can be processed by a PC sound card. This is one of the special features of my design to simplify the VNWA. Since a standard PC sound device has only two simultaneously sampled signal inputs, namely stereo left and right, some kind of switch is required to multiplex the three test signals to the two audio channels. Care has to be taken to achieve a sufficiently high switch isolation of about 100 dB. Alternatively, one could add a second sound card to the PC. The current software version does not support two sound cards, though. Since most sound cards utilize 16 bit AD-converters, a dynamic range of  $20 \cdot \log(2^{16})$  dB  $\approx$  96 dB is to be expected and indeed, also realized. Experiments with a 24-bit sound card<sup>5</sup> yielded no significant improvement of the dynamic range (theoretically 144 dB) though, since the least significant data byte is dominated by noise and on top, a systematic phase error between left and right channel was observed.<sup>6</sup>

### In the Labyrinth of a Microsoft Windows PC

The PC's tasks are basically quite simple now:

1. Set DDS oscillators to new test frequency.
2. Wait until DUT reaches steady state (especially important for DUTs with high Q-values).

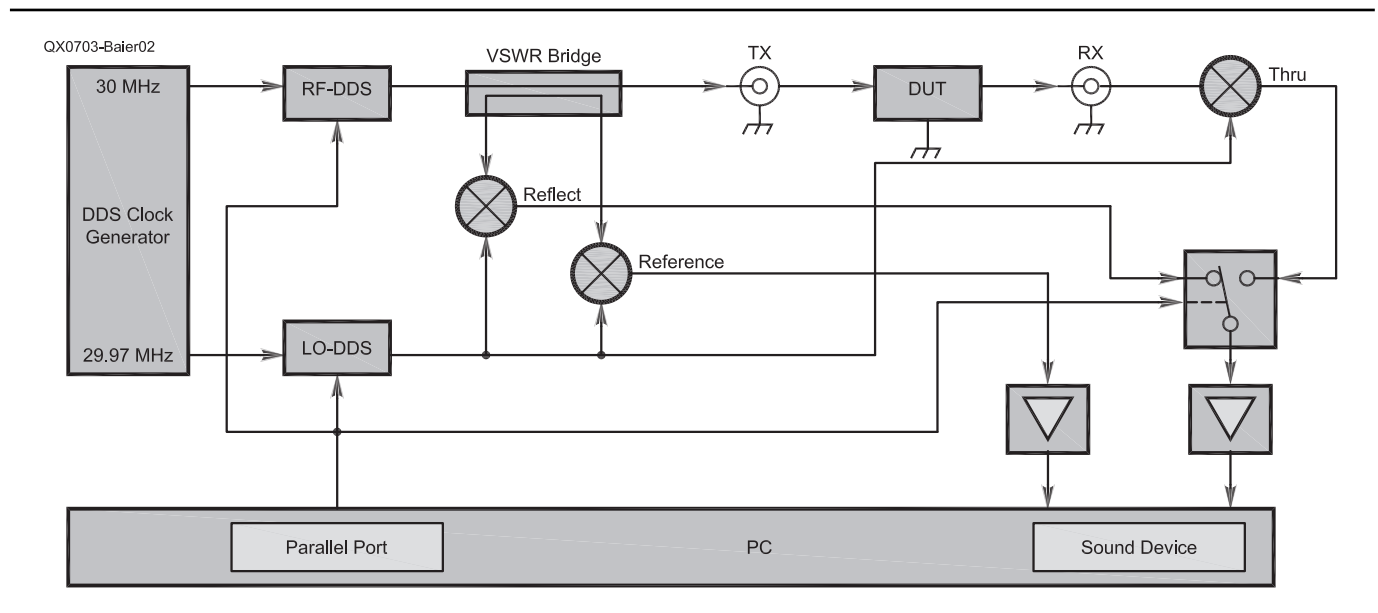


Figure 2 — Basic construction of the described vector network analyzer.

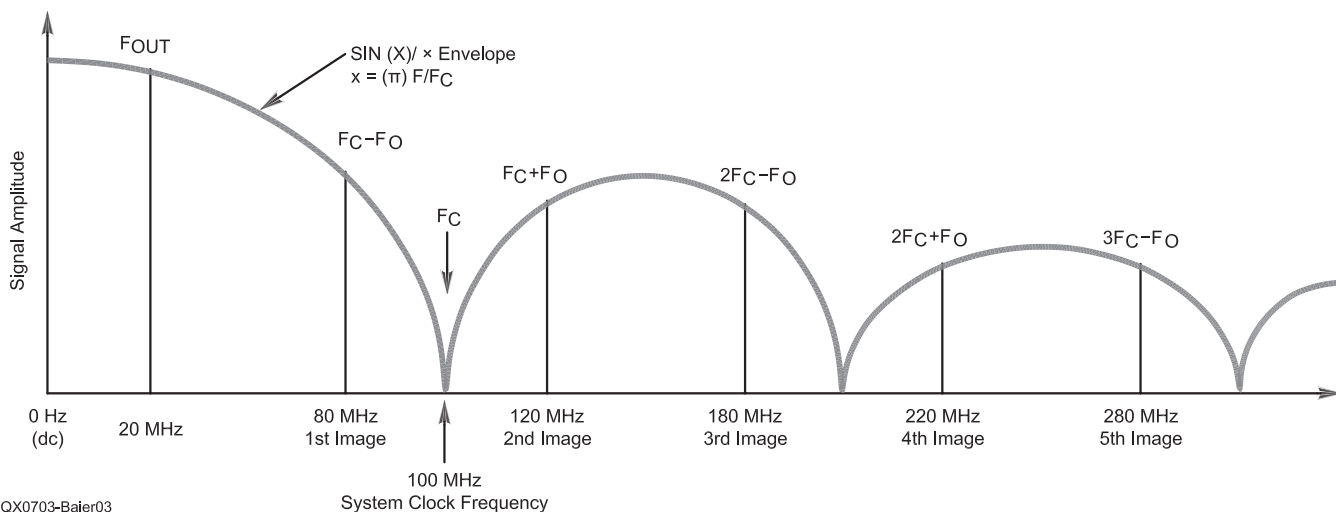


Figure 3 — Unfiltered output spectrum of a DDS oscillator (from Note 7).

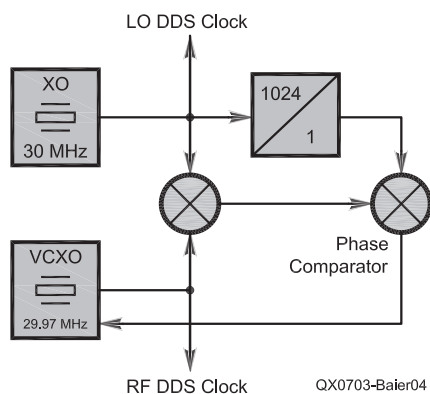


Figure 4 — Generation of two interlocked DDS clocks via phase locked loop.

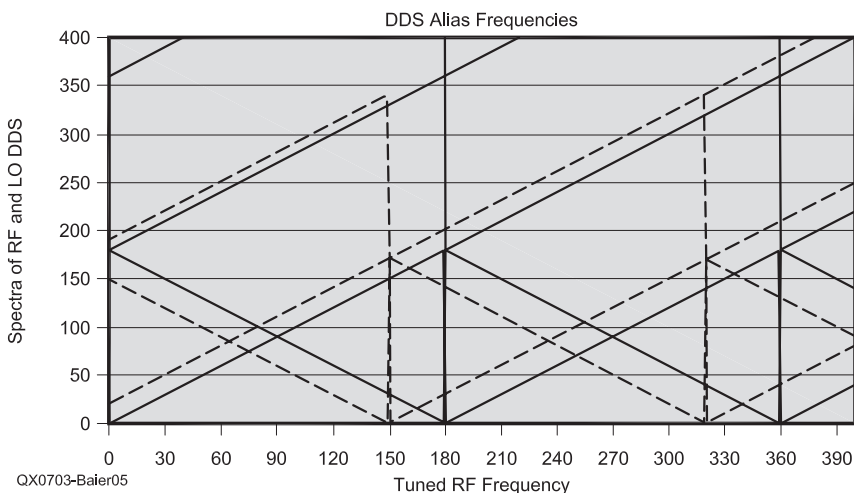


Figure 5 — Utilization of DDS alias frequencies. The RF spectrum is plotted solid; the LO spectrum is plotted dashed. Obviously, there is only one frequency pair mixing to the example IF, which is chosen to 10 MHz for better visibility. In this calculation LO-DDS and RF-DDS clocks are chosen as 170 MHz and 180 MHz, respectively.

3. Measure reference and reflect signals or reference and through signals.
4. Calculate  $S_{11}$  or  $S_{21}$ .
5. Plot data point to the screen.
6. Repeat measurement cycle with new test frequency at step 1.

Here the timing is the real challenge. Care has to be taken that the measured signals can precisely be related to the set test frequency. On the other hand, the sweep time should be as short as possible (up to 1000 frequency points per second). Finally the software should run under the widespread Microsoft *Windows 2000* or *XP* operating system, which makes coding challenging, since Microsoft *Windows* is not a real-time operating system.

Additionally, the standard PC contains a multitude of clock oscillators that are usually not synchronized with each other. The important clocks for the VNWA application are the

sound card clock oscillator, determining the sampling rate; a performance counter, which can be used to measure points in time with a resolution of about 1 microsecond; and the *Windows* multimedia timer which can fire up to 1000 *Windows* events per second. The latter is used to increment the test frequency. Since the multimedia timer fires quite randomly, even though the average firing rate is quite precise, it is necessary to measure the time of every frequency increment event with the performance counter and memorize it for the further analysis. Now these points in time need to be relocated precisely in the

audio data stream coming from the sound card. Since the sound card clock is usually decoupled from the rest of the PC and on top is not very accurate, it needs to be measured once against the *Windows* performance counter for a later time calibration. Additionally, the time delay between the actual start of the audio acquisition and the sending of the *Windows* command that starts acquisition is unknown. This time delay depends on the actual sound card hardware and on the set sampling rate. It can amount to up to 1 millisecond! I measure it once with a correlational method for time calibration. These two time

calibration data enable us to exactly find the data segment in the audio stream that belongs to a certain test frequency.

## Building Blocks

### Oscillators

DDS-oscillators<sup>7</sup> are a perfect choice to generate the RF and LO signals. They offer crystal stability, low phase noise and their frequency can be controlled digitally—and fast—with millihertz resolution. DDS oscillators work similarly to CD audio players. They approximate the wanted sine signal with a step function generated by a D/A converter. Because of this approximation, their output spectrums do not only contain the wanted frequency, but also quite a number of aliased frequencies. Figure 3 shows the unfiltered output spectrum of a DDS oscillator. Usually these aliasing frequencies are unwanted and blocked with a low-pass filter. Since real low-pass filters do not exhibit infinitely steep skirts, DDS oscillators can practically be used to generate sine wave signals of up to about one third of the DDS clock frequency. I selected an AD9851 with a maximum 180 MHz internal clock frequency, which can therefore generate sine waves up to about 60 MHz. I used this DDS type because its package is still big enough to be manually solderable with a soldering iron and I could use an available PC-board layout for my experiments.<sup>8</sup>

However, I soon found that the limited frequency range and the necessity for high-suppression filters (with their temperature stability problems) were bugging me. So I thought about how to explicitly make use of the DDS aliasing frequencies instead of suppressing them. I had to avoid all the aliasing frequencies of the RF oscillator mixing with those from the LO to the very same IF. The simple solution was to use slightly different clock frequencies for the two DDS oscilla-

tors. Experiments revealed that the two clocks must be tied to each other with a PLL circuit. Otherwise strong fluctuations of the IF would occur and deteriorate the phase accuracy. Figure 4 shows how I have generated the two interlocked clock frequencies of 30 MHz and 29.97 MHz with a simple PLL circuit. The 30 MHz XO signal is divided by 1024. The resulting 30 kHz signal is locked to the frequency difference obtained by mixing the XO signal with a 29.97 MHz VCXO signal. Alternatively, another AD9851 could be used to generate the 29.97 MHz clock out of the original 30 MHz DDS clock. This is possible since the AD9851 contains an internal clock multiplier  $\times 6$ .

Figure 5 shows an example calculation of how any aliasing frequency can be selected for the measurement by appropriate choice of the RF to LO offset. As can be seen from Figure 4, the DDS output power becomes zero at integer multiples of the DDS clock frequency  $f_{\text{clock}}$ . In the vicinity of these frequencies no measurements are possible because of lack of signal power.

Interference due to the lack of anti-aliasing filters occurs at frequencies where two spectral lines cross, for example at  $0.5 \times f_{\text{clock}}$ ,  $1.5 \times f_{\text{clock}}$ ,  $2.5 \times f_{\text{clock}}$  .... Thus, with some exceptions, the usable frequency range of the VNWA is extended dramatically.

Figure 6 displays the measured convolution

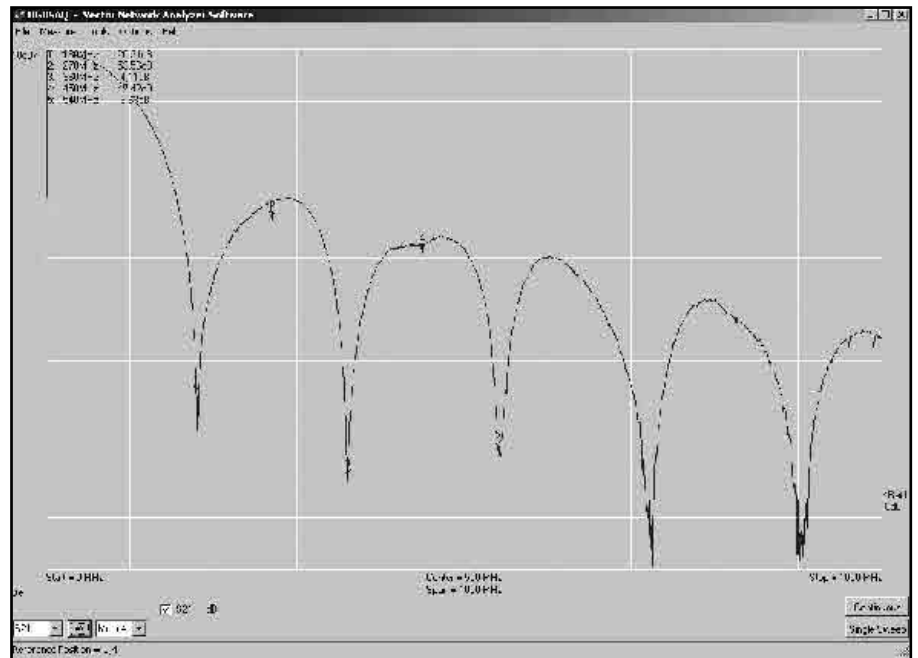


Figure 6 — Reference signal amplitude measured with the VNWA. Clearly, the structure resembles Figure 3.

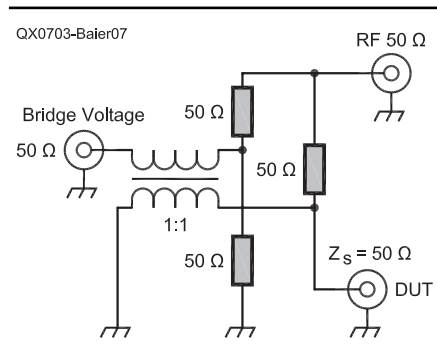


Figure 7 — Standard SWR bridge design.

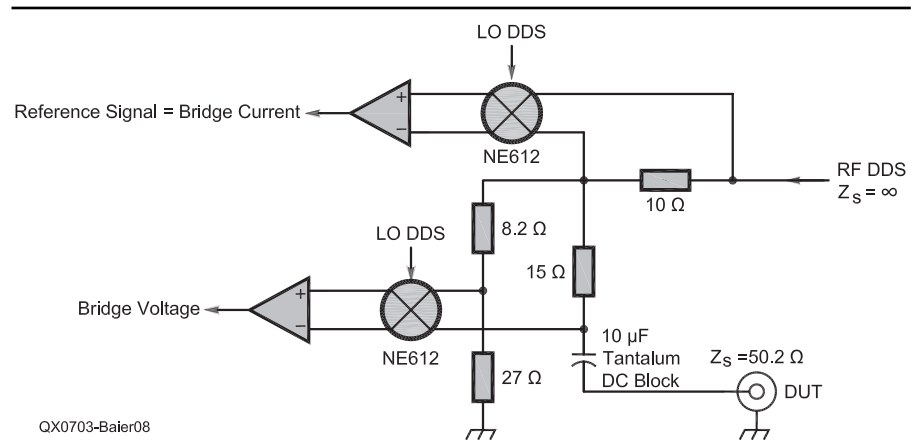


Figure 8 — Modified SWR bridge of the VNWA.

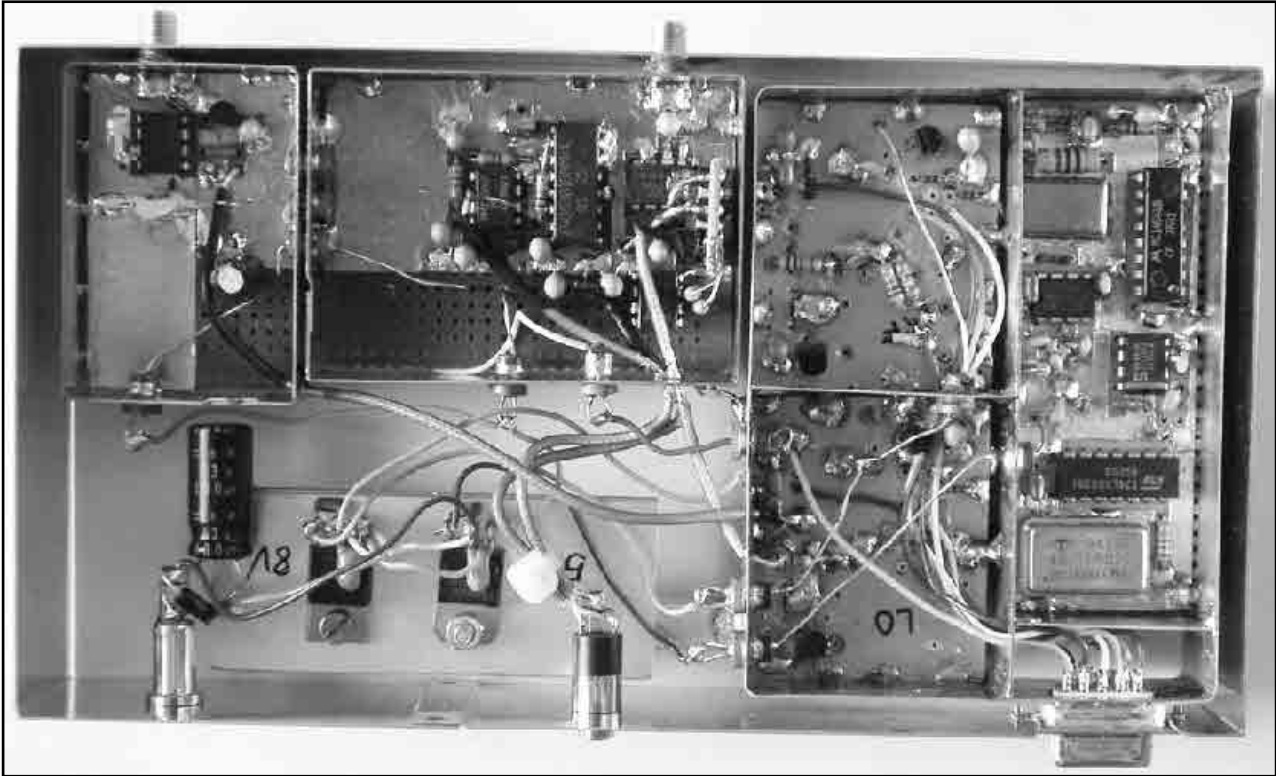


Figure 9 — Top view of the VNWA. From left to right one recognizes: RX mixer, TX mixers, DDS-oscillators, clock generator. Outer dimensions are 185 × 100 × 40 mm.

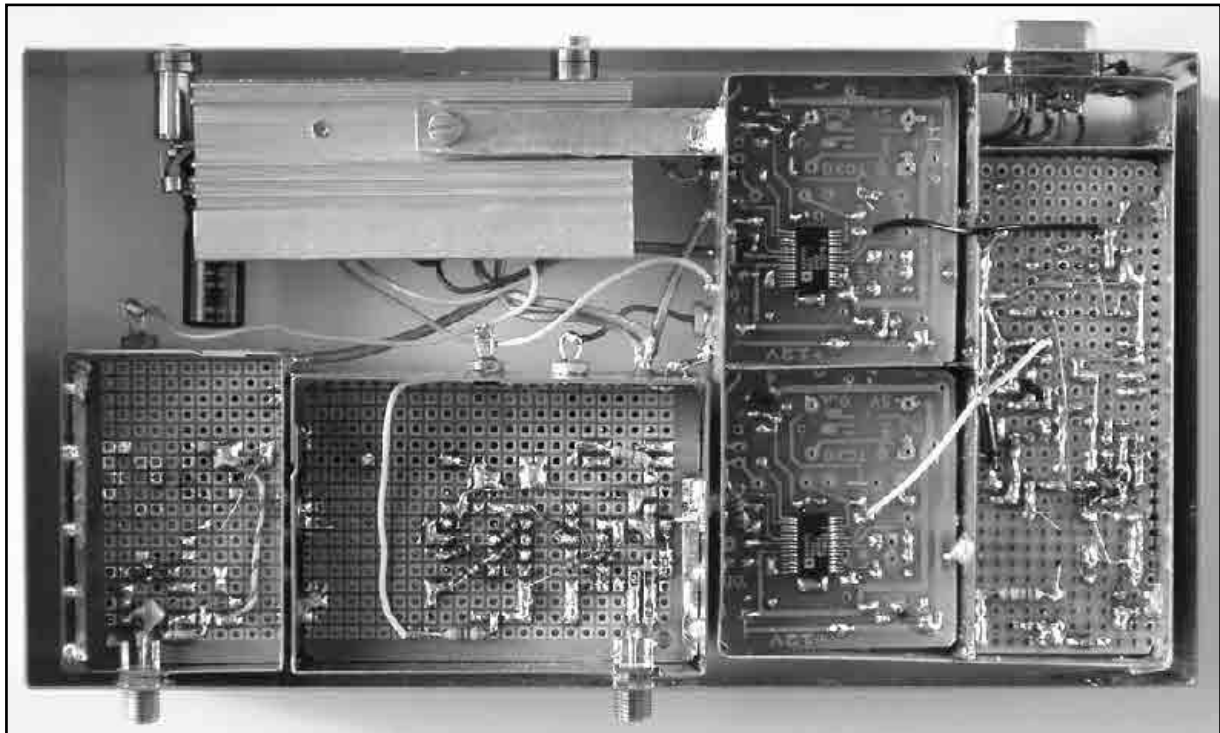


Figure 10 — Bottom view of the VNWA. Here, the two DDS chips and the SWR bridge can be seen.



of the RF and LO DDS spectra in the frequency range 0-1 GHz. It was obtained by detecting the reference signal amplitude with my homebrew VNWA. Clearly the spectral structure of Figure 3 can be recognized. Precise measurements can be performed in the frequency range 200 Hz to 160 MHz and 200 MHz to 330 MHz. Measurements in the 70 centimeter amateur band and above are still possible but are limited in precision because of low signal strength and poor mixer performance. It is remarkable that at 1 GHz a signal can still be detected stronger than 30 dB above the noise level.

### SWR Bridge and Mixer

Since I wanted to use my VNWA down to the audio frequency range, I could not use a directional coupler or a hybrid coupler for the reflection measurement, as in the designs of Notes 1 and 2. Instead, I selected a simple Wheatstone type SWR bridge, which works theoretically from dc to several GHz. Figure 7 shows the schematic of such an SWR bridge. This bridge type can readily be found in commercial equipment.<sup>9</sup> An important feature of SWR bridges is the well-defined 50-Ω source impedance at the DUT port as discussed above. In our example, this is guaranteed when all other ports are terminated with 50 Ω. The bridge voltage is detected through a 1:1 balun. It depends on the input impedance of the DUT and becomes zero if the DUT impedance is 50 Ω. Since it's close to impossible to build a passive BALUN operating from a few hertz to UHF, I used a generic balanced Gilbert-cell mixer of type NE612 instead to detect the bridge voltage. The same mixer type is also used for down conversion of the reference and through signals.

Because of its high input impedance of about 1 kΩ and the fact that the DDS output is a current source with almost infinite source impedance, the bridge resistor values required some redesign. Figure 8 shows my SWR bridge, which works nicely with standard resistor values. My prototype, which is built with non pre-selected resistors, achieves a directivity of 30 dB at 160 MHz. Also important: A good fraction of the DDS output power reaches the DUT.

At this point, I started to consider what signal the SWR bridge exactly measures. I considered the bridge as a 4-port device with the DDS connecting to port 1, port 2 connecting to the reference path, port 3 connecting to the reflect path and port 4 connecting to the DUT. Most interestingly, I found that no matter what the bridge S matrix looks like, the measured signal  $M$  = reflection signal / reference signal always depends on the reflection coefficient  $S_{11}$  of DUT in the very same way:

$$M = \frac{a \cdot S + b}{c \cdot S + 1} \quad [\text{Eq 2}]$$

If the bridge is of perfect design, then the constants  $b$  and  $c$  are zero (basic function of a good SWR bridge). In reality, the three numbers  $a$ ,  $b$  and  $c$  have to be found with the aid of three calibration measurements. These are performed with three different well known terminations, the so-called calibration standards. Usually the standards are chosen to be short, open and load=50 Ω.

Coming back to the hardware, I use a

CMOS switch matrix CD4053 to multiplex the reflected and the through signals. To improve the switch isolation from 50 dB to 100 dB, I use low-resistance HexFETs to short the unselected switch inputs. Finally, the two IF signals are amplified by a factor of 10 with differential amplifiers built out of op amps of type OP07 before they are fed into the sound card. Figures 9 and 10 show my prototype VNWA built into a 185 × 100 ×

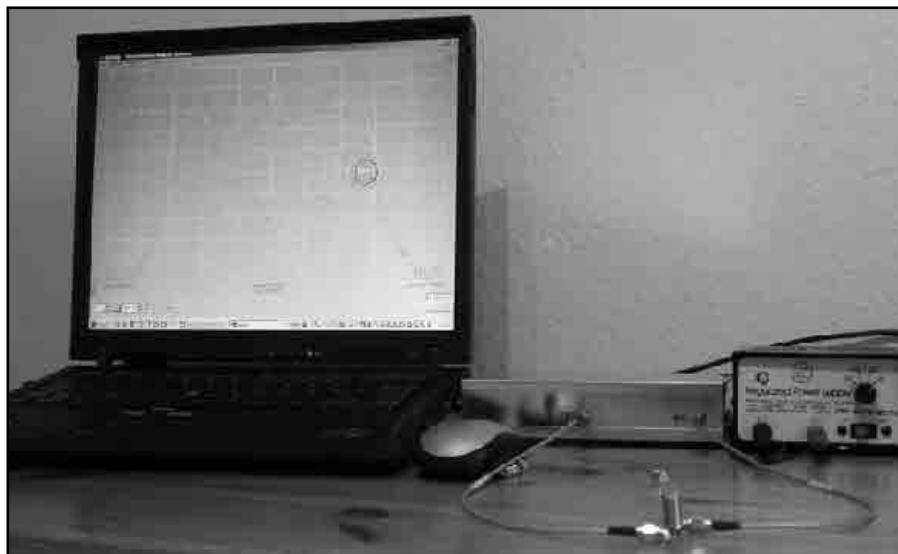


Figure 11 — Complete measurement setup with a monolithic crystal filter connected.

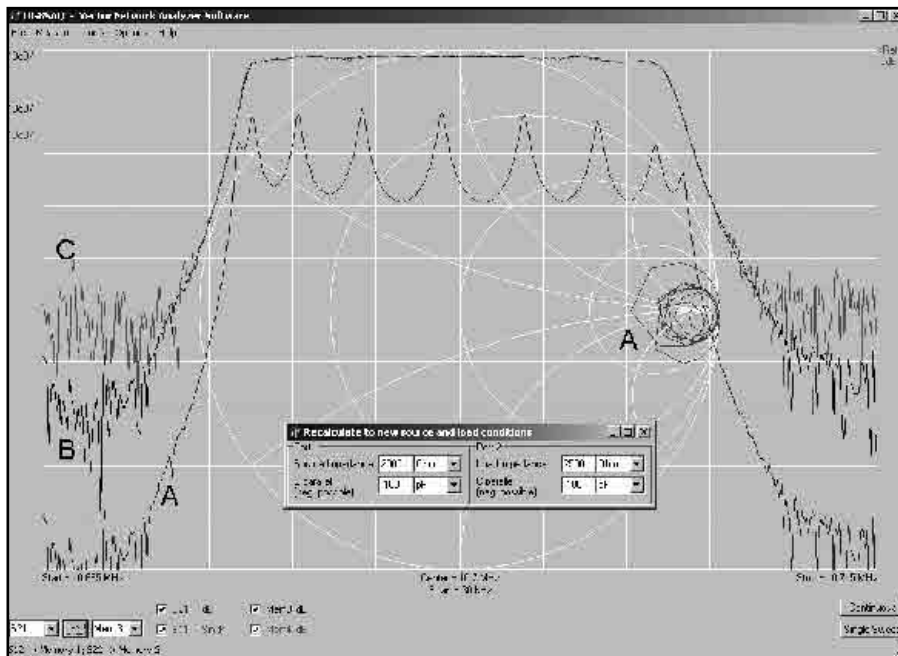


Figure 12 — Unmatched (A) and numerically matched (B) S-parameters of a 10.7 MHz monolithic crystal filter. For comparison, a numerically matched reference measurement obtained on an HP8753C is also plotted (C). The color version is available at [www.arrl.org/qxfiles/3x07\\_Baier.zip](http://www.arrl.org/qxfiles/3x07_Baier.zip).

40 mm sheet-metal enclosure. Except the DDS part, all components have been assembled onto experimental multipurpose PC boards that have been covered on the upper side with thin adhesive copper sheets for grounding and shielding. Figure 11 shows the complete measurement setup with a monolithic crystal filter connected to the VNWA.

### Test Results

Figure 12 shows S parameters of a 10.7 MHz monolithic crystal filter measured with 50 Ω source and load impedance (A). Because of the strong impedance mismatch between filter and VNWA, the filter transmission shows a considerable passband ripple. With a simulation tool embedded in my VNWA software, I have recalculated the measured filter S parameters to a 2000 Ω / 2500 Ω impedance environment (B). In addition, a reference measurement obtained on a HP8753C is also recalculated to the high-impedance environment and plotted (C). The match between my VNWA data and the HP8753C data is excellent. Another indicator for the good quality and consistency of the S-parameters measured on my VNWA is that the filter passband becomes perfectly smooth after impedance transformation. Erroneous measurements can be recognized by severe spikes in the pass band of high Q devices after impedance transformation as extreme impedance transformations magnify the effect of measurement errors.

Figure 13 shows the measured input reflection coefficients ( $S_{11}$ ) of two crystals unsoldered from a bridge type crystal filter. I have imported the very same measured S parameters into the simulation tool APLAC in order to calculate how the crystals would behave in a bridge type filter (Figure 14). The simulation results are shown in Figure 15. Apparently the measured S-parameters are well suited for a system simulation.

To test my VNWA at very low frequencies, I measured an old commercial three-pole 11 kHz LC band-pass filter. Figure 16 displays the results. Curve A shows the measured filter transmission in the original 50-Ω impedance environment. The same measurement recalculated to 610 Ω source and load impedances is also plotted (B). Curve C (noisy curve) was obtained by measuring the very same filter with 560 Ω series resistors between VNWA TX port and filter input and between filter output and RX port respectively. The 560 Ω resistors connected in series to the 50 Ω VNWA impedances form 610 Ω source and load impedances for the filter. Obviously, the calculated trace (B) and the measured trace (C) match nicely. Also, an additional insertion attenuation of calculated 21.7 dB caused by the resistors is basically observed. These measurements had been performed with a

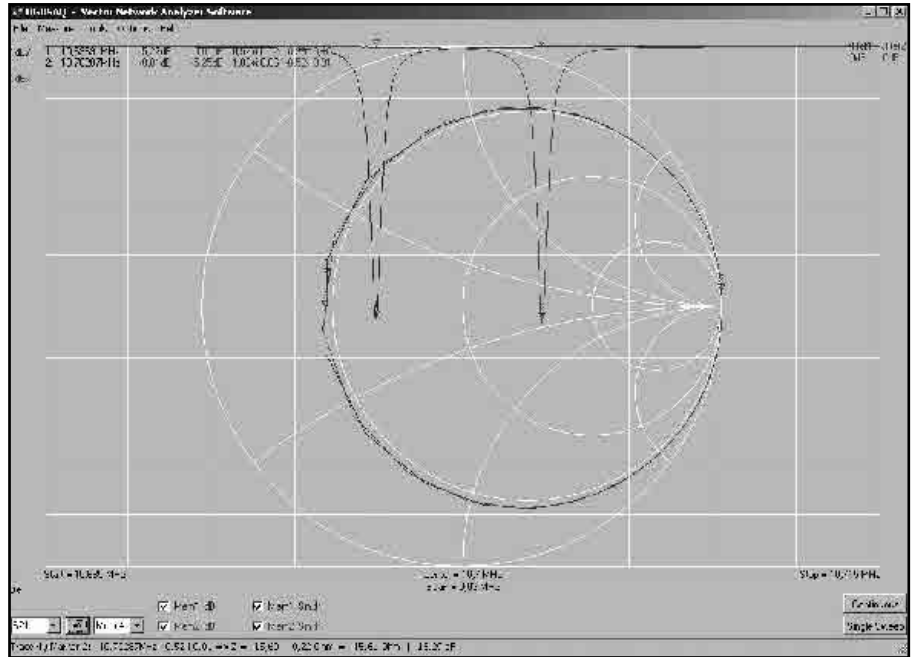


Figure 13 — Reflection coefficients of two different 10.7 MHz filter crystals.

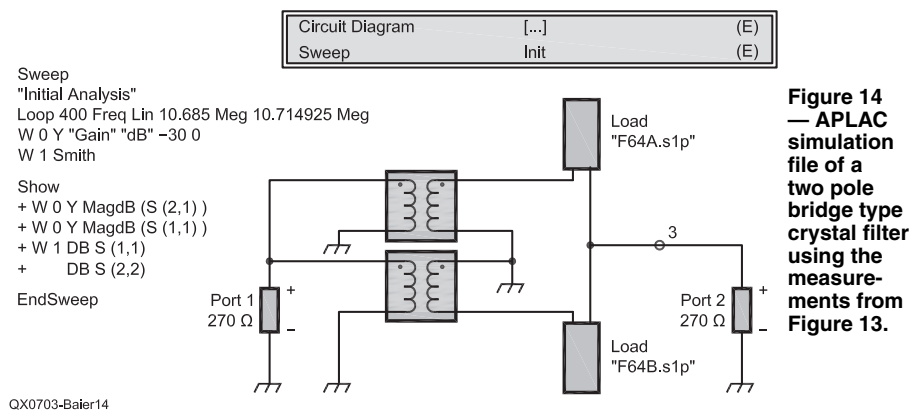


Figure 14 — APLAC simulation file of a two pole bridge type crystal filter using the measurements from Figure 13.

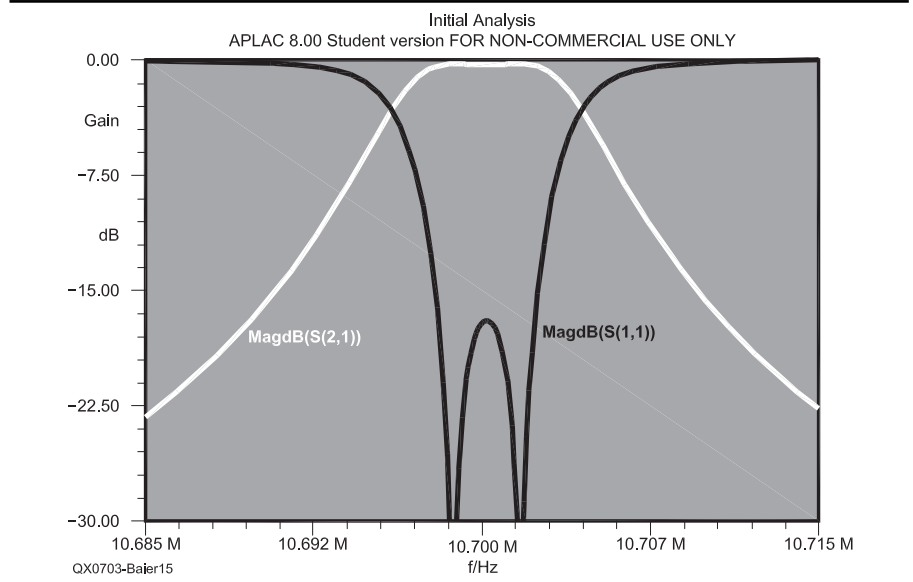


Figure 15 — Simulation results of the bridge type crystal filter from Figure 14.

10 dB coaxial attenuator connected to the VNWA TX port in order to obtain a well-defined 50  $\Omega$  source impedance of the TX port. At these very low frequencies, the dc blocking capacitor changes the bridge impedance.

Figure 17 shows a measurement performed in the UHF range. I have measured the S parameters of a 400 MHz crystal surface acoustic wave IF filter out of a GSM mobile phone (A). The reference measurements obtained on a HP8753C (B) prove that measurements are still possible at this high frequency range. The dynamic range is limited but impedances can still be measured reasonably accurately for Amateur Radio purposes. Figure 18 displays the very same measurements recalculated to 550  $\Omega$  source and load impedances, with inductors equivalent to negative capacitors of -40 pF connected in parallel to the filter input and output. Apparently, the obtained S parameters are still good enough to calculate a matching network. A 10 dB coaxial attenuator in front of the RX port additionally degraded the dynamic range during this measurement. It was necessary to obtain a well defined 50  $\Omega$  load impedance at the filter output.

### Summary and Outlook

I have described a very simple homebrew PC supported vector network analyzer which operates on all Amateur Radio bands below 500 MHz and even beyond. The wide operating frequency range was obtained by deliberately using aliasing frequencies generated by the DDS oscillators. The simplicity of design was reached by utilizing an IBM compatible PC to the greatest extent possible. The parallel printer port was used for control and the sound card was used for data acquisition. With this setup, a measurement resolution of 0.01 dB and 0.1° can be achieved. A dynamic range of over 100 dB can be reached.

The concept offers many possibilities for further improvement. With higher clocked DDS chips (for example, AD9858, 1 GHz clock) and improved mixers, the frequency range could simply be extended to beyond 2 GHz. Look at Note 10 for new developments and for my most recent VNWA software.

### Acknowledgments

Thanks to the following:

Wolfgang Schneider, DJ8ES for helping me get started with DDS technology.

All the people at Swiss Delphi Center who helped me solve coding problems and particularly to Marco Senn alias Jailbird who kindly provided some graphics code snippets.

Thanks to Stefan Fuchs for support with the reference measurements.

Last but not least thanks to Mike

Alferman, WA2NAS, for brushing up the wording of this manuscript.

### Notes

<sup>1</sup>Tom McDermott, N5EG, and Karl Ireland, "A Low-Cost 100 MHz Vector Network Analyzer with USB Interface", *QEX*, Jul/Aug 2004,

ARRL. See also [www.tapr.org/kits\\_vna.html](http://www.tapr.org/kits_vna.html).

<sup>2</sup>Homebrew-VNA by Paul Kiciak, N2PK; [n2pk.com/index.html](http://n2pk.com/index.html).

<sup>3</sup>[www.aplac.com/](http://www.aplac.com/).

<sup>4</sup>[eesof.tm.agilent.com/products/ads\\_main.html](http://eesof.tm.agilent.com/products/ads_main.html).

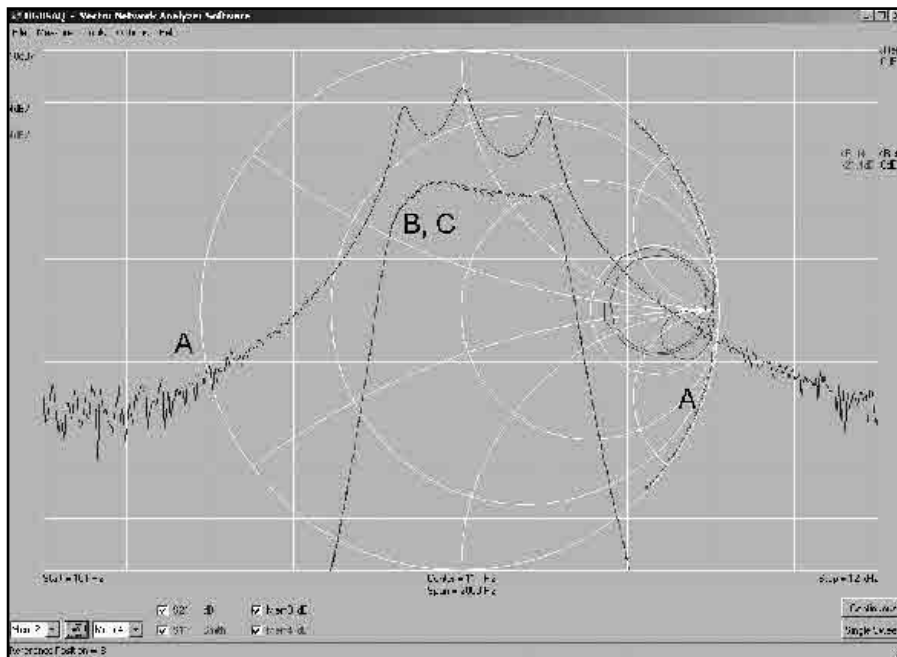


**Figure 16 — Unmatched (A, 10 dB/div) and numerically matched (B, 4 dB/div) S-parameters of a three pole 11 kHz LC-filter. A measurement of the same filter matched with two 560  $\Omega$  series resistors is also plotted (C, noisy trace, 4 dB/div, 21.4 dB offset to trace B). The color version is available at [www.arrl.org/qexfiles/3x07\\_Baier.zip](http://www.arrl.org/qexfiles/3x07_Baier.zip).**

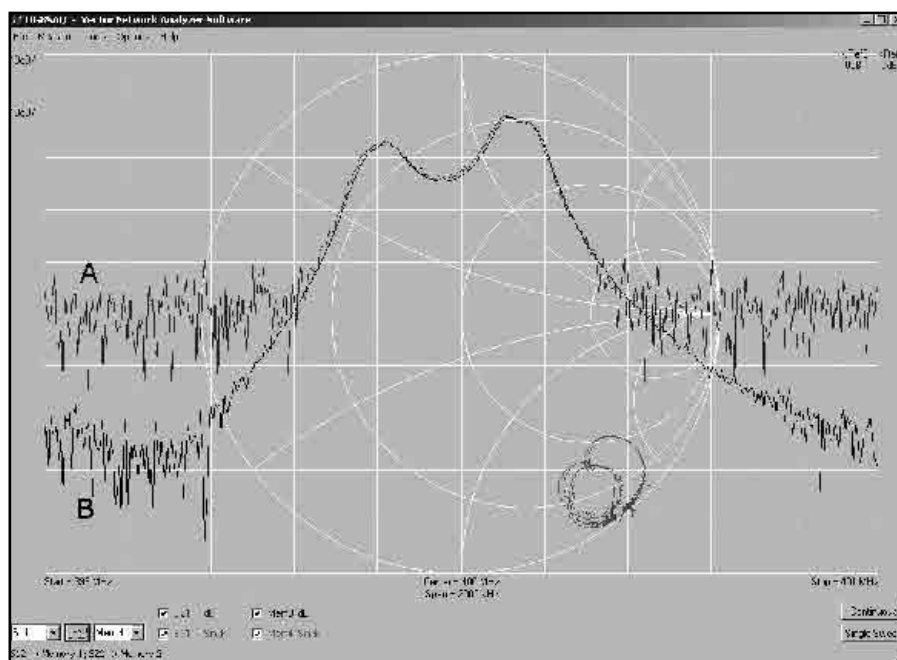


**Figure 17 — S-parameters of a 400 MHz crystal surface acoustic wave filter measured with VNWA (A) compared to HP8753C reference measurement (B). The color version is available at [www.arrl.org/qexfiles/3x07\\_Baier.zip](http://www.arrl.org/qexfiles/3x07_Baier.zip).**

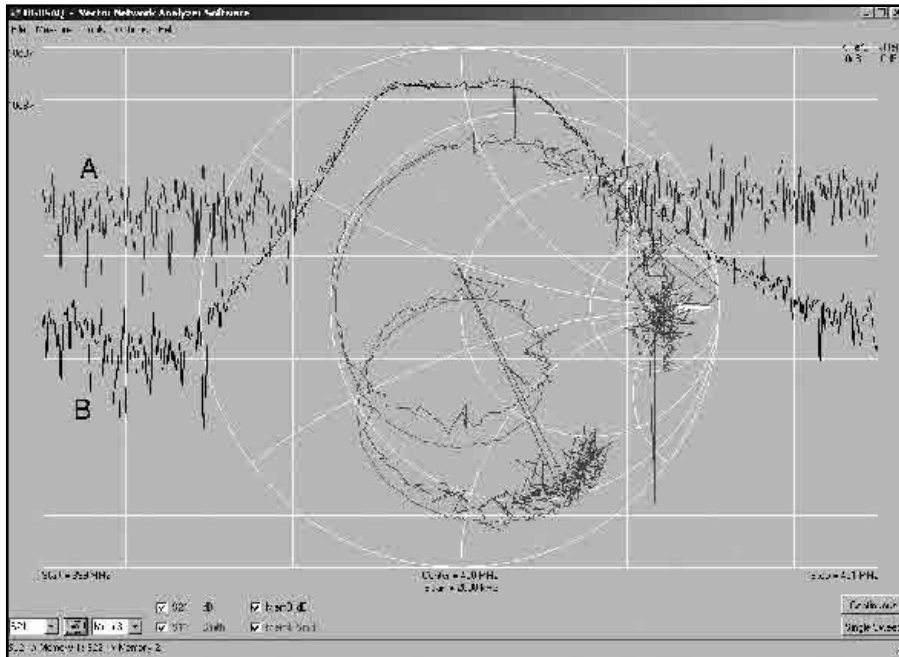


Figure 18 — S-parameters of Figure 17 numerically recalculated to an impedance level of  $550 \Omega$  with parallel inductors equivalent to  $-40 \text{ pF}$ .

<sup>5</sup>Sound Blaster Live! 24-bit; [www.soundblaster.com](http://www.soundblaster.com).

<sup>6</sup>[www.mydarc.de/DG8SAQ/SoundBlaster/index.shtml](http://www.mydarc.de/DG8SAQ/SoundBlaster/index.shtml).

<sup>7</sup>AD9851 data sheet by Analog Devices to be found at [www.analog.com](http://www.analog.com). Thanks for the free samples!

<sup>8</sup>C. W. Preuss, WB2V, "Building a Direct Digital Synthesis VFO," QEX, Jul 1997, ARRL.


<sup>9</sup>eg. Rohde & Schwarz SWR bridge ZRC.

<sup>10</sup>[www.mydarc.de/DG8SAQ/VNWA/index.shtml](http://www.mydarc.de/DG8SAQ/VNWA/index.shtml).

*Professor Dr Thomas Baier, MA, teaches physics, mathematics and electronics at the University of Applied Sciences in Ulm, Germany. Before his teaching assignment, he spent 10 years of work on research and development of surface acoustic wave filters for mobile communication with Siemens and EPCOS. He holds 10 patents. Tom, DG8SAQ, has been a licensed radio amateur since 1980. He prefers the soldering iron to the microphone, though. His interests span from microwave technology to microcontrollers. Lately, he has started Windows programming with Delphi. Tom spent one year in Oregon USA rock climbing and working on his master's degree.* **QEX**

1010 Jorie Blvd. #332  
 Oak Brook, IL 60523  
 1-800-985-8463  
[www.atomictime.com](http://www.atomictime.com)

# ATOMIC TIME



**14" LaCrosse Black Wall**  
WT-3143A     \$26.95

This wall clock is great for an office, school, or home. It has a professional look, along with professional reliability. Features easy time zone buttons, just set the zone and go! Runs on 1 AA battery and has a safe plastic lens.

**Digital Chronograph Watch**  
ADWA101     \$49.95


Our feature packed Chrono-Alarm watch is now available for under \$50! It has date and time alarms, stopwatch backlight, UTC time, and much more!

**LaCrosse Digital Alarm**  
WS-8248U-A     \$64.95


This deluxe wall/desk clock features 4" mil easy to read digits. It also shows temperature, humidity, moon phase, month, day, and date. Also included is a remote thermometer for reading the outside temperature on the main unit. approx. 12" x 12" x 1.5"

**LaCrosse WS-9412U Clock**     \$19.95


This digital wall / desk clock is great for travel or to fit in a small space. Shows indoor temp, day, and date along with 12/24 hr time. appx 6" x 6" x 1"



**WT-3143A - \$26.95**



**WS-8248 - \$64.95**



**WS-9412U - \$19.95**

1-800-985-8463  
[www.atomictime.com](http://www.atomictime.com)  
 Quantity discounts available!

Telling time by the U.S. Atomic Clock - The official U.S. time that governs ship movements, radio stations, space flights, and warplanes. With small radio receivers hidden inside our timepieces, they automatically synchronize to the U.S. Atomic Clock (which measures each second of time as 9,192,631,770 vibrations of a cesium 133 atom in a vacuum) and give time which is accurate to approx. 1 second every millenium. Our timepieces even account automatically for daylight saving time, leap years, and leap seconds. \$7.95 Shipping & Handling via UPS. (Rush available at additional cost) Call M-F 9-5 CST for our free catalog.

# Ceramic Resonator Ladder Filters

The author shows us how to design band-pass ladder filters using readily available ceramic resonators.

Dave Gordon-Smith, G3UUR

## Introduction

Ceramic resonators usefully fill the gap between LC tuned circuits and quartz crystal resonators in terms of their Q and frequency stability. They were originally developed for use in oscillators as a cheap alternative to quartz crystals, but they can also play a useful role as the main frequency-determining ele-

ments in band-pass ladder filters. The range of frequencies now covered by ceramic resonators is roughly 200 kHz to 32 MHz. Within this range there are many standard frequencies that are particularly useful for IF filtering applications in surplus receivers (250 kHz, 500 kHz, 560 kHz, and 1 MHz), and some that are extremely handy for front-end filtering on the amateur bands (2 MHz, 3.58 MHz, 3.69 MHz, 4 MHz and so on). In contrast to their quartz counterparts, the motional parameters of ceramic resonators give very convenient termination impedances and coupling capacitor values in the USB version

of the crystal ladder filter, which is shown in Figure 1A. Unfortunately, this configuration has not received much attention in Amateur Radio publications in the past, and its advantages in certain applications have been largely ignored.

The basis of the USB ladder configuration is the parallel-tuned circuit, coupled in a well-defined way to other tuned circuits and terminated appropriately, as shown in Figure 1B. To predict the values of coupling capacitors and termination resistances, the effective values of the parallel capacitances and inductances of the ceramic resonators

Whitehall Lodge, Salhouse Rd  
Rackheath, Norwich NR13 6LB  
United Kingdom  
g3uur@dg-s.fsnet.co.uk

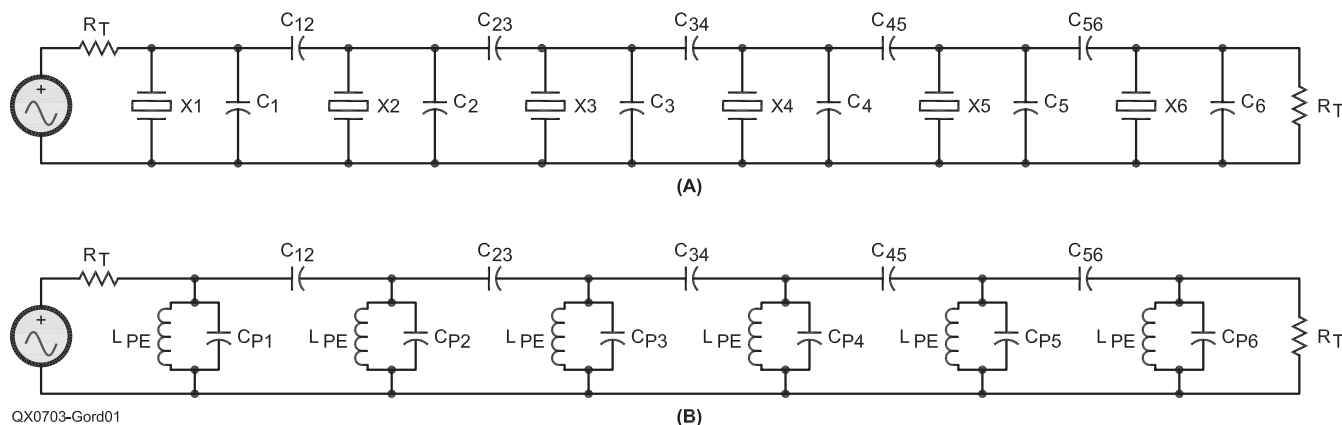
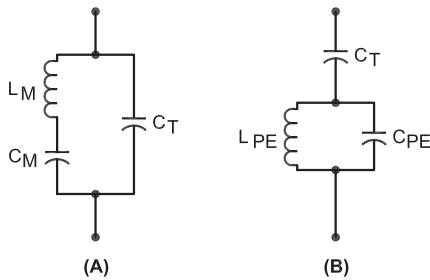


Figure 1 — Part A shows the circuit of the USB version of the standard crystal ladder filter. Part B shows the equivalent LC ladder filter on which the USB version is based.

Table 1  
3-dB-Down k and q Values for 0.01-dB-Ripple Chebyshev Filters

Order	q	$k_{12}$	$k_{23}$	$k_{34}$	$k_{45}$	$k_{56}$	$k_{67}$	$k_{78}$	$k_{89}$	$k_{9A}$	$k_{AB}$	$k_{BC}$
2	1.4829	0.7075										
3	1.1811	0.6818	0.6818									
4	1.0457	0.7370	0.5413	0.7370								
5	0.9766	0.7796	0.5398	0.5398	0.7796							
6	0.9372	0.8088	0.5500	0.5177	0.5500	0.8088						
7	0.9127	0.8289	0.5597	0.5168	0.5168	0.5597	0.8289					
8	0.8966	0.8430	0.5673	0.5198	0.5098	0.5198	0.5673	0.8430				
9	0.8854	0.8533	0.5733	0.5233	0.5092	0.5092	0.5233	0.5733	0.8533			
10	0.8773	0.8609	0.5778	0.5265	0.5103	0.5063	0.5103	0.5265	0.5778	0.8609		
12	0.8667	0.8712	0.5842	0.5313	0.5133	0.5063	0.5043	0.5063	0.5133	0.5313	0.5842	0.8712





**Figure 2 — Part A shows the standard electrical equivalent circuit of a piezoelectric resonator. Part B is the parallel-tuned equivalent of the resonator circuit shown in Part A.**

need to be determined. Since it is the reactance variation of these resonators that establishes the pass band, it is not simply a matter of working out the total parallel capacitance of the standard electrical equivalent circuit of Figure 2A. Instead, the change of reactance with frequency of these resonators has to be matched with a parallel-tuned version of the resonator equivalent electrical circuit as given in Figure 2B. The parallel equivalent capacitance ( $C_{PE}$ ) is then found to be equal to  $C_T(1 + (C_T / C_M))$ , where  $C_T$  is the total parallel capacitance across the series-tuned circuit ( $C_M$  and  $L_M$ ) of the resonator equivalent in Figure 2A. This total includes the static capacitance, any parallel tuning capacitance and the sum of the capacitors coupling to resonators on either side of the one being considered.  $C_M$  and  $L_M$  are the motional capacitance and inductance of the resonator, which are determined by the mechanical mode of vibration and the physical properties of the resonator material.

As can be seen from Figure 2B, the actual parallel equivalent circuit is a little bit more complicated than just a simple parallel-tuned circuit with this value of effective capacitance. In practical terms, however, ignoring the series capacitor only incurs an error of a few percent, provided that the interval between the filter center frequency and the series resonance of  $L_M$  and  $C_M$  is at least equivalent to 1.5 times the

–3 dB bandwidth ( $BW_{-3}$ ). Going beyond this limit badly compromises the stop-band performance, and also produces severe asymmetry in the transition region, so it is not worthwhile devising a more exact method of calculating the filter component values to include these cases. The simple method described here works well for cases that provide good stop-band performance with only a moderate worsening of the asymmetry. For a fixed frequency interval between the center frequency and the ceramic resonator series-resonant point, the symmetry of the filter response improves as the bandwidth is reduced. The ultimate attenuation also increases as the bandwidth decreases, just as with the LSB configuration. Greater ultimate attenuation and improved symmetry can also be obtained by using more resonators in the filter, but at the expense of increased insertion loss.

### Background Information

The values of the components of the electrical equivalent circuit of ceramic resonators have to be established in order to be able to predict the coupling capacitors and terminations required for a particular bandwidth and center frequency. Ideally, these should be obtained by characterizing the actual resonators to be used in the filter. Manufacturers have published some data on the electrical equivalents of their ceramic resonators, but this is difficult for amateurs to obtain. This information gives typical figures that appear to be within  $\pm 10\%$  of the measured values, which, of course, have their own error. If the manufacturer's figures are used as a basis for design, the parallel-resonant frequencies of individual resonators must still be measured in an oscillator circuit with a specific load capacitance ( $C_L = C_{I2} + C_{23} + C_2$ ) for matching purposes. Generally, the frequencies of the resonators should be matched to better than one-tenth of  $BW_{-3}$  at this stage. Small changes in the theoretical values of the parallel trimming capacitors can then be made, to allow for actual frequency differences, and each cell in the filter adjusted to resonate on the center frequency to better than one-twentieth

of  $BW_{-3}$  when the filter is put together — the closer, the better, as far as the perfection of the pass-band response is concerned.

A rough estimate of the motional capacitance of the widely-used Murata ceramic resonators can be made by measuring their static capacitance on a bridge or capacitance meter, and then dividing by 15.5 for the LF CSB series (suffixes D, E, J, and P), dividing by 9 for the HF CSA (MG) series, and dividing by 6.6 for the HF CSA (MT) series of resonators. This should provide values of motional capacitance within  $\pm 20\%$ , which is close enough for many applications. Usually, careful measurement of the motional parameters with special jigs will only provide results within  $\pm 5$  to  $\pm 10\%$ , so this crude estimate can be quite an effective way of getting near enough to the real values for practical purposes with little effort. The values of the coupling capacitors might have to be adjusted to get the desired bandwidth, however, if the initial figure is too far out to be acceptable.

### Design Procedure

Starting from a position where the resonators have been thoroughly characterized, or the manufacturer's data is available, the capacitance required to set the resonators at the desired center frequency,  $f_c$ , is calculated. It is most convenient to do this in terms of the shift,  $\Delta f$ , relative to the series-resonant frequency,  $f_R$ . The shift is calculated from:

$$\Delta f = f_c - f_R \quad (\text{Eq 1})$$

Then, the required total capacitance,  $C_T$ , to achieve this center frequency is calculated using:

$$C_T = C_M f_R / 2 \Delta f \quad (\text{Eq 2})$$

Alternatively, measurements of the static capacitance ( $C_0$ ) of the resonators, combined with oscillator checks on the load capacitance ( $C_L$ ) required to achieve the desired center frequency, can also provide a value for  $C_T$ .

$$C_T = C_L + C_0 \quad (\text{Eq 3})$$

Then using the divisors suggested previ-

**Table 2**  
**3-dB-Down k and q Values for 1-dB-Ripple Chebyshev Filters**

Order	q	k <sub>12</sub>	k <sub>23</sub>	k <sub>34</sub>	k <sub>45</sub>	k <sub>56</sub>	k <sub>67</sub>	k <sub>78</sub>	k <sub>89</sub>	k <sub>9A</sub>	k <sub>AB</sub>	k <sub>BC</sub>
2	2.218	0.7351										
3	2.216	0.6440	0.6440									
4	2.210	0.6353	0.5471	0.6353								
5	2.207	0.6338	0.5346	0.5346	0.6338							
6	2.205	0.6335	0.5313	0.5202	0.5313	0.6335						
7	2.204	0.6335	0.5301	0.5160	0.5160	0.5301	0.6335					
8	2.203	0.6336	0.5297	0.5143	0.5112	0.5143	0.5297	0.6336				
9	2.202	0.6337	0.5295	0.5136	0.5093	0.5093	0.5136	0.5295	0.6337			
10	2.202	0.6337	0.5294	0.5132	0.5084	0.5071	0.5084	0.5132	0.5294	0.6337		
12	2.201	0.6339	0.5294	0.5129	0.5076	0.5055	0.5049	0.5055	0.5076	0.5129	0.5294	0.6339

ously for the various series of Murata ceramic resonators, the value of  $C_M$  for the type chosen for the filter can be estimated, crudely, from measured values of  $C_O$ .

Next, the parallel equivalent capacitance is calculated from:

$$C_{PE} = C_T + C_T^2 / C_M \quad (\text{Eq 4})$$

All of the coupling capacitors can then be worked out using:

$$C_{nm} = C_{PE} \times k_{nm} / Q \quad (\text{Eq 5})$$

where  $n$  and  $m$  are integer numbers that correspond to the positions of the resonators on either side of the coupling capacitor being considered.  $Q$  is defined in the usual way as the quotient of  $f_c$  and  $BW_{-3}$ . The value of  $k_{nm}$  is determined by the type of filter required, and can be found in tables for the various types of filter response. Tables 1 and 2 give the values of  $k_{nm}$  and  $q$  for 0.01 dB and 1 dB ripple Chebyshev filters. These are the most appropriate choices for front-end and IF filtering, respectively.

Ideally, each resonator in the filter should be identical, and must experience the same total capacitance ( $C_T$ ) surrounding it. This includes the coupling capacitors and any additional parallel capacitance across the resonators. Note that with regard to tuning each resonant cell of the filter, the coupling capacitors appear as if they are in parallel with the resonators to which they are connected. Note also, that the filter design is symmetrical about the center component. Therefore, the theoretical parallel-tuning capacitors for each resonator in a six-pole filter are:

$$C_1 = C_6 = C_T - C_O - C_{12} \quad (\text{Eq 6})$$

$$C_2 = C_5 = C_T - C_O - C_{12} - C_{23} \quad (\text{Eq 7})$$

$$C_3 = C_4 = C_T - C_O - C_{23} - C_{34} \quad (\text{Eq 8})$$

The end resonators should have the largest values of capacitance across them because they have only one coupling capacitor connected to them, and the second and penultimate resonators should have the least because they have the two largest coupling capacitors associated with them. In practice, these values need to be adjusted to trim the resonance of individual ceramic resonators to the right frequency. The amount by which the adjustment should be made,  $C_A$ , can be roughly predicted for a small frequency change,  $\delta f$ , by the approximation:

$$C_A = C_T / ((C_M \times f_r / 2C_T \times \delta f) - 1) \quad (\text{Eq 9})$$

$C_A$  should be added to the theoretical value of  $C_n$  when the resonator frequency is higher than the ideal frequency by  $\delta f$ , and subtracted when it is low.

The upper limit of the center frequency of any filter made from a particular set of resonators depends on the desired bandwidth, and the difference between the natural parallel-resonant frequency of the resonators and

the target center frequency of the filter. The bandwidth can be too wide to be achievable if a center frequency is chosen that is too close to the natural parallel resonance of the available ceramic resonators. Whether there is a difficulty in this regard can be assessed by working out a design for a particular center frequency, and then checking to see if the total capacitance required exceeds the amount necessary to achieve the desired center frequency. If it does, a lower center frequency will have to be accepted, or other resonators with a higher parallel-resonant frequency must be sought for use in the filter.

The resistance required to terminate the filter is:

$$R_T = 2\pi q BW_{-3} L_{PE} Q^2 = qQ / (2\pi f_c C_{PE}) \quad (\text{Eq 10})$$

If a complex termination is required to absorb the reactance of devices, or circuit strays at either end of the filter, the values of the parallel capacitors across the end resonators can be adjusted accordingly, to allow for this.

### Design Example

An example that nicely illustrates the problem of choosing too high a bandwidth, or center frequency, for a given set of resonators is a 50 kHz wide, 6-pole, 0.01 dB ripple Chebyshev front-end filter using Murata CSA 3.69MG ceramic resonators, with a target center frequency of 3.75 MHz. The measured parameters for a batch of Murata 3.69 MHz resonators were  $C_M = 5.26$  pF,  $C_O = 37$  pF,  $f_r = 3.543$  MHz, and  $Q$  of around 1200. The spread in the series-resonant frequency of these resonators was  $\pm 3$  kHz, and in the parallel-resonant frequency with 8 pF load it was  $\pm 2$  kHz. Using these values, it can be established that the desired center frequency of the filter is an average of 207 kHz above the series-resonant frequency of these resonators. Therefore we can use Equation 2:

$$C_T = C_M f_r / 2 \Delta f \quad (\text{Eq 2})$$

$$C_T = 5.26 \text{ pF} \times 3.543 \times 10^6 \text{ Hz} / (2 \times 207 \times 10^3 \text{ Hz})$$

$$C_T = 45.0 \text{ pF}$$

Using this value of  $C_T$ , the effective parallel capacitance of the resonator at the desired center frequency can be calculated using Equation 4:

$$C_{PE} = C_T + C_T^2 / C_M \quad (\text{Eq 4})$$

$$C_{PE} = 45 \text{ pF} + (45^2 \text{ pF}^2 / 5.26 \text{ pF})$$

$$C_{PE} = 430.1 \text{ pF}$$

Then, this allows the coupling capacitors to be predicted using  $k$  values from Table 1 and Equation 5.

$$C_{nm} = C_{PE} \times k_{nm} / Q \quad (\text{Eq 5})$$

$$C_{12} = C_{PE} \times k_{12} / Q$$

$$C_{12} = 430.1 \text{ pF} \times 0.8088 / 75 = 4.64 \text{ pF}$$

$$C_{23} = C_{PE} \times k_{23} / Q$$

$$C_{23} = 430.1 \text{ pF} \times 0.5500 / 75 = 3.15 \text{ pF}$$

$$C_{34} = C_{PE} \times k_{34} / Q$$

$$C_{34} = 430.1 \text{ pF} \times 0.5177 / 75 = 2.97 \text{ pF}$$

Reference should be made to Figure 1A for the component designations used in this design example. Design symmetry about  $C_{34}$  gives  $C_{45} = C_{23}$ , and  $C_{56} = C_{12}$ . The second and penultimate resonators in the filter have the highest combination of coupling capacitance across them, and are a good indication of whether the choice of center frequency and bandwidth are feasible for a given set of resonators. The sum of  $C_{12}$  and  $C_{23}$  comes to 7.79 pF. Adding this to  $C_O$  gives a total of 44.79 pF, which is just under the value required for a center frequency of 3.75 MHz. For convenience, however, it is best to use preferred-value, fixed capacitors for coupling, and using the nearest ones to those predicted will cause the total capacitance across resonators 2 and 5 to increase to 45 pF (for  $C_{12} = C_{56} = 4.7$  pF,  $C_{23} = C_{45} = 3.3$  pF, and  $C_{34} = 3.0$  pF =  $2 \times 1.5$  pF), with  $C_2$  and  $C_5$  equal to zero.

This bandwidth is right on the limit for a center frequency of 3.75 MHz with these resonators. Increasing the values of the coupling capacitors to achieve a  $BW_{-3}$  greater than 50 kHz would necessitate a commensurate reduction in the center frequency. Note that, in this case, there is no need for parallel-tuning capacitors across resonators 2 and 5. Theoretically. The two resonators used in these positions must be exactly on frequency if the desired response is to be achieved, but in practice variations in the nominal capacitance of the coupling capacitors will allow some variation in the frequency of these resonators, as will the tolerance of the design. Small frequency adjustments can be made to individual cells in the filter, by making use of the tolerance variations in the nominal value of the parallel trimming capacitors and juggling the positions of the resonators used. The best strategy, however, is often to buy far more resonators than needed for the filter, and carefully select a set that don't require additional trimming to frequency at all. Otherwise considerable time can be spent matching the right trimming capacitors to individual resonators. The other parallel trimming capacitors required to complete the design are  $C_1 = C_6 = 3.3$  pF, and  $C_3 = C_4 = 1.7$  pF. The latter can be made 1.8 pF without much effect on the response.

The value of 430.1 pF for  $C_{PE}$  resonates at the center frequency of 3.75 MHz with  $L_{PE} = 4.188$   $\mu$ H. Therefore, the termination resistance for the filter is given by:

$$R_T = 2\pi q BW_{-3} L_{PE} Q^2 \quad (\text{Eq 10})$$

$$R_T = 2 \pi \times 0.9372 \times 50 \times 10^3 \text{ Hz} \times 4.188 \times 10^{-6} \text{ H} \times 75^2 = 6.936 \text{ k}\Omega$$

Obviously, this must be transformed down to 50  $\Omega$  for use in the front-end of a receiver. In order to provide the filter with source and

load impedances that are essentially resistive over the entire BW<sub>-3</sub> of the ceramic filter, the tuned transformers used for this transformation should have a maximum working Q of one-third the filter working Q. Convenience will determine the exact Q chosen below this maximum figure, and that will depend mainly on the inductance that gives a suitable number of turns to provide the right transformation ratio. This, of course, depends on the construction method and core material used, and is a matter of personal preference, or availability.

### Performance

The curve shown in Figure 3 gives some indication of the sort of attenuation that can be achieved on adjacent frequencies with a 6-pole, 0.01 dB ripple Chebyshev front-end filter. The insertion loss is about 3 dB for ceramic resonator Q values of around 1000 to 1200, and the bandwidth slightly short of the design figure at 49 kHz. The center frequency is also lower than the design target of 3.750 MHz by 3 kHz. The ultimate attenuation of signals at the low end of 80 m is in excess of 120 dB. The stop-band attenuation of this type of filter will always be asymmetrical because of the notch produced by each resonator at its series resonance, but this can often be used to advantage. The perfection of the pass-band response is very dependant on

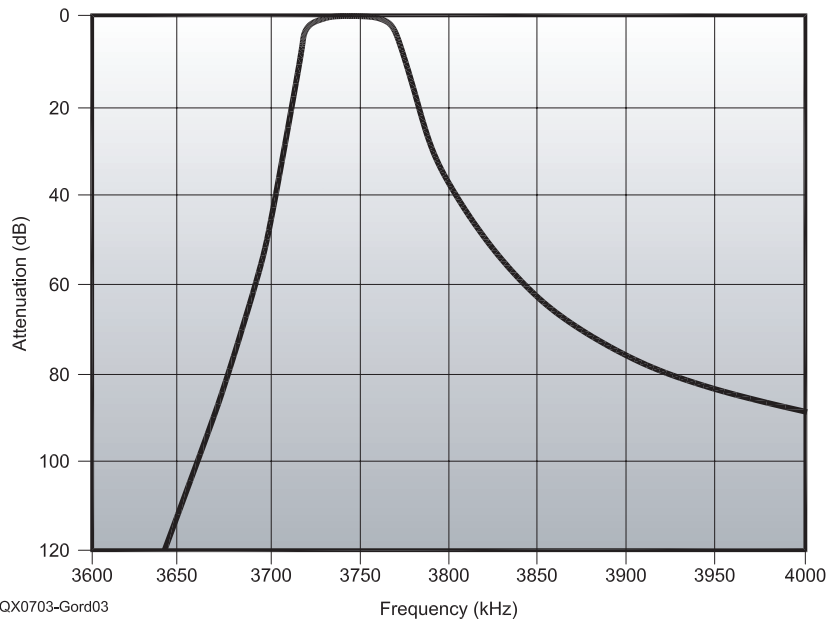


**Figure 3** — This graph shows the frequency response of a six-pole ceramic resonator USB ladder filter centered on 3747 kHz.

the care taken in selecting component values and trimming the resonators to frequency. Actual bandwidths will usually be smaller than the design value because the finite Q of the resonators reduces the effective coupling between them. If it is important to achieve a certain minimum bandwidth, the design bandwidth should be increased by 5 to 10% to allow for the effect of finite resonator Q.

### Conclusions

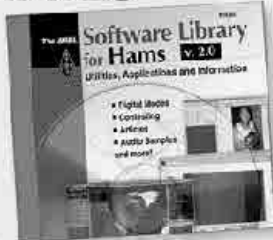
Despite its simplicity, the technique described in this article predicts coupling capacitor and termination resistance values that are close (within 5 %, usually) to the ideal values for the USB ladder configuration. The coupling capacitor and termination resistance calculations are consistent within themselves, in that they will produce the right response even though the bandwidth and center frequency might be in error because of inaccuracies in the measurement of resonator parameters. Generally, the bandwidth and center frequency accuracy will be limited more by the latter, and the effect of the finite Q of the resonators, than it will by the approximations used to simplify the design procedure.

USB ladder filters using ceramic resonators usefully fill a gap between LC band-pass filters and quartz crystal filters. The range of frequencies for which ceramic resonators are available encompasses both superhet IFs and several HF amateur bands. For front-end filtering applications, the same type of resonators can be used in the LSB ladder

configuration to provide a filter at the low end of an amateur band, and in the USB configuration to provide one at the high end. Using low frequency ceramic resonators in the 250 kHz to 1 MHz range, SSB and AM IF filters can be made with bandwidths and center frequencies that are not commonly available to the amateur.

*First licensed in 1965, Dave concentrated mainly on home construction and 160 meter DXing during his first few years on the air. Constructing his own equipment was a necessity in those early days because he was an impoverished schoolboy, but later it became a great source of fun and satisfaction. He holds a PhD in materials science from the University of Bath, and was a tenured member of the academic staff at Warwick University for many years, specializing in the characterization and study of defects in crystalline solids. During this time he was also a Visiting Professor at the State University of New York (Stony Brook) and a regular Guest Scientist at Brookhaven National Laboratory on Long Island. While at BNL, in the late '80s, he discovered a ham shack that was full of old tube radio gear from the '50s and '60s, and this revived his flagging interest in Amateur Radio. He's now semi-retired and a confirmed vintage radio enthusiast, spending much of his hobby time restoring and operating old tube equipment, as well as writing articles on that and his Amateur Radio experimental work from the past. You can reach the author at g3uur@dg-s.fsnet.co.uk.*

**NEW v. 2.0**




**The ARRL Software Library for Hams**

Quick access to utilities, applications and information:

- **Book excerpts** and a selection of articles from QST
- **Contesting software**
- **Jason** low-frequency digital software
- **Weather Satellite** software
- **WinDRM** digital voice software
- **HF digital software** for PSK31, MFSK16, MT63, RTTY and more
- **WSJT** software for meteor scatter and moonbounce **and more!**

**CD-ROM, version 2.0**  
ARRL Order No. 9825  
**Only \$19.95\***

\*shipping: \$6 US (ground)/\$11.00 International



**ARRL** The national association for **AMATEUR RADIO**

SHOP DIRECT or call for a dealer near you.  
ONLINE WWW.ARRL.ORG/SHOP  
ORDER TOLL-FREE 888/277-5289 (US)

QEX 3/2007

# Upcoming Conferences

## 2007 Eastern VHF/UHF Conference

The 33<sup>rd</sup> Annual Eastern VHF/UHF Conference will be held April 20, 21 and 22, 2007 once again at the Crowne Plaza Hotel in Enfield, CT. This year we will sponsor a Saturday afternoon mini conference — **Introduction to Microwaves** in addition to our regular 3 day conference activities. Friday night hospitality suite, Saturday lectures, band session discussions, vendor displays and noise figure measurements and evening banquet. Outdoor flea market Sunday morning (weather permitting) specializing in VHF and Up items.

Directions: Take Interstate 91 to Exit 49, bear right at end of the ramp, and take your immediate right (at the Friendly's) onto Bright Meadow Blvd. The hotel will be on your left.

See [www.newsvhf.com](http://www.newsvhf.com) or contact Bruce Wood, N2LIV, Conference Chairman at [n2liv@arrl.net](mailto:n2liv@arrl.net) or (516) 938-0698 ext 210, (days) for further info.

If you interested in presenting a talk or preparing a paper for inclusion in the Conference Proceedings please contact Bruce Wood. Paper submittal deadline March 1, 2007.

## 2007 Southeastern VHF Society Conference

The Southeastern VHF Society is calling for the submission of papers and presentations for the upcoming 11<sup>th</sup> Annual Southeastern VHF Society Conference to be held in Atlanta, Georgia on April 27 and 28, 2007.

Papers and presentations are solicited on both the technical and operational aspects of VHF, UHF and Microwave weak signal Amateur Radio. Some suggested areas of interest are: Transmitters; Receivers; Transverters; RF Power Amplifiers; RF Low Noise Pre-amplifiers; Antennas; Construction Projects; Test Equipment and Station Accessories; Station Design and Construction; Contesting; Roving; DXpeditions; EME; Propagation (Sporadic E, Meteor Scatter, Troposphere Ducting, etc.) ; Digital Modes (WSJT, etc); Digital Signal Processing (DSP) ; Software Defined Radio (SDR); Amateur Satellites; Amateur Television.

In general, papers and presentations on non-weak-signal-related topics such as FM repeaters and packet will not be accepted but exceptions may be made if the topic is related to weak signal. For example, a paper or presentation on the use of APRS to track rovers during contests would be considered.

The deadline for the submission of pa-

pers and presentations is March 2, 2007. All submissions should be in Microsoft *Word* (.doc) or alternatively Adobe *Acrobat* (.pdf) files. Pages are 8½ by 11 inches with a 1 inch margin on the bottom and ¾ inch margin on the other three sides. All text, drawings, photos, and so on should be black and white only (no color). Please indicate when you submit your paper or presentation if you plan to attend the conference and present it there, or if you are submitting just for publication. Papers and presentations will be published in bound proceedings by the ARRL. Send all questions, comments and submissions to the technical program chair, Jim Worsham, W4KXY, at [w4kxy@bellsouth.net](mailto:w4kxy@bellsouth.net). For further information about the conference please go to [www.svhfs.org](http://www.svhfs.org).

## Microwave Update 2007, October 18-20, 2007

### Call For Papers


Any topics related to microwave theory, construction, communication, deployment, propagation, antennas, activity, transmitters, receivers, components, amplifiers, communication modes, LASER and practical experiences welcome. Abstracts should be submitted by June 1 and completed papers and articles by August 15, 2007.

Please submit your papers, articles and abstracts to W2PED, [pdrexler@hotmail.com](mailto:pdrexler@hotmail.com) or to N2UO, [lu6dw@yahoo.com](mailto:lu6dw@yahoo.com) in Microsoft *Word* or as an Adobe PDF file. Diagrams, photos and illustrations should be in black and white. Hard copies may be mailed to Paul E. Drexler, 28 West Squan Rd, Clarksburg, NJ 08510.

### Microwave Update 2007 Details

Microwave Update 2007 will be held at historic Valley Forge, near Philadelphia, Pennsylvania. Thursday sightseeing or possible surplus tour. Conference Friday and Saturday; Flea Market Friday night, Vendors on site; Banquet Saturday night; Door prizes and raffles; Hospitality room. Hosted by the Pack Rats — Mt Airy VHF Radio Club. Spouses, friends and family invited. Alternative family/spouse programs available.

\$79 early-bird registration until 9/1 includes Conference, proceedings and banquet; \$89 from 9/1-10/1; \$99 thereafter. Extra banquet Tickets \$39. Special hotel rate \$92 per night. Full info and registration at [www.microwaveupdate.org](http://www.microwaveupdate.org).

Questions to chairpersons Philip Theis, Jr, K3TUF, e-mail [Phil@k3tuf.com](mailto:Phil@k3tuf.com) or David Fleming, KB3HCL, e-mail [kb3hcl@arrl.net](mailto:kb3hcl@arrl.net) 

## WANTED: C++ PROGRAMMER

We need a part time C++ programmer who likes to work at home but lives in the Orange County/Los Angeles area. We need to automate our test procedures, which involve RF transmitters and receivers to determine if production products pass or fail. Tests include determining RF output, current consumption, PLL lock range, frequency accuracy, and receiver sensitivity by checking each section with a fully or semi-automated test program.

We need the following:

- Someone with experience writing Visual C++ programs allowing the PC to control the test equipment with RS-232 and/or GPIB.
- You need to be familiar with RF test equipment such as spectrum analyzers, oscilloscopes, signal generators, and frequency counters.
- Be familiar with troubleshooting of RF and digital circuits.
- Be able to control relays, switches, etc. through PC I/Os with Visual C++.
- Have TCP/IP programming experience with Visual C++.
- Have CGI programming experience in any language.
- Robotic experience a plus.
- We would like to see examples and/or samples of your past work.



**COMMUNICATIONS SPECIALISTS, INC.**  
426 WEST TAFT AVENUE • ORANGE, CA 92865-4296  
714.998.3021 • FAX 714.974.3420  
US & CANADA 800.854.0547 • FAX 800.850.0547  
[www.com-spec.com](http://www.com-spec.com) E-mail: [spence@com-spec.com](mailto:spence@com-spec.com)

## Advanced Power Technology Acquired by Microsemi

Several recent *QEX* articles have mentioned Advanced Power Technology parts. Advanced Power Technology was acquired by Microsemi Corporation in 2006. For the immediate future you will still find their Web site at [www.advancedpower.com](http://www.advancedpower.com) but you can also find them listed under [www.microsemi.com](http://www.microsemi.com) going forward. The internal email addresses have changed to the microsemi.com domain. They continue to sell and support the RF power transistor lines that you have seen in *QEX*.

## American Technical Ceramics Adds Wideband Capacitor

ATC has added another component to the list of wideband capacitors. The UBC™ ATC 545L series of capacitors feature low insertion loss from 16 kHz through 40 GHz. The line has only two parts so far. One is 100 nF at 10 working voltage (WV) and the other is 100 nF at 16 WV. Normal ceramic capacitors in the 100 nF range have significant equiva-

lent resistance and inductance near 100 MHz, so you need to parallel them with ceramic or porcelain capacitors in the 20 pF to 100 pF range to achieve useful transmission across a wide frequency range.

These new capacitors come in a 0402 surface-mount package that can be mounted in any orientation. Some other wideband capacitors are asymmetrical and require a particular orientation for mounting. Another problem with normal ceramic capacitors is a significant temperature coefficient of capacitance. These new parts have  $\pm 15\%$  temperature coefficient.

American Technical Ceramics, One Norden Lane, Huntington Station, NY 11746; Phone (631) 622-4700; Fax (631) 622-4748; Email [sales@atceramics.com](mailto:sales@atceramics.com)

These parts are available through distribution, including Richardson Electronics. Find them on the Web at [www.rell.com/](http://www.rell.com/). Go to the RF/Wireless Communications Group to find the ATC capacitors. Phone: 1-800-RF POWER (1-800-737-6937); E-mail: [rwc@rell.com](mailto:rwc@rell.com)

## Hittite Announces Low Noise Amplifiers

Hittite has announced two new GaAs Phemtp MMIC low noise amplifiers for the microwave bands. The HMC564LC4 is rated at 1.8 dB noise figure and covers 7 GHz to 14 GHz. It has a 13 dBm 1-dB compression point. It still has full gain in the 5.6 GHz band and useful (but reduced) gain down to the 3.4 GHz amateur band. The HMC565LC5 is rated from 6 GHz to 20 GHz with a 2.4 dB noise figure. It has a 10 dBm 1-dB compression point. It has useful gain from 5 GHz to 25 GHz, so it covers three amateur bands. Both parts require no external matching to 50  $\Omega$  and have an internal dc block on both input and output.

Parts can be ordered directly from the Hittite Web site with a minimum order of 10 parts. The HMC564LC4 is \$17.98 each and the HMC565LC5 is \$20.79 each.

Hittite Microwave Corporation, 20 Alpha Rd, Chelmsford, MA 01824; Phone (978) 250-3343; Fax (978) 250-3373; Web site [www.hittite.com](http://www.hittite.com)

**QEX**

# New Books

Doug Smith, KF6DX  
[kf6dx@arrl.org](mailto:kf6dx@arrl.org)

## Digital Communications Systems Using SystemVue

By D. Silage, *Da Vinci Engineering Press, Charles River Media, Hingham, MA, 2006, ISBN 1-58450-850-7, 365 pp plus CD. Cover price: \$49.95 US, \$66.95 Canada.*

Two timeless truths reverberate down the halls of academia, throughout engineering laboratories and around production shops worldwide. They are: "You must have the right tools for the job," and "It's nice to know what you're doing at every stage of the game." To those utterances, I'd have to add what Mom told me: "Son, there's no substitute for experience." *Digital Communications Systems Using SystemVue* gives all that to students of digital communications systems over a broad range of levels.

This new book is an outgrowth of the author's direct experience teaching the theory and practice of both analog and digital systems. What makes it truly outstanding is its emphasis on simulating practical systems in realistic environments, rather than on the exact numerical solutions to equations.

Thus, the book includes little discussion of the underlying theory of digital systems; but as a supplement to theoretical studies, it is excellent and *SystemVue* is quite a versatile tool.

The Textbook Edition of the *SystemVue* software included with the book allows you to view block diagrams of digital communications systems on your computer screen and to analyze performance. Without doubt, such schematic entry makes it relatively fast and easy to explore trade-offs among noise, nonlinearities and other deleterious effects while optimizing the design. Results may be presented in time and frequency domains. The proper approach to, and limitations of, simulation are illustrated.

The book specifically addresses various forms of digital modulation, including just about everything from pulse amplitude modulation (PAM) and frequency shift keying (FSK) to direct-sequence (DSSS) and frequency-hopping spread-spectrum (FHSS). Synchronization, channel modeling and equalization get fair coverage.

Naturally, a good understanding of analog signals is necessary for any communications designer, too. Chapter 6 contains a treatment of sampling and quantization, featuring spectra of sampled signals and analyses of coding schemes for audio. That part of the book deserves particular attention, since digital signal processors (DSPs) often embody the preferred implementations of systems these days.

The application of the Textbook Edition software included is intentionally limited to what's described in the book. An evaluation version of *SystemVue Professional* would allow models to be extended and new designs to be investigated. Check it out because it's very powerful software. Additional instructional and experimental materials are available on the author's Web site at: [astro.temple.edu/~silage](http://astro.temple.edu/~silage).

Dennis Silage, PhD, K3DS, is Professor of Electrical and Computer Engineering at Temple University in Philadelphia. Dennis graciously gives his time to those interested in Amateur Radio.

**QEX**



# Letters to the Editor

## Q Calculations of L-C Circuits and Transmission Lines: A Unified Approach (Sep/Oct 2006)

Hello Doug,

I would like to add the following corrections to Equations 30 and 31 of my article.

They should read as follows: (Thanks to Dan Maguire, AC6LA for reporting these errors).

$$R = 2 \alpha_c \operatorname{Re} [ Z_o ] \quad (\text{Eq 30})$$

Where  $R$  is in ohms / foot and  $\alpha_c$  is the attenuation in nepers / foot due to conductor losses.

$$G = \frac{2 \alpha_d \operatorname{Re} [ Z_o ]}{| Z_o |^2} \quad (\text{Eq 31})$$

Where  $G$  is in siemens / foot and  $\alpha_d$  is the attenuation in nepers / foot due to dielectric losses.

The coefficients  $\alpha_c$  and  $\alpha_d$  are obtained from  $A_{o,c}$  and  $A_{o,d}$ , as in Equations 18 through 21.

Please add a PDF version of the MathCad files on ARRL Web at [www.arrl.org/qex-files/](http://www.arrl.org/qex-files/). (This has been done. Look for **9x06\_Audet.zip** in the files for the September 2006 issue. — Ed.)

MathCad Explorer for MathCad files, V8 and below, may also be downloaded from: [www.ecs.soton.ac.uk/~msn/book/mcexp802.exe](http://www.ecs.soton.ac.uk/~msn/book/mcexp802.exe)

— Thanks, Jacques Audet, VE2AZX; [ve2azx@amsat.org](mailto:ve2azx@amsat.org); Web: [www.geocities.com/ve2\\_azx](http://www.geocities.com/ve2_azx)

## An Alternative Transmission Line Equation (Jan/Feb 2007)

Doug,

Oops! On page 15 in Equations A6A and A6B (last step in both) [you are wrong]. After one finishes the hard/interesting part it's easy to lose focus and mess up something basic. — 73, Martin Davidoff, K2UBC; [MDAVIDOFF@ccbcmd.edu](mailto:MDAVIDOFF@ccbcmd.edu)

Martin,

You're right! The expressions at the right-hand sides of those equations are wrong; but in the center section, they are correct.

$$\sinh 2x = \frac{e^{2x} - e^{-2x}}{2} = \frac{e^2 (e^x - e^{-x})}{2} \quad (\text{Eq A6A})$$

$$\cosh 2x = \frac{e^{2x} + e^{-2x}}{2} = \frac{e^2 (e^x + e^{-x})}{2} \quad (\text{Eq A6B})$$

— 73, Doug Smith, KF6DX, QEX Editor; [kf6dx@arrl.org](mailto:kf6dx@arrl.org)

Doug,

Thanks for the presentation of Ron Barker's novel approach to the transmission line equation. Since I am one of those who has struggled with hyperbolic functions in the past, Ron is providing relief to a most vexing problem. I anticipate that his new equations will be the standard we hams will be using in the future. His article and others like it are why I subscribe to QEX magazine: to get answers that I won't find anywhere else. — 73, Patrick Wintheiser, W0OP; [patw@goproweb.com](mailto:patw@goproweb.com)

Dear Doug and Ron,

I read carefully this article, which I found very interesting. I would like to add two thoughts about the paper:

1) By looking at Equation 6, we could think that voltage across the load ( $V_A$ ) only depends on the load impedance ( $Z_A$ ), the characteristic impedance of the line ( $Z_0$ ), and the input voltage ( $V_S$ ). Equation 6 is actually valid in a very particular case.

Indeed,  $V_A$  generally also depends on the length of the line.  $V_A$  can be independent of the line length in some very particular cases, such as when the line is terminated in a matched load and the line has no loss.

2) You say that Equation 7 is only valid when the line is terminated in a matched load. This is indeed the case. After that, Equation 7 is used to deduce Equation 10. So the validity of Equation 10 has only been proven for matched loads, and leads to  $P_A = 0$  because our hypothesis is  $Z_A = Z_0$ ! But is Equation 10 still valid for the unmatched load case, and is it correct to use it to compute Equation 11A (non-matched load)?

The answer is actually yes, but the proof is quite more complicated than in the article, and requires solving differential equations.

Congratulation on your article.

— 73, Christophe Bourguignat, F4DAN; Web site [f4dan.free.fr](http://f4dan.free.fr)

Hello Christophe,

Thank you for your e-mail and for your interest in my article. I would first like to apologize for the delayed response. When I downloaded your e-mail I was in the final stages of preparing to leave for a six-week trip to visit family in Australia, where I am now, still somewhat jetlagged.

With regards to your first point Equation 6 is not a "very particular case."  $V_A$  is a vector quantity and the equation gives it in rectangular form as a complex number. The magnitude of  $V_A$  is independent of line length for any termination other than the effect due to line loss.

Turning now to your second point I think

that the Thevenin derivation of Equation 10 is valid but maybe I was economical with the detail in my explanation. Essentially what the Thevenin Theorem states is that any linear network of voltage sources and impedances, however complex, has an equivalent circuit comprised of one zero impedance voltage source (emf) in series with one fixed impedance, the source impedance,  $Z_0$ .

A consequence of the theorem is that the maximum power that can be drawn occurs when the load impedance is equal to the source impedance, and the voltage across the load will be half that of the source voltage (emf). For any other value of load impedance the power delivered will be less and  $V_A$  will no longer be  $V_S / 2$ .

By virtue of its characteristic impedance, a transmission line meets the definition of a linear network to which the Thevenin theorem can be applied. When the line is terminated into a matched load  $V_F$  is equal to  $V_A$  and  $V_S$  (emf) must be equal to twice  $V_F$  as per Equation 7. When there is a mismatch,  $V_A$  is not equal to  $V_F$ , the difference being  $V_R$  as per Equation 8. Your assertion that the derivation of Equation 10 was based on a matched load situation failed to take account of Equation 8, which is a key stage of the derivation.

I have seen the differential equation derivation of Equation 10 somewhere but my math was not up to understanding it and I can't remember where I saw it. — 73, Ron, G4JNH; [g4jnh@onetel.com](mailto:g4jnh@onetel.com)

Doug,

Regarding this article in QEX, I mentioned in a letter to Ron only one of several problems I have. After pouring over it in great detail I decided it was all there because there might be someone who wanted to apply the transmission line equation and didn't have access to "modern machines" to do the job.

I went to my trusty Microsoft Excel spreadsheet and found that the hyperbolic functions are an integral part of the tool set to do functional calculations. It should be easy for any up-to-date ham to do calculations in Excel. If not, then I think the scarce resource of available pages and available time should be used to teach hams how to calculate things. Of course, their use of antenna modeling programs suggests that they have, as a group, a sufficient sophistication to handle Excel. So, I think that Ron's article was not the best use of the space in QEX. It was, however, entertaining. I offer these comments only as a "soft" suggestion.

I really appreciate your work as editor and author and moderator of the journal. The quality of QEX is high and I know that



you, probably, do any refereeing that gets done. If that is so, another suggestion I have is that a number of the readers be enlisted as a group of reader/reviewers to comment to you on publications under consideration. I'm sure you have much experience with reading refereed publications. Or this is already going on and I am just ignorant of it?

Again, thank you very much for a great publication.

— 73, Steven Bomba, K9IER; [steven@sjbomba.com](mailto:steven@sjbomba.com)

**Hi Steven,**

I'm a bit puzzled about the nature of your argument. Yes, the article is there for the purpose of explaining how computations may be simplified enough to be done on a standard hand calculator. Underlying that, though, is the exposure of basic facts about transmission line behavior that may not otherwise have been recognized by readers.

At *QEX*, we employ a team of Technical Advisors who review articles and make recommendations. While the final decisions rest with me, the weight of their comments is considerable. Our Contributing Editors also have a big say in what gets published and how. On the other hand, we are not swamped with submissions and we welcome your contributions. Perhaps you have some particular subject about which you are passionate, that you'd like to see grace our pages, eh? My door is always open.

— 73, Doug

**Hello Doug,**

I have found that many technicians have difficulty in understanding logarithms, so I found a simple method of calculating them

without using a table or a calculator. Check out this page on my Web site:

[www.science-site.net/logcalc.htm/](http://www.science-site.net/logcalc.htm/)  
— 73, Weldon Vlasak, KCØFYW; [adaptent@alltel.net](mailto:adaptent@alltel.net)

**Remote Possibilities (Empirical Outlook, Jan/Feb 2007)**

**Hi Doug,**

I am a relatively new subscriber to *QEX* (I joined at Dayton last year) and am enjoying the technical content, particularly your articles on receiver performance.

I have just received the Jan/Feb issue and was immediately drawn to the heading of your editorial, as I wrote a series of articles in RSGB *RadCom* 18 months ago called "There's a remote possibility." You may or may not know that December 1, 2006 was a major milestone for amateurs in the UK when a new license was introduced by Ofcom to allow remote operation to take place. This was largely as a result of the work I have been doing since 2000 under a special "research permit" that I obtained from the regulatory authority with the help of the RSGB that allowed me to experiment with remote operation.

I started off with a Kachina 505DSP complete with remote system, which worked very well but was limited for me by the audio delays on the single dial-up line. I don't like the idea of having an unattended PC at the remote site so I have gone down the route of using port redirection software and Ethernet-to-serial servers at the remote site. I used an ISDN line where I could use one line for control and one line for the audio. Unfortunately, I have just lost my remote site; it was sold and the new owners required me to move out.

The key issues as far as I am concerned are:

- 1) Latency: The system has to be able to

work well under contest search-and-pounce mode.

2) A PC makes a lousy tool for tuning a rig! I used a technique available in *TRX-Manager* to tune a rig normally at home, and the remote rig was kept in sync through the software.

3) I think there is scope to use remote head rigs such as the Kenwood TS-480, which would give a more normal feel to tuning. I have been planning to implement two TTL-to-Ethernet adapters back to back, to allow the remote head to be used over an (extended) LAN or even WAN.

4) I would like to see an SDR with a proper hardware front panel to give a good user interface and facilitate remote operation.

5) We need to think about the feedback necessary to ensure the actions commanded have taken place.

It will be interesting to see how remote operation develops and what *QEX* can do to push it forwards. If I can assist in any way I would be willing to do so.

— 73, Dave, G3UEG; [dave@g3ueg.co.uk](mailto:dave@g3ueg.co.uk)

**Octave for Transmission Lines (Jan/Feb 2007)**

**Hi Doug,**

I received a query from a reader asking whether the code for my article would be posted for download from [www.arrl.org](http://www.arrl.org). I don't see it there, maybe because I submitted the code embedded in the Word file that contained the text.

If you would be interested in making the code available, I'll send you the source code from Table 1 as a text file.

— 73, Maynard Wright, W6PAP; [m-wright@eskimo.com](mailto:m-wright@eskimo.com)

**Hi Maynard,**

It is done. The file is available at [www.arrl.org/qexfiles](http://www.arrl.org/qexfiles). Look for **1x07\_Wright.zip** with the files under the January 2007 issue.

— Doug, KF6DX



**ARRL**  
225 Main Street  
Newington, CT 06111-1494 USA

For one year (6 bi-monthly issues) of *QEX*:

**In the US**

ARRL Member \$24.00  
 Non-Member \$35.00

**In the US by First Class mail**

ARRL Member \$37.00  
 Non-Member \$49.00

**Elsewhere by Surface Mail (4-8 week delivery)**

ARRL Member \$31.00  
 Non-Member \$43.00

**Canada by Airmail**

ARRL Member \$40.00  
 Non-Member \$52.00

**Elsewhere by Airmail**

ARRL Member \$59.00  
 Non-Member \$71.00

Remittance must be in US funds and checks must be drawn on a bank in the US. Prices subject to change without notice.

## QEX Subscription Order Card

**QEX**, the Forum for Communications Experimenters is available at the rates shown at left. Maximum term is 6 issues, and because of the uncertainty of postal rates, prices are subject to change without notice.

Subscribe toll-free with your credit card **1-888-277-5289**

Renewal     New Subscription

Name: \_\_\_\_\_ Call: \_\_\_\_\_

Address: \_\_\_\_\_

City: \_\_\_\_\_ State or Province: \_\_\_\_\_ Postal Code: \_\_\_\_\_

Payment Enclosed to ARRL.

Charge:

Account # \_\_\_\_\_ Good thru \_\_\_\_\_

Signature \_\_\_\_\_ Date \_\_\_\_\_

06/01

**In the next issue of**



In the May/June issue of *QEX*, Rod Brink, KQ6F, describes his phasing SSB rig for ragchewing on 75 and 40 m. Quality of sound and an image-rejecting mixer are featured in a direct-conversion design. Older hams will remember some of the requirements for good opposite-sideband rejection that Rod points out. In fact, what we now call the I-Q method is used in DSP to do the same thing that KQ6F has done in analog. Check it out!



# CD-ROM Collections



## NEW EDITION! ARRL Periodicals on CD-ROM are

fully-searchable collections of popular ARRL journals. Every word and photo published throughout the year is included!

SEARCH the full text of every article by entering titles, call signs, names—almost any word. SEE every word, photo (including color images), drawing and table in technical and general-interest features, columns and product reviews, plus all advertisements. PRINT what you see, or copy it into other applications.

### System Requirements:

Microsoft Windows™. 1999, 2000, 2001, 2002, 2003, 2004, 2005 and 2006 editions support Windows and Macintosh systems, using the industry standard Adobe Acrobat Reader® (included).

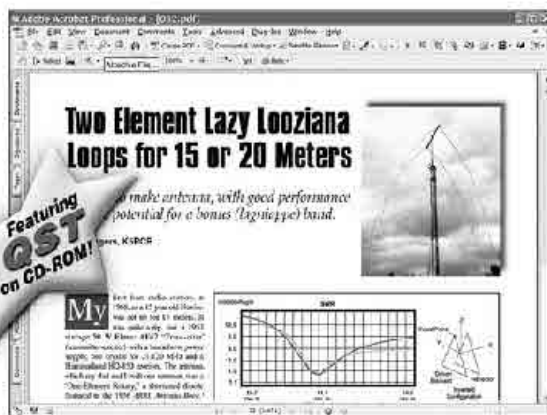
### Communications Quarterly CD-ROM

This CD-ROM collection covers volumes of *Communications Quarterly* published from 1990-1999. Gain access to advanced technical topics in articles which cover transmitter, receiver and transceiver projects, theory, antennas, troubleshooting and much more. High quality black-and-white page scans can be read on your computer screen or printed. Quickly **search** for articles by title and author, **select** specific year and issue, and **browse** individual articles and columns. Requires Microsoft Windows™.

### QST View

Every page of *QST*—all the ads, articles, columns and covers—has been scanned as a black-and-white image that can be viewed or printed.

**BONUS!** Latest, enhanced viewer—**AView**—included with any **QST View** purchase. **AView** is compatible with all sets of **QST View**.



### ARRL CD-ROM Collections

#### ARRL Periodicals CD-ROM

(includes *QST*, *QEX*, *NCJ*)

#9841 Year 2006	..... <b>NEW!</b>	..... <b>\$19.95</b>
#9574 Year 2005	.....	..... <b>\$19.95</b>
#9396 Year 2004	.....	..... <b>\$19.95</b>
#9124 Year 2003	.....	..... <b>\$19.95</b>
#8802 Year 2002	.....	..... <b>\$19.95</b>
#8632 Year 2001	.....	..... <b>\$19.95</b>
#8209 Year 2000	.....	..... <b>\$19.95</b>
#7881 Year 1999	.....	..... <b>\$19.95</b>
#7377 Year 1998	.....	..... <b>\$19.95</b>
#6729 Year 1997	.....	..... <b>\$19.95</b>
#6109 Year 1996	.....	..... <b>\$19.95</b>
#5579 Year 1995	.....	..... <b>\$19.95</b>

#### QST View CD-ROM

#7008 Years 1915-29	.....	..... <b>\$39.95</b>
#6710 Years 1930-39	.....	..... <b>\$39.95</b>
#6648 Years 1940-49	.....	..... <b>\$39.95</b>
#6435 Years 1950-59	.....	..... <b>\$39.95</b>
#6443 Years 1960-64	.....	..... <b>\$39.95</b>
#6451 Years 1965-69	.....	..... <b>\$39.95</b>
#5781 Years 1970-74	.....	..... <b>\$39.95</b>
#5773 Years 1975-79	.....	..... <b>\$39.95</b>
#5765 Years 1980-84	.....	..... <b>\$39.95</b>
#5757 Years 1985-89	.....	..... <b>\$39.95</b>
#5749 Years 1990-94	.....	..... <b>\$39.95</b>
#8497 Years 1995-99	.....	..... <b>\$39.95</b>
#9418 Years 2000-2004	.....	..... <b>\$39.95</b>
#QSTV (all 13 sets) ...	.....	..... <b>Only \$399</b> (Save \$120)

#### Communications Quarterly CD-ROM

#8780 (1990-1999)	.....	..... <b>\$39.95</b>
<b>Ham Radio Magazine CD-ROM*</b>		
#8381 Years 1968-76	.....	..... <b>\$59.95</b>
#8403 Years 1977-83	.....	..... <b>\$59.95</b>
#8411 Years 1984-90	.....	..... <b>\$59.95</b>
#HRCD (all three sets)	.....	..... <b>\$149.85</b>
<b>QEX Collection CD-ROM</b>		
#7660 (1981-1998)	.....	..... <b>\$39.95</b>
<b>NCJ Collection CD-ROM</b>		
#7733 (1973-1998)	.....	..... <b>\$39.95</b>



[www.arrl.org/shop](http://www.arrl.org/shop)  
**1-888-277-5289 (US)**

\*Ham Radio CD-ROM, © 2001, American Radio Relay League, Inc. Ham Radio Magazine © 1968-1990, CQ Communications, Inc.

**Shipping & Handling charges apply:** US orders add \$6 for one CD, plus \$2 for each additional CD (\$12 max.). International orders add \$5.00 to US rate (\$17.00 max.). Or, contact ARRL to locate a dealer. Sales Tax is required for orders shipped to CA, CT, VA, and Canada.

# Electronics Officers Needed for U.S. Flag Commercial Ships Worldwide

Skills required: Computer, networking, instrumentation and analog electronics systems maintenance and operation. Will assist in obtaining all licenses. Outstanding pay and benefits. Call, Fax or e-mail for more information.

## American Radio Association AFL-CIO

"The Electronics and Information Technology  
Affiliate of the ILWU"



Phone: 510-281-0706

Fax: 775-828-6994

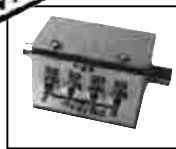
[arawest@earthlink.net](mailto:arawest@earthlink.net)



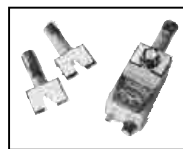
### NATIONAL RF, INC.



**VECTOR-FINDER**  
Handheld VHF direction finder. Uses any FM xcvr. Audible & LED display.  
VF-142Q, 130-300 MHz \$239.95  
VF-142QM, 130-500 MHz \$289.95



**ATTENUATOR**  
Switchable, T-Pad Attenuator, 100 dB max - 10 dB min BNC connectors  
AT-100, \$89.95



**DIP METER**  
Find the resonant frequency of tuned circuits or resonant networks—ie antennas.  
NRM-2, with 1 coil set, \$219.95  
NRM-2D, with 3 coil sets (1.5-40 MHz), and Pelican case, \$299.95  
Additional coils (ranges between 400 kHz and 70 MHz avail.), \$39.95 each



**DIAL SCALES**  
The perfect finishing touch for your homebrew projects. 1/4-inch shaft couplings.  
NPD-1, 3 3/4 x 2 3/4 inches 7:1 drive, \$34.95  
NPD-2, 5 1/2 x 3 3/8 inches 8:1 drive, \$44.95  
NPD-3, 5 1/2 x 3 3/8 inches 6:1 drive, \$49.95

S/H Extra, CA add tax

**NATIONAL RF, INC**  
7969 ENGINEER ROAD, #102  
SAN DIEGO, CA 92111

858.565.1319 FAX 858.571.5909  
[www.NationalRF.com](http://www.NationalRF.com)

# ELECTRONICS OFFICER TRAINING ACADEMY

The Complete Package To Become A Marine  
Radio Officer/Electronics Officer

ELKINS, with its 54-year history in the radio and communications field, is the only school in the country providing all the training and licensing certification needed to prepare for the exciting vocation of Radio Officer/Electronics Officer in the Merchant Marines.

Great Training | Great Jobs | Great Pay



Call, Fax or Email for More Information:

**ELKINS Marine Training International**

P.O. Box 2677; Santa Rosa, CA 95405

Phone: 800-821-0906, 707-792-5678

Fax: 707-792-5677

Email: [info@elkinsmarine.com](mailto:info@elkinsmarine.com)

Website: [www.elkinsmarine.com](http://www.elkinsmarine.com)

## Down East Microwave Inc.

We are your #1 source for 50MHz to 10GHz components, kits and assemblies for all your amateur radio and Satellite projects.

Transverters & Down Converters, Linear power amplifiers, Low Noise preamps, coaxial components, hybrid power modules, relays, GaAsFET, PHEMT's, & FET's, MMIC's, mixers, chip components, and other hard to find items for small signal and low noise applications.

**We can interface our transverters with most radios.**

Please call, write or see our web site  
**[www.downeastmicrowave.com](http://www.downeastmicrowave.com)**  
for our Catalog, detailed Product descriptions and interfacing details.

Down East Microwave Inc.  
954 Rt. 519  
Frenchtown, NJ 08825 USA  
Tel. (908) 996-3584  
Fax. (908) 996-3702

# Big Winners from Array Solutions



## PowerMaster Watt/VSWR Meter

- Sets the leading edge for all watt/vswr meters to follow
- Unheard of accuracy for the price
- Fast Bright reading meter
- Application software included
- Upgradeable via Internet

**\$430**



## AIM 4170 Antenna Analyzer

- Most advanced vector impedance analyzer at a fraction of the cost
- Accurate and easy to use
- Application software included
- Lab instrument quality
- Upgradeable via Internet

**\$400**



OptiBeam 3 element 80 Yagi

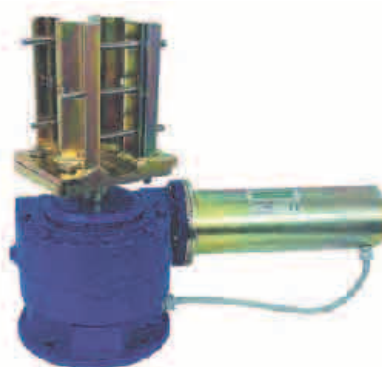
**OB3-80+**

## OptiBeam Antennas

German Engineering means High Performance and Reliability

## Prosistel Rotators

Strongest Rotators  
on the Market  
Prosistel  
PST 71 DC



## AS-AYL-4

NEW 4 Direction K9AY Loop Antenna  
Hear What You've Been Missing on the Low Bands

[www.arrayolutions.com](http://www.arrayolutions.com)

Phone 972-203-2008

[sales@arrayolutions.com](mailto:sales@arrayolutions.com)

Fax 972-203-8811



**We've got your stuff!**



# KENWOOD

Listen to the Future

# KENWOOD SKYCOMMAND TURN IT ON!

**Kenwood SkyCommand has FCC approval.**

Allows Global communication through remote operation on HF frequencies at home or in the field utilizing Kenwood's TS-2000 series transceivers.

Kenwood's TH-D7AG or TM-D700A required for remote use.

Perfect for use in hurricane or tornado zones, as well as Search and Rescue areas for Long Distance Communications when other normal modes of communications are out.

A great tool to monitor propagation while doing other things at home!

No cables or adaptors to fool with or buy!

No software or computer required!!

Step by step setup and programming taking only minutes.

Ease of use.



*See your local dealer for details.*

**KENWOOD U.S.A. CORPORATION**  
Communications Sector Headquarters

3975 Johns Creek Court, Suite 300, Suwanee, GA 30024-1265

**Customer Support/Distribution**

P.O. Box 22745, 2201 East Dominguez St., Long Beach, CA 90801-5745

Customer Support: (310) 639-4200 Fax: (310) 537-8235

**INTERNET**

Kenwood News & Products

<http://www.kenwoodusa.com>

ADSP44606



QUALITY SYSTEM  
JQA-1205

001-A

ISO9001 Registered

Kenwood Corporation

ISO9001 certified